BioMed Research International

Signal Transduction Inhibitors as Promising Anticancer Agents

Guest Editors: Raj Kumar, Cedric Dos Santos, Tarunveer Singh Ahluwalia, and Sandeep Singh

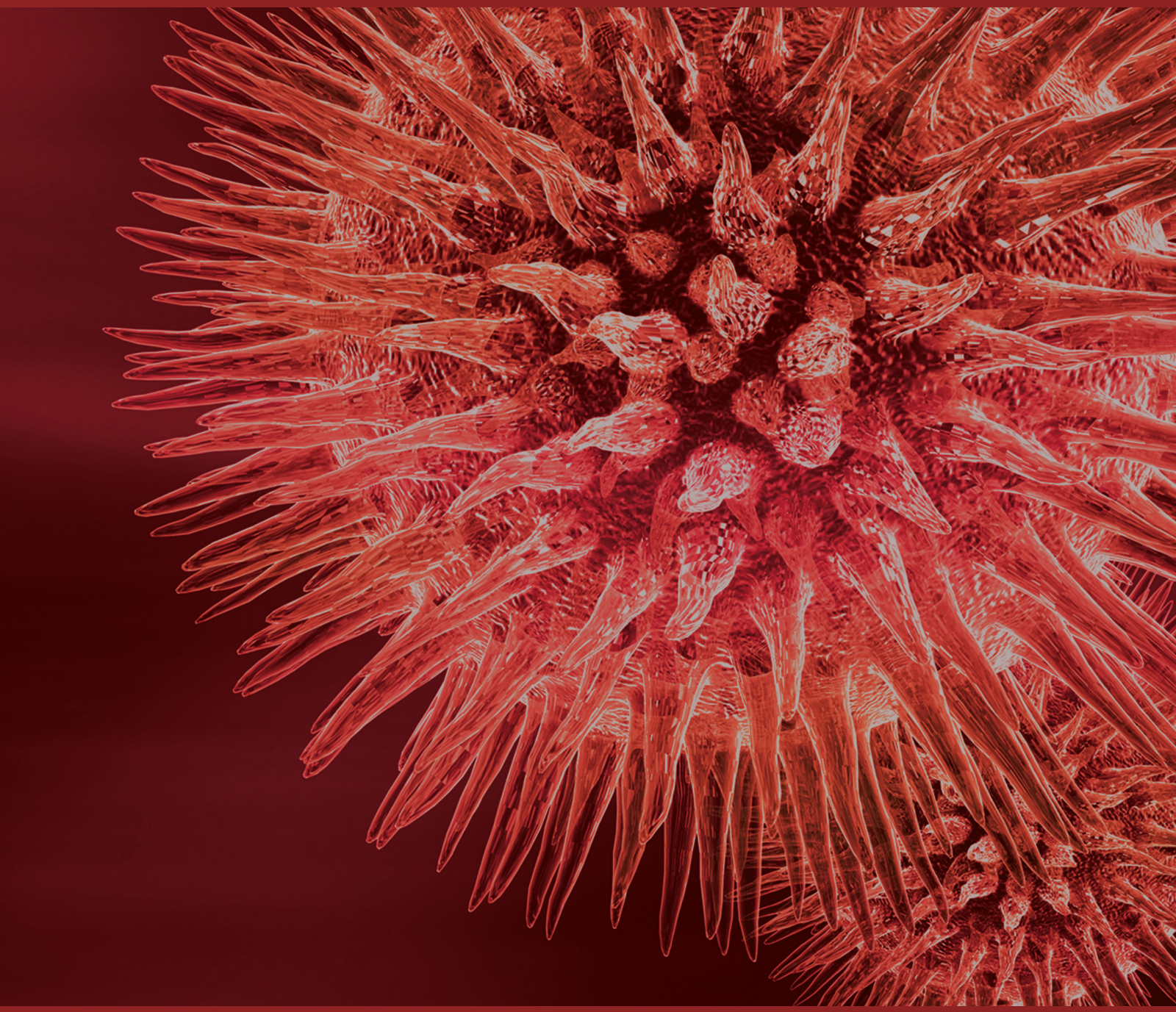

Signal Transduction Inhibitors as Promising Anticancer Agents

BioMed Research International

Signal Transduction Inhibitors as Promising Anticancer Agents

Guest Editors: Raj Kumar, Cedric Dos Santos,
Tarunveer Singh Ahluwalia, and Sandeep Singh

Contents

Hindawi Publishing Corporation
BioMed Research International
Volume 2015, Article ID 584170, 2 pages
http://dx.doi.org/10.1155/2015/584170

Editorial

Signal Transduction Inhibitors as Promising Anticancer Agents

Raj Kumar,[1] Cedric Dos Santos,[2] Tarunveer Singh Ahluwalia,[3] and Sandeep Singh[4]

[1]*Laboratory for Drug Design and Synthesis, Centre for Chemical and Pharmaceutical Sciences, Central University of Punjab, Bathinda Punjab 151001, India*
[2]*Hematology-Oncology, Perelman School of Medicine, University of Pennsylvania, 720 BRB-II/III, 421 Curie Boulevard Philadelphia, PA 19104-6160, USA*
[3]*The Novo Nordisk Foundation Centre for Basic Metabolic Research, Section of Metabolic Genetics, Faculty of Medical and Health Sciences, University of Copenhagen, Universitetsparken 1, DIKU Building, 2100 Copenhagen, Denmark*
[4]*Centre for Genetic Diseases and Molecular Medicine, Central University of Punjab, Bathinda Punjab 151001, India*

Correspondence should be addressed to Raj Kumar; raj.khunger@gmail.com

Received 5 April 2015; Accepted 5 April 2015

Cancer is a group of diseases sharing common features like unrestrictive growth, metastasis, and angiogenesis; however the basic signal transduction pathways are deregulated to such an extent that every cancer case itself poses new challenges for the therapeutics. Worldwide approximately 7.6 million people died of cancer in year 2008 and it has been projected that 13.1 million deaths will be due to cancer by year 2030.

Understanding the disease etiology and dysregulation of tissue microenvironment, signal transduction pathways are the potential directions, which may help us find the possible cure for the disease. However, recent advances in cancer therapeutics are proving to be beneficial for the patients but there is still a lot to be desired. Continuous research worldwide is focusing on developing better therapeutics as well as finding novel druggable targets for better efficacy. Another recent development is novel multitarget drugs, which may increase the efficacy manyfold.

In the current special issue a total of twelve articles were received which were of the highest quality indicating the level of interest worldwide on the issue. The articles were having potential topics including (i) understanding of signal transduction alteration in cancer development, (ii) experimental studies highlighting the role of various cell signaling molecules involved in carcinogenesis, (iii) mechanistic studies involving better (novel) animal/cell culture models for signal transduction studies in cancer, and (iv) evaluation of synthetic and natural products as cell signaling inhibitors in cancer development, angiogenesis, and metastasis. Out of the twelve articles received, five were accepted for publication in the special issue.

In study entitled "Deguelin Induces Apoptosis by Targeting Both EGFR-Akt and IGF1R-Akt Pathways in Head and Neck Squamous Cell Cancer Cell Lines," Y. Baba et al. investigated potential anticancer mechanisms of a retinoid compound named deguelin derived from the African plant *Mundulea sericea* (Leguminosae) in head and neck squamous cell carcinoma (HNSCC). The flow cytometry data showed accumulation of proapoptotic cells in deguelin treated cells. The compound inhibited IGF-1 and EGF induced Akt activation. Cell death induced by the compound was reported to be via reduction of phospho-IGF1R, Akt, and ERK1/2. Overall, the study showed potential mechanisms behind antitumor activity of deguelin and suggested that it may be applicable therapeutic strategy for head and neck squamous cell cancer.

S. J. Assinder et al. proposed novel role of negative regulators of receptor tyrosine kinase in clinical settings. The study "Cosuppression of Sprouty and Sprouty-Related Negative Regulators of FGF Signalling in Prostate Cancer: A Working Hypothesis" targeted FGF RTK signaling which is commonly involved in prostate cancer. The authors explored potential role of sprouty and sprouty-related antagonists in prostate intraepithelial neoplasia using various knock-out mice models. By performing various *in vivo* and clinical

analyses, the authors conclude that in prostate cancer sprouty and sprouty-related antagonists are significantly repressed demonstrating the importance of negative regulators of RTK and highlighted their importance for future pharmacopeia.

In research article "Biological and Molecular Effects of Small Molecule Kinase Inhibitors on Low-Passage Human Colorectal Cancer Cell Lines," F. Lange et al. tested various small molecule kinase inhibitors such as vemurafenib, trametinib, perifosine, and regorafenib in 4 cancer cell lines (CRC) established from colon cancer patients. The mutant BRAF inhibitor vemurafenib and MEK1/2 inhibitor trametinib efficiently inhibited DNA synthesis in BRAF mutant cells. On the other hand, the AKT inhibitor perifosine was effective in three cell lines but the fourth cell line was resistant to it. Regorafenib, which is multikinase inhibitor, suppressed proliferation in all the cell lines irrespective of KRAS, BRAF, PIK3CA, and TP53 mutations or expression. In conclusion, the authors stressed on use of low-passage CRC cell lines for preclinical investigations to test small molecule inhibitors.

In the paper "Roles of ERβ and GPR30 in Proliferative Response of Human Bladder Cancer Cell to Estrogen," W. Huang et al. probed potential involvement of estrogen receptors in progression of bladder cancer. Cells were treated with different doses of 17β-estradiol followed by cell proliferation analysis. Further mechanistic insights indicated that 17β-estradiol effect is EGFR-MAPK pathway independent and primarily happens due to GPR30. On the other hand, c-FOS, BCL-2, and cyclin D1 expression was increased by estradiol treatment that was independently associated with EGFR-MAPK pathway.

M. Xie et al. in their study entitled "Progesterone and Src Family Inhibitor PP1 Synergistically Inhibit Cell Migration and Invasion of Human Basal Phenotype Breast Cancer Cells" demonstrated antimetastatic effects of PP1 in aggressive breast cancer cell lines. The authors detected moderate expression levels in brain-metastatic BPBC cell line MB231Br, which was derived from the parent mPRα undetectable MB231 cells. The work provided interesting and novel findings towards development of novel anticancer agents targeting nuclear hormonal receptors and endocrine-resistant breast cancers.

Raj Kumar
Cedric Dos Santos
Tarunveer Singh Ahluwalia
Sandeep Singh

Hindawi Publishing Corporation
BioMed Research International
Volume 2015, Article ID 251780, 10 pages
http://dx.doi.org/10.1155/2015/251780

Research Article

Roles of ERβ and GPR30 in Proliferative Response of Human Bladder Cancer Cell to Estrogen

Weiren Huang,[1,2] Yuanbin Chen,[1,3,4] Yuchen Liu,[2,5] Qiaoxia Zhang,[2] Zhou Yu,[1,6] Lisha Mou,[1,2] Hanwei Wu,[1] Li Zhao,[1] Ting Long,[3] Danian Qin,[3] and Yaoting Gui[1]

[1]*Guangdong and Shenzhen Key Laboratory of Male Reproductive Medicine and Genetics, Institute of Urology, Peking University Shenzhen Hospital, Shenzhen PKU-HKUST Medical Center, Shenzhen 518036, China*
[2]*Key Laboratory of Medical Reprogramming Technology, Shenzhen Second People's Hospital, First Affiliated Hospital of Shenzhen University, Shenzhen 518035, China*
[3]*Department of Physiology, Shantou University School of Medicine, Shantou 515031, China*
[4]*Department of Physiology, Medical College of Jiaying University, Meizhou 514031, China*
[5]*Anhui Medical University, Hefei 230032, China*
[6]*The Institute of Plastic Surgery, Xijing Hospital, Fourth Military Medical University, Xi'an 710032, China*

Correspondence should be addressed to Danian Qin; dnqin@stu.edu.cn and Yaoting Gui; guiyaoting@hotmail.com

Received 2 July 2014; Revised 14 September 2014; Accepted 1 October 2014

Academic Editor: Tarunveer S. Ahluwalia

Bladder cancer belongs to one of the most common cancers and is a leading cause of deaths in our society. Urothelial carcinoma of the bladder (UCB) is the main type of this cancer, and the estrogen receptors in UCB remain to be studied. Our experiment aimed to investigate the possible biological effect of 17β-estradiol on human bladder-derived T24 carcinoma cells and to indicate its related mechanisms. T24 cells were treated with various doses of 17β-estradiol, and cell proliferation was detected using MTT assays. 17β-estradiol promoted T24 cell proliferation independent of ERβ/GPR30-regulated EGFR-MAPK pathway, while it inhibited cell growth via GPR30. Furthermore, the expression levels of downstream genes (*c-FOS, BCL-2,* and *CYCLIN D1*) were increased by 17β-estradiol and this effect was independently associated with activity of the EGFR-MAPK pathway. The two estrogen receptors might be potential therapeutic targets for the treatment of bladder cancer.

1. Introduction

Bladder cancer is currently the fourth most common cancer worldwide and accounts for a high number of deaths every year [1]. It is widely acknowledged that sex hormones exert a complicated function *in vivo*. Previous studies showed that estrogens play important roles in the initiation and proliferation of bladder cancer through specific receptors-induced signaling pathways [2–5]. However, reports also showed that females who are treated with estrogens have reduced risk of bladder cancer [6, 7], implying that estrogens may contribute to the prevention of bladder cancer. Estrogens exert their biological function primarily through binding to estrogen receptors (ERs), which include the classic nuclear ERs (ERα and ERβ) [8] and/or the membrane ERs [9]. ERα is rarely expressed in bladder cancer cells [5, 10], while ERβ is expressed at high levels in both normal urothelial and bladder cancer cells [5]. Furthermore, it is considered that ERβ expression is abundant in cases of both low-grade and high-grade cancers [5], implying that ERβ plays important roles in bladder cancer.

GPR30 (G protein-coupled receptor 30), a novel membrane ER with high-affinity and low-capacity binding to estrogens, is structurally dissimilar to nuclear ERs [11] and localizes to both the plasma membrane and endoplasmic reticulum [12, 13]. GPR30 has been detected in multiple tumors and plays important roles in cell proliferation and differentiation [14–17]. Activation of GPR30 results in inhibition of prostate cancer PC-3 cell proliferation [16] and stimulation of testicular germ cell-JKT-1 cell proliferation [17]. These

effects are probably not induced by the same signaling pathways.

Several studies have investigated the effects mediated by ERs [4, 5, 18] and GPR30 in bladder cancer [19]; however, the observations were controversial. In addition, few studies have explored the function regulated by the two ERs subtypes. In this study, we aimed to elucidate the biological action of 17β-estradiol (E2, <1 μmol/L) on bladder cancer *in vitro* and to investigate the involved mechanisms. As 90% of the cases of bladder cancer are transitional cell carcinoma (TCC) [20], we used T24, a human bladder transitional cell carcinoma line, as an experimental model.

2. Materials and Methods

2.1. Cell Culture. T24 human carcinoma cells (ATCC HTB-4) were cultured at 37°C with 5% CO_2 in RPMI 1640 medium (Gibco-BRL, Grand Island, NY, USA) supplemented with 10% dextran-coated charcoal-treated fetal bovine serum (FBS; Hyclone, UT, USA) and 100 U/mL penicillin and streptomycin. Cells were plated in 6-well plates at a density of 1×10^5 cell/well. The experimental reagents were added to fresh phenol-red-free RPMI 1640 medium after one night of serum starvation. After specific treatment times, the exponentially proliferating cells in this study were used for quantitative real time PCR and western blotting analyses.

2.2. MTT Assays. To observe the effect of E2, T24 cells were seeded in 96-well plates at a density of approximately 2×10^3 cells/well. Then E2 or E2-BSA was added at final concentrations of 0.1 nM, 1 nM, 10 nM, 100 nM, or 1 μM, and 0.1% DMSO was used as the basal control group. Cells were treated in quadruplicate for each condition. After the cells were incubated for 0, 24, 48, 72, and 96 h, 20 μL 3-(4,5-dimethythiazol-2-yl)-2,5-diphenyltetrazolium bromide (MTT) (Sigma-Aldrich, St. Louis, MO) solution [5 g/mL in phosphate buffered saline (PBS)] was added to each well. The cells were incubated at 37°C for 4 h; then media were removed and 150 μL dimethyl sulfoxide (DMSO) was added per well to solubilize the formazan. The microplate was shaken on a rotary platform for 10 mins at room temperature, and then the optical density (OD) values were measured at 490 nM using a Wellscan reader (Bio-Rad Laboratories, Hercules, CA, USA). To investigate the signaling pathways activated by E2, T24 cells were pretreated with specific siRNA or inhibitors prior to E2 addition, and the results were examined as described above. The cell inhibition rate = (control group value − experimental group value)/control group value × 100%. Three dependent experiments were performed. The data presented here was from one representative experiment.

2.3. Quantitative PCR. Total RNA from T24 cells was extracted using TRIzol reagent (Invitrogen, Carlsbad, CA, USA) and reverse transcribed using PrimeScript RT Kit (Takara, Shiga, Japan). We determined the expression of *c-FOS*, *BCL-2*, *CYCLIN D1*, and *β-actin* using the ABI PRISM 7000 instrument (ABI, CA, USA). The primers were as follows:

c-FOS (forward, 5′-AGGAGAATCCGAAGGGAA-AG-3′; reverse, 5′-CAAGGGAAGCCACAGACATC-3′),

BCL-2 (forward, 5′-GGGAGGATTGTGGCCTTC-TT-3′; reverse, 5′-ATCCCAGCCTCCGTTATCCT-3′),

CYCLIN D1 (forward, 5′-CATGGAAGCGAATCA-ATGGACT-3′; reverse, 5′-CCTCCTTCTGCACAC-ATTTGAA-3′),

β-actin (forward, 5′-CTGGAACGGTGAAGGTGA-CA-3′; reverse, 5′-AAGGGACTTCCTGTAA-3′).

The PCR cycling parameters were denaturation at 95°C for 30 s, followed by 40 cycles at 95°C for 5 s and 60°C for 30 s.

2.4. Western Blotting. T24 cells exposed to reagents in 6-well plates were lysed in 200 μL RIPA buffer (Invitrogen, Carlsbad, CA, USA), which contained a final concentration of 1 mM NaF (Sigma-Aldrich, St. Louis, MO) and 1 mM Na_3VO_4 (Sigma-Aldrich, St. Louis, MO), and cells were then sonicated on ice for 10 s. After centrifugation at 12,000 ×g for 10 min, the supernatant was transferred to a clean Eppendorf tube and then boiled at 100°C for 5 min in loading buffer containing mercaptoethanol. The whole proteins (20 μg) extracted from each sample were resolved on a gradient SDS-PAGE gel and electrotransferred onto PVDF membranes (Millipore, Billerica, MA) using a wet transfer cell (Bio-Rad Laboratories, Hercules, CA) at 200 mA for 2 h. Membranes were preblocked in Tris-buffered saline containing 0.1% Tween 20 and 5% BSA (TBST-BSA) and then were incubated with phospho-ERK-specific antibodies (Cell Signaling Technology, Beverly, MA, USA) diluted at 1 : 1000 in TBST-BSA overnight at 4°C, followed by species-specific HRP-conjugated secondary antibodies (KPL, Gaithersburg, MD, USA) diluted at 1 : 2500 in TBST-BSA for 1 h at room temperature. Blots were developed using ECL procedures. Relative expression levels of total ERK protein in each sample were determined by stripping the phospho-ERK-specific antibodies from the membranes and reincubating with ERK antibodies (Cell Signaling Technology, Beverly, MA, USA).

ECL results were scanned and the protein bands were quantified using Image J analysis software (National Institutes of Health, USA). Histograms were generated by normalizing the amount of each protein to the total ERK level detected in the same extracted sample. Each experiment was repeated three times. The data presented here were from one representative experiment.

2.5. siRNA and Plasmids. T24 cells were transfected using siRNA transfection regent (Qiagen, Hilden, Germany) with 10 nM *ERβ* or *GPPR30* siRNA (Qiagen, Hilden, Germany) according to the manufacturer's instructions; negative siRNA (Qiagen, Hilden, Germany) was used as a negative control. The target sequence of the used *ERβ* siRNA was 5′-CAG-CGATTACGCATCGGGATA-3′, and the sequence of used *GPR30* siRNA was 5′-CGGCCACGTCATGTCTCTAAA-3′.

After culturing in phenol-red-free RPMI 1640 medium containing 10% dextran-coated charcoal-treated FBS for 24 h, E2 was added to 6-well plates for the qPCR and western blot experiments or to 96-well plates for the MTT assays.

Mammalian expression vectors encoding *ERβ* or *GPPR30* were constructed by inserting PCR-amplified fragments into pcDNA3 (Invitrogen). Lipofectamine 2000 reagent was used for transfections according to the standard protocols (Invitrogen).

2.6. Data Analysis and Statistical Methods. Results from three independent experiments were analyzed using standard error of the mean (SEM). The comparison among groups was analyzed by one-way ANOVA. Values of $P < 0.05$ were considered statistically significant and values of $P < 0.01$ were considered highly significant. All of the statistical analysis was performed using SPSS for Windows Release 13.0 (SPSS, Chicago, IL, USA).

3. Results

3.1. T24 Cell Proliferation Was Promoted by E2. To investigate the biological function of E2 in T24 cells, we first explored the expression of estrogen receptors using qPCR and western blotting, which showed that T24 cells expressed *ERβ* and *GPR30* but not *ERα* (Figures 1(a) and 1(b)). To better understand the exact effect of E2 on T24 cells, we incubated the cells with increasing concentrations of E2: 0.1 nM, 1 nM, 10 nM, 100 nM, and 1 μM. Cell proliferation was examined after 0 h, 24 h, 48 h, 72 h, and 96 h using MTT assays, in which the absorbance of formazan indirectly reflected cell activity and cell numbers (Figure 1(c)). These data demonstrated that E2 stimulated T24 cell proliferation in a dose- and time-dependent manner. We selected 10 nM E2 for subsequent experiments due to its higher efficiency and lower toxicity.

3.2. GPR30 May Mediate the Inhibitory Effect Induced by E2 in T24 Cells. T24 cells express ERβ and GPR30, but it was not known exactly which receptor mediated the cell proliferation stimulated by E2. Cells were transfected with siRNA against *ERβ* (Figures 2(a) and 2(b)) or *ERβ* ORF expression vector, and the effect of 10 nM E2 on proliferation was investigated using MTT assays (Figure 2(c)). Surprisingly, cell proliferation was inhibited at 48 h ($P < 0.01$) when cells were transfected with *ERβ* siRNA. After incubation for 96 h, the inhibition rate was increased to 16.58% ($P < 0.01$). However, upregulated cell proliferation was observed from 24 h ($P < 0.05$) in the cells that were only treated with 10 nM E2, and this effect was time-dependent (Figure 2(c)). In contrast, cell proliferation was further promoted by E2 in cells overexpressing *ERβ* (Figure 2(c)).

It has previously been suggested that GPR30 mediates an inhibitory effect in T24 cells [19]. 17β-estradiol-17-hemisuccinate-BSA (E2-BSA, Sigma-Aldrich, St. Louis, MO, USA) is too large to pass through the cell plasma membrane. Thus, it could be considered that E2-BSA binds to GPR30, which is localized on the plasma membrane. To validate the biological effect of E2-BSA mediated by GPR30 in T24 cells, the cells were treated with 0.1 nM, 1 nM, 10 nM, 100 nM, and 1 μM E2-BSA for 0–96 h, and MTT assays were performed to measure the cell numbers (Figure 2(d)). The inhibition rate of T24 cells was about 18.06% at 48 h ($P < 0.01$), and the inhibition rate reached 20.38% at 96 h when the cells were treated with 10 nM E2-BSA ($P < 0.01$). Next, we silenced or overexpressed *GPR30* in T24 cells (Figures 2(d) and 2(f)), followed by 10 nM E2-BSA-treatment or 10 nM E2-treatment for 0–96 h (Figure 2(g)). No significant difference was observed between cells treated with 10 nM E2-BSA and control cells, perhaps because E2-BSA can not bind to a receptor. Cell proliferation was promoted when the *GPR30*-silenced cells were treated with 10 nM E2 ($P < 0.01$). In contrast, cell proliferation was further inhibited by E2 in cells overexpressing *GPR30*. Thus, we concluded that the E2 could inhibit cell proliferation in the presence of GPR30 and promoted cell proliferation in other circumstances. This finding may indicate that GPR30 mediated an inhibitory effect on T24 cell proliferation.

3.3. Either ERβ Or GPR30 Mediated Phosphorylation of ERK Induced by E2 through the EGFR-MAPK Pathway. Estrogens can generate a rapid nongenomic effect via second messengers, such as G protein, and then activate various downstream kinases such as ERK in cancer cells [21]. Our study showed that phosphorylation of ERK in T24 cells could be rapidly induced after treatment with E2 for 5 min (Figure 3). To evaluate which estrogen receptor (ERβ or GPR30) was involved in this response, T24 cells were transfected with specific siRNAs against *ERβ* or *GPR30* and incubated for 24 h. Then the phosphorylation of ERK was monitored after treatment with 10 nM E2 for 5 min. Although total levels of ERK were not changed by E2 in both the presence or absence of related siRNAs ($P < 0.01$), the extent of phosphorylated ERK was reduced when *ERβ* or *GPR30* was silenced (Figure 3). This suggests that ERK phosphorylation was mediated by either ERβ or GPR30 and that there may be a cross talk between the two receptors. When the cells were pretreated with the EGFR (epidermal growth factor receptor) antagonist AG1478 (100 nM) or the MAPK antagonist PD98059 (20 μM) for half an hour, this effect induced by E2 was also blocked (Figure 3). These results indicated that EGFR and MAPK were required for phosphorylation of ERK. We proposed that either ERβ or GPR30 could mediate the phosphorylation of ERK induced by E2 and hypothesized that activation of ERK in this context was mediated by the EGFR-MAPK pathway via cross talk between ERβ and GPR30.

3.4. E2 Altered the Expression Levels of Relative mRNAs in T24 Cells. As described above, E2 transduced signals through rapid activation of ERK (Figure 3). According to our hypothesis, this response could involve the activation of both ERβ and GPR30. *c-FOS* is one of the target genes in the estrogen response [22, 23] and participates in the regulation of cell cycle [24]. BCL-2 is closely associated with apoptosis [25, 26] and CYCLIN D1 is an essential cell cycle regulatory molecule. Therefore, we evaluated the mRNA expression levels of these targets using qPCR after normalization against *β-actin* levels

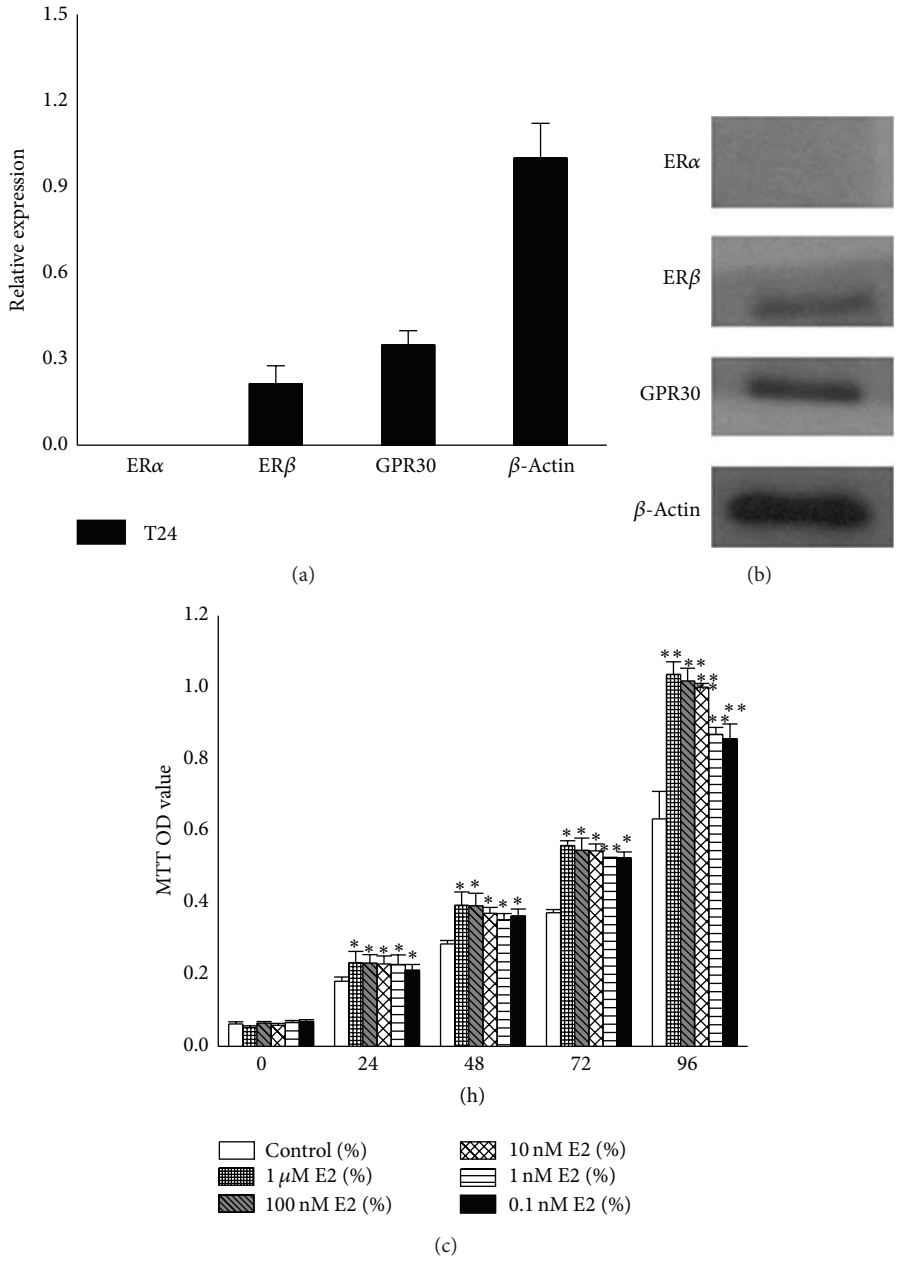

Figure 1: Proliferation of T24 cell was promoted by E2. (a) qPCR analysis of expression of estrogen receptor in T24 cells. *ERα* mRNA was rarely expressed in the cells, and the relative expression levels of *ERβ* and *GPR30* were 0.21 and 0.35, respectively (normalization to *β-actin*). (b) Expression of estrogen receptors in human T24 bladder cancer cells. Twenty micrograms of whole protein extracts was used for western blot analysis. ERα was not detected. (c) Cell proliferation promoted by E2. T24 cells were seeded in 96-well plates at a density of approximately 2×10^3 for each well and incubated with E2; then the OD values were examined after 0, 24, 48, 72, and 96 h by MTT assays. 0.1% DMSO was used as the negative control. The values represent the mean ± SD of the data from three independent experiments. $^{*}P < 0.05$; $^{**}P < 0.01$.

(Figure 4). After treatment with 10 nM E2 for 48 h, the expression levels of *c-FOS*, *BCL-2*, and *CYCLIN D1* mRNA were 5.5-, 2.8-, and 2.7-fold higher than that of the control, respectively (Figure 4). However, *BCL-2* and *CYCLIN D1* expression levels were inhibited when the cells were transfected with *ERβ* siRNA (Figures 4(b) and 4(c)), with inhibition rates of 42% and 22%, respectively. In contrast, E2 increases the expression levels of these genes in *GPR30*-silenced T24 cells. These results indicated that ERβ mediated cell proliferation and GPR30 mediated cell growth inhibition. Furthermore, *BCL-2* and *CYCLIN D1* gene expression levels were increased in the presence of EGFR antagonist and MAPK antagonist, suggesting that the cell proliferation promoted by E2 may be independent of the EGFR-MAPK pathway.

3.5. E2 Promoted T24 Cell Proliferation Independent of the EGFR-MAPK Pathway. To further confirm the molecular

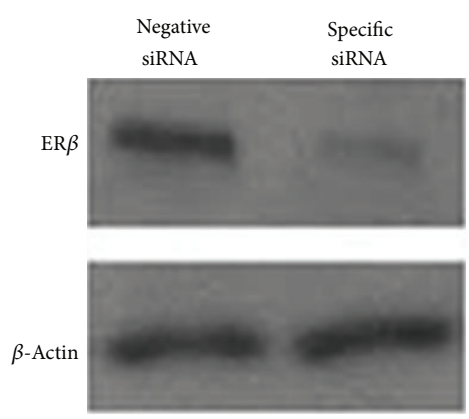

(a)

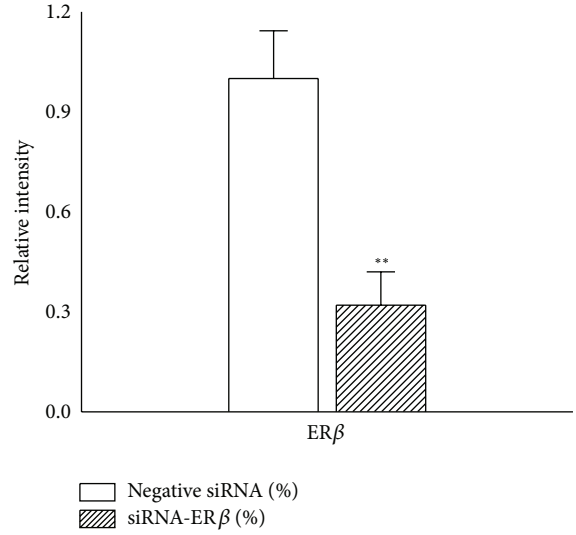

(b)

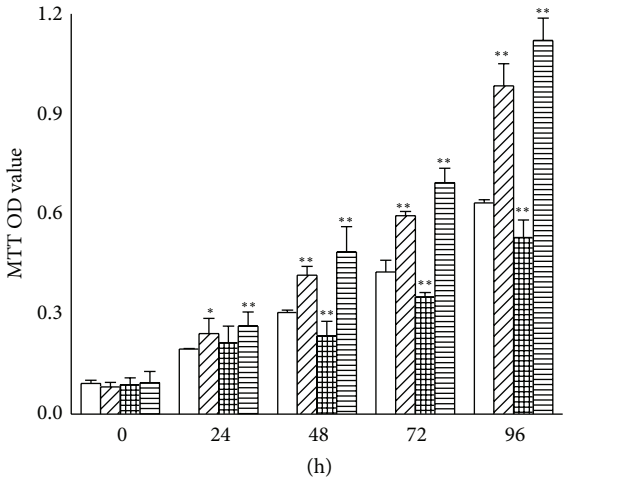

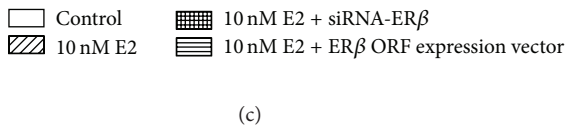

(c)

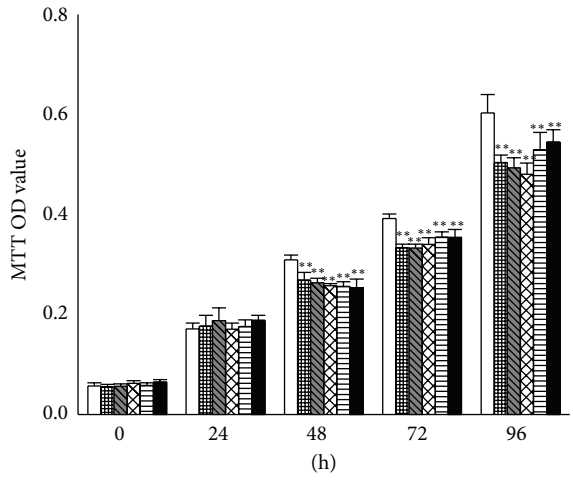

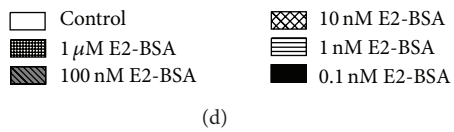

(d)

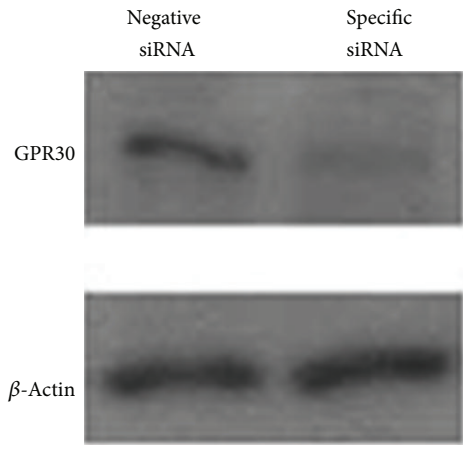

(e)

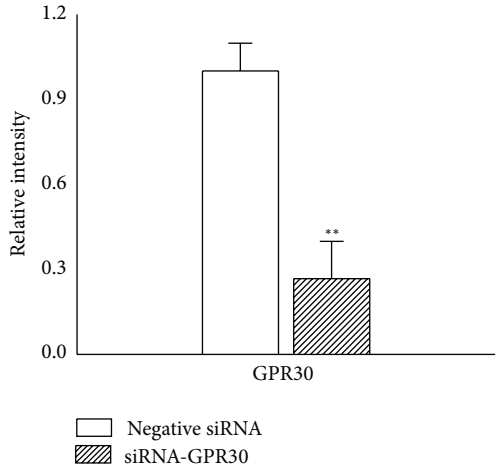

(f)

Figure 2: Continued.

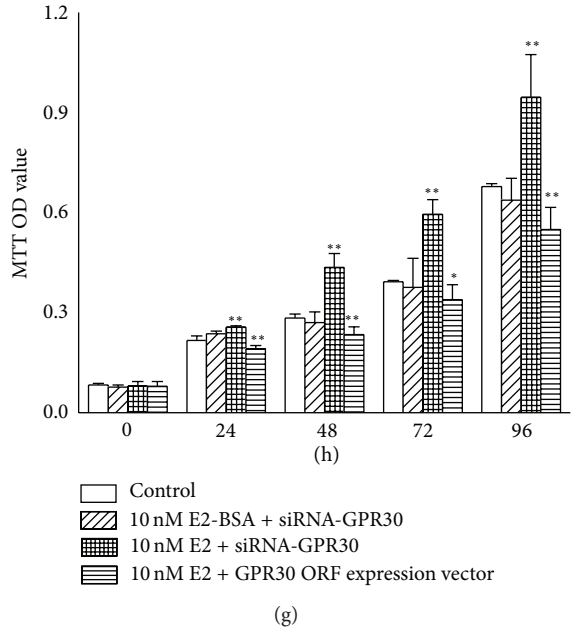

Figure 2: GPR30 mediated an inhibitory effect in T24 cells. (a) T24 cells were transfected with 10 nM specific siRNA against *ERβ*, and then protein expression levels were measured by western blot. (b) *ERβ* mRNA expression levels by qPCR analysis. The level of *ERβ* in control cells was defined as 1.0. (c) E2 inhibited T24 cell proliferation in the absence of ER*β*. Cells were transfected with siRNA against *ERβ* or *ERβ* ORF expression vector and then treated with 10 nM E2 for 0–96 h. MTT assays were performed to measure the cell activity. (d) Cell proliferation was inhibited by E2-BSA. T24 cells were treated as shown in Figure 1(c), and MTT assays were used to monitor the effect of E2-BSA. (e) T24 cells were transfected with siRNA against *GPR30*. The cells were treated as shown in (a), and protein levels were measured by western blot analysis. (f) Expression levels of *GPR30* mRNA by qPCR analysis. The level of *GPR30* was defined as 1.0. (g) *GPR30* mediated inhibition of T24 cell proliferation. The cells were transfected with 10 nM siRNA against *GPR30* or *GPR30* ORF expression vector and then treated with 10 nM E2 or 10 nM E2-BSA for 0–96 h. MTT assays were used to detect cell activity. The data presented here is one typical experiment from three independent experiments. $^{*}P < 0.05$; $^{**}P < 0.01$.

mechanisms induced by E2 in T24 cells, we performed additional MTT assays (Figure 5). The data showed that 10 nM E2 stimulated proliferation of T24 cell but inhibited the proliferation of *ERβ*-silenced T24 cells. Furthermore, the proliferation of T24 cells was not affected by 100 nM AG1478 or 20 μM PD98059 in the presence of E2. This experiment provided evidence that there may be cross talk between ER*β* and GPR30, the expression levels of which may determine the cellular responses to E2. ER*β* may play key roles in general response of T24 cells to E2 when the function of GPR30 was weakened or even lost. Finally, the cell proliferation stimulated by E2 was probably independent of the EGFR-MAPK pathway.

4. Discussion

Estrogens, particularly 17*β*-estradiol (E2), are widely acknowledged to be potent regulators of cell proliferation in tissues. Estrogens mediate their effects in target tissues through ERs, and ERs were found to be expressed in most cancer cells. Some studies demonstrated that ER*α* is required for carcinogenesis of the mammary gland [27, 28] and prostate [29]. Reports also suggested that ER*α* contributes to the stimulation of cell proliferation. For instance, ER*α* mediates the induction of breast cancer cell proliferation [30] and the promotion of cell proliferation of ovarian cancer [31] and bladder cancer [5]. However, ER*β* has been observed to exert an inhibitory effect on cell proliferation [30, 32, 33]. In our study, we aimed to investigate the effects mediated by ERs in response to estrogens in bladder cancer. Previous reports published contradictory results regarding the expression levels of ER*α* in bladder cancer cells. Teng et al. reported that the expression of ER*α* in human bladder tumor cells was significantly higher than that in bladder urothelial cells [4]. However, Shen et al. and Tuygun et al. only found weak expression levels of ER*α* in the tumor samples of hundreds of patients [5, 10, 18]. It has also been reported that bladder urothelial cells [4] and tumor cells [4, 5] express equally high levels of ER*β*, suggesting that ER*β* plays more crucial roles in urothelial and bladder cancer cells. Our results are not in agreement with studies, in which the results showed that ER*α* is expressed at high levels in T24 cells and that E2 induced cell proliferation in the absence of *ERβ* [4]. Here, we found that T24 cells expressed ER*β* but rarely ER*α*, and proliferation was stimulated by E2. It was interesting to note that these results were not consistent with the view that ER*β* has an inhibitory effect on cancer cells. Therefore, there may be other receptors involved in this function.

GPR30 is a novel membrane ER [13] and potentially mediates rapid E2-dependent cancer cell proliferation [15, 16, 34, 35]. Our findings suggest that GPR30 may be involved

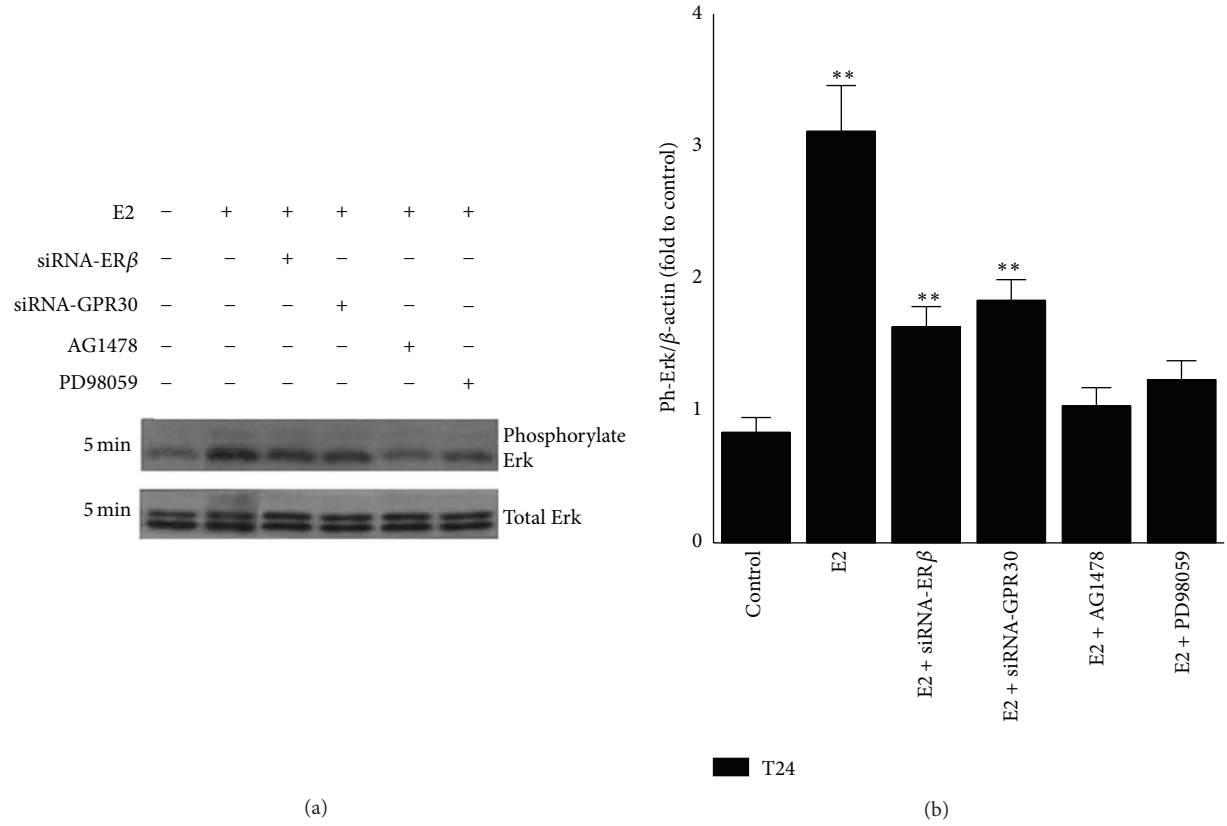

Figure 3: E2 induced activation of ERK through ERβ/GPR30-regulated EGFR-MAPK pathway in T24 cells. (a) E2 rapidly induced activation of ERK in T24 cells. Cells were transfected with specific siRNA against *ERβ* or *GPR30*, or pretreated with 100 nM AG1478 or 20 μM PD98059 for 30 min. Then 10 nM E2 was added and phosphorylated and total ERK levels were measured by western blot analysis. (b) Histogram of phosphorylation of ERK. The values were normalized to total ERK for each sample. The control was defined as 1.0. Blots are representative of three independent experiments with similar results. $^{**}P < 0.01$.

in promoting T24 cell proliferation induced by E2. The proliferation of cells transfected with siRNA against *ERβ* was inhibited in the presence of E2. We considered that nuclear ERβ may play a key role in the cell proliferation stimulated by E2, and we hypothesized that GPR30 mediated an inhibitory effect in T24 cells. Cell proliferation was stimulated by E2 when *GPR30* was silenced, providing evidence that nuclear ERβ and GPR30 had opposing effects on cell proliferation in T24 cells: nuclear ERβ mediated promotion of T24 cell proliferation and GPR30 mediated cell growth inhibition. We considered that the action of ERβ in response to estrogens should not be generally extrapolated to all tissues.

Here, we found that nuclear ERβ binding protein E2 stimulated T24 cell proliferation in parallel with immediate phosphorylation of ERK. Either GPR30 or ERβ can mediate the rapid activation of ERK [36–38]. We examined the activation of ERK induced by E2 after the cells were transfected with siRNA against *GPR30* and found that the extent of ERK phosphorylation was reduced compared to that of the control cells. Furthermore, MTT assays indicated that the effects induced by E2 were reversed when *ERβ* and *GPR30* were silenced. Thus, nuclear ERβ may play a key role in the response to E2 and was not activated by GPR30 in T24 cells. In some cases, for instance, when *ERβ* was silenced, GPR30 could exert its function to mediate inhibition of cell proliferation.

c-FOS gene is a protooncogene upregulated by numerous stimuli that enhance its expression and interaction with c-JUN to form heterodimers to regulate cell proliferation and differentiation [12]. In our study, 10 nM E2 increased *c-FOS* gene expression through the EGFR-MAPK pathway when either of the two receptors was knocked down. Hence, we considered that both receptors could mediate *c-FOS* gene expression. BCL-2 protein is known to regulate apoptosis [25, 26] and normally results in the promotion of tumor cell survival by blocking programmed cell death. Here, E2-induced T24 cell proliferation was associated with an increase in *BCL-2* expression. CYCLIN D1 reflects the G1 to S phase transition in cell cycle, and it plays a specific role in mitosis [39]. We found the expression level of CYCLIN D1 mRNA was more than two-fold higher than that of the control. However, the results were inconsistent with those observed by Teng et al. When *GPR30* was silenced [4], Teng et al. found that E2 increased CYCLIN D1 mRNA levels in T24 cells [19] but did not increase its expression level in the absence of *GPR30* [19]. These two views are incompatible because ERβ can also mediate the expression of this gene. In our study, this gene was expressed at significantly higher levels in the absence of

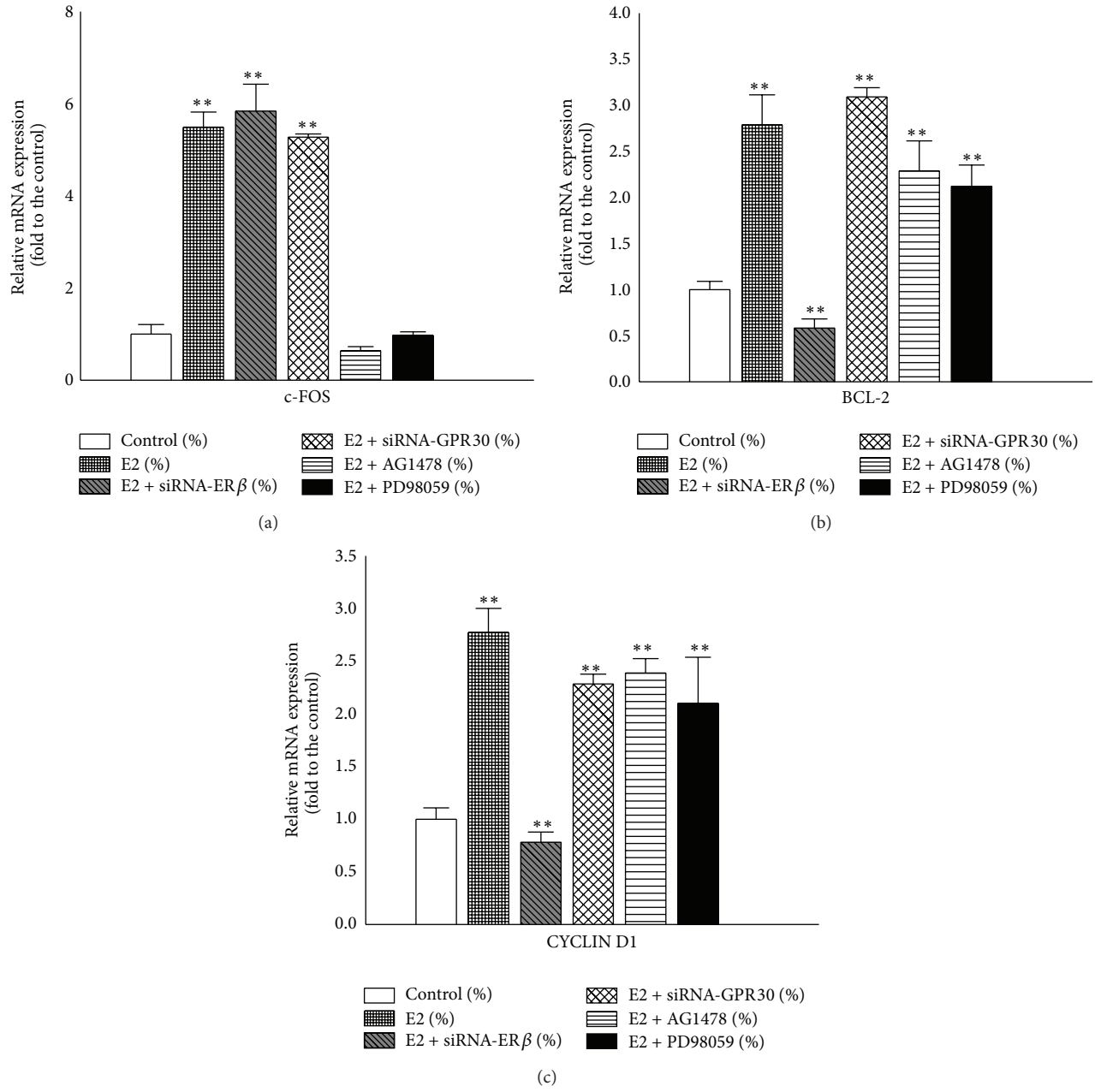

Figure 4: Relative expression levels of genes in T24 cells after treatment with E2. ((a)–(c)) Cells were pretreated as described in Figure 3(a) and then incubated with 10 nM E2 for 48 h. Total RNA was extracted for qPCR. *c-FOS*, *BCL-2,* and *CYCLIN D1* mRNA expression levels were evaluated and normalized to *β-actin* level. The values represent the mean ± SD of the data from three independent experiments. $^{**}P < 0.01$.

either ERβ or GPR30. We supposed that E2 increased the expression of the *c-FOS* gene, and the resulting c-FOS/c-JUN heterodimers increased the expression of the *BCL-2* gene to protect the cells from apoptosis. The c-FOS/c-JUN heterodimers could also increase the relative gene expression, such as CYCLIN D1, which resulted in promoting cell proliferation. Barkhem et al. hypothesized that the long-term effects of estrogens may be mediated by both ERα and ERβ through alterations of gene expression and protein synthesis [40]. In our study, we presumed that the cross talk between nuclear ERβ and GPR30 mediated E2-promoted T24 cell proliferation. Nuclear ERβ mainly performed the genomic action, and GPR30 assisted it to execute this response.

Our data indicated that the cell proliferation promoted by E2 was independent of the EGFR-MAPK pathway, because the inhibition of EGFR or MAPK by specific inhibitors could not abolish E2-stimulation of T24 cell proliferation. Silencing of *ERβ* or *GPR30* did not inhibit ERK activation. GPR30 could transactivate EGFR in response to E2 and then induced ERK phosphorylation [30]. And, according to previous reports, ERβ could also lead to rapid activation of ERK [36, 37]. The activation of ERK was probably not correlated

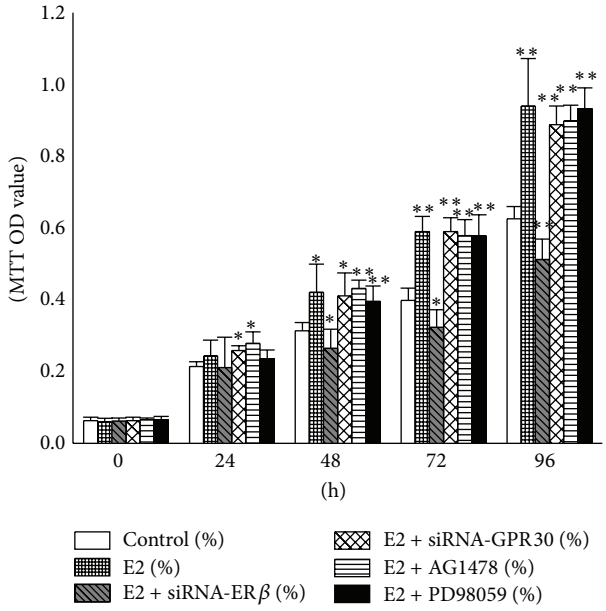

Figure 5: E2 promoted T24 cell proliferation independent of the EGFR-MAPK pathway. T24 cells were pretreated as described in Figure 3. Cells were seeded in 96-well plates at a density of 2×10^3 cells/well and incubated with 10 nM E2. OD values were measured after 0, 24, 48, 72, and 96 h. The values presented here are representative of three independent experiments. $^*P < 0.05$; $^{**}P < 0.01$.

with the cell proliferation in the presence of both nuclear ERβ and GPR30, and the antagonists of the EGFR-MAPK pathway blocked ERK activation but did not inhibit the cell proliferation stimulated by E2. We presumed that this cell proliferation was possibly mediated by nuclear ERβ through other pathways, which will be the focus of our future work. GPR30 probably did not exert the key roles in the cells unless its expression level or the ratio of the two receptors reached a crucial level.

5. Conclusions

Our data provide evidence that E2 could stimulate the proliferation of T24 cells. ERβ and GPR30 receptors can affect EGFR-MAPK/ERK activation, but this stimulation is independent of cell proliferation. ERβ promoted cell proliferation, while GPR30 inhibited cell proliferation. Since the function of GPR30 is weakened or lost, ERβ may play the main roles in response to E2 in T24 cells. This study suggests new insights in the understanding of bladder cancer and indicates that ERβ and GPR30 might be potential new targets for bladder cancer therapy.

Conflict of Interests

The authors declare that there is no conflict of interests regarding the publication of this paper.

Authors' Contribution

Weiren Huang and Yuchen Liu carried out the siRNA design and codrafted the paper with Yuanbin Chen. Yuanbin Chen performed the MTT assays. Zhou Yu carried out the western blot analysis. Hanwei Wu performed the qPCR. Lisha Mou and Qiaoxia Zhang performed the statistical analysis. Ting Long carried out the siRNA transfection. Danian Qin and Yaoting Gui conceived the study and helped to draft the paper. All authors read and approved the final paper. Weiren Huang, Yuanbin Chen, and Yuchen Liu contributed equally to this work.

Acknowledgments

This project was supported by Grants from the National Basic Research Program of China (973 Program) (2014CB745201), the National Natural Science Foundation of China (nos. 81100460, 81270686, and 31271244), Science and Technology Program of Shenzhen (201202055, 201202057), Guangdong Natural Science Foundation (S2012010008200), and Basic Research Program of Shenzhen (JCYJ20120614155650545). The authors acknowledge the graduate students in their lab for their assistance.

References

[1] A. Jemal, F. Bray, M. M. Center, J. Ferlay, E. Ward, and D. Forman, "Global cancer statistics," *Cancer Journal for Clinicians*, vol. 61, no. 2, pp. 69–90, 2011.

[2] H. Miyamoto, Z. Yang, Y.-T. Chen et al., "Promotion of bladder cancer development and progression by androgen receptor signals," *Journal of the National Cancer Institute*, vol. 99, no. 7, pp. 558–568, 2007.

[3] J.-T. Wu, B.-M. Han, S.-Q. Yu, H.-P. Wang, and S.-J. Xia, "Androgen receptor is a potential therapeutic target for bladder cancer," *Urology*, vol. 75, no. 4, pp. 820–827, 2010.

[4] J. Teng, Z.-Y. Wang, D. F. Jarrard, and D. E. Bjorling, "Roles of estrogen receptor α and β in modulating urothelial cell proliferation," *Endocrine-Related Cancer*, vol. 15, no. 1, pp. 351–364, 2008.

[5] S. S. Shen, C. L. Smith, J.-T. Hsieh et al., "Expression of estrogen receptors-α and -β in bladder cancer cell lines and human bladder tumor tissue," *Cancer*, vol. 106, no. 12, pp. 2610–2616, 2006.

[6] B. J. Wolpert, S. Amr, S. Ezzat et al., "Estrogen exposure and bladder cancer risk in Egyptian women," *Maturitas*, vol. 67, no. 4, pp. 353–357, 2010.

[7] C. A. Davis-Dao, K. D. Henderson, J. Sullivan-Halley et al., "Lower risk in parous women suggests that hormonal factors are important in bladder cancer etiology," *Cancer Epidemiology Biomarkers and Prevention*, vol. 20, no. 6, pp. 1156–1170, 2011.

[8] M.-J. Tsai and B. W. O'Malley, "Molecular mechanisms of action of steroid/thyroid receptor superfamily members," *Annual Review of Biochemistry*, vol. 63, pp. 451–486, 1994.

[9] A. P. Govind and R. V. Thampan, "Membrane associated estrogen receptors and related proteins: localization at the plasma membrane and the endoplasmic reticulum," *Molecular and Cellular Biochemistry*, vol. 253, no. 1-2, pp. 233–240, 2003.

[10] C. Bolenz, Y. Lotan, R. Ashfaq, and S. F. Shariat, "Estrogen and progesterone hormonal receptor expression in urothelial

carcinoma of the bladder," *European Urology*, vol. 56, no. 6, pp. 1093–1095, 2009.

[11] P. Thomas and J. Dong, "Binding and activation of the seven-transmembrane estrogen receptor GPR30 by environmental estrogens: a potential novel mechanism of endocrine disruption," *The Journal of Steroid Biochemistry and Molecular Biology*, vol. 102, no. 1–5, pp. 175–179, 2006.

[12] E. J. Filardo, J. A. Quinn, K. I. Bland, and A. R. Frackelton Jr., "Estrogen-induced activation of Erk-1 and Erk-2 requires the G protein-coupled receptor homolog, GPR30, and occurs via trans-activation of the epidermal growth factor receptor through release of HB-EGF," *Molecular Endocrinology*, vol. 14, no. 10, pp. 1649–1660, 2000.

[13] C. M. Revankar, D. F. Cimino, L. A. Sklar, J. B. Arterburn, and E. R. Prossnitz, "A transmembrane intracellular estrogen receptor mediates rapid cell signaling," *Science*, vol. 307, no. 5715, pp. 1625–1630, 2005.

[14] S. Dong, S. Terasaka, and R. Kiyama, "Bisphenol A induces a rapid activation of Erk1/2 through GPR30 in human breast cancer cells," *Environmental Pollution*, vol. 159, no. 1, pp. 212–218, 2011.

[15] L. Albanito, A. Madeo, R. Lappano et al., "G protein-coupled receptor 30 (GPR30) mediates gene expression changes and growth response to 17β-estradiol and selective GPR30 ligand G-1 in ovarian cancer cells," *Cancer Research*, vol. 67, no. 4, pp. 1859–1866, 2007.

[16] Q. K. Y. Chan, H.-M. Lam, C.-F. Ng et al., "Activation of GPR30 inhibits the growth of prostate cancer cells through sustained activation of Erk1/2, c-jun/c-fos-dependent upregulation of p21, and induction of G2 cell-cycle arrest," *Cell Death and Differentiation*, vol. 17, no. 9, pp. 1511–1523, 2010.

[17] N. Chevalier, A. Bouskine, and P. Fenichel, "Role of GPER/GPR30 in tumoral testicular germ cells proliferation," *Cancer Biology and Therapy*, vol. 12, no. 1, pp. 2–3, 2011.

[18] C. Tuygun, D. Kankaya, A. Imamoglu et al., "Sex-specific hormone receptors in urothelial carcinomas of the human urinary bladder: a comparative analysis of clinicopathological features and survival outcomes according to receptor expression," *Urologic Oncology: Seminars and Original Investigations*, vol. 29, no. 1, pp. 43–51, 2011.

[19] J. Teng, Z. Y. Wang, E. R. Prossnitz, and D. E. Bjorling, "The G protein-coupled receptor GPR30 inhibits human urothelial cell proliferation," *Endocrinology*, vol. 149, no. 8, pp. 4024–4034, 2008.

[20] J. E. Castelao, J.-M. Yuan, P. L. Skipper et al., "Gender- and smoking- related bladder cancer risk," *Journal of the National Cancer Institute*, vol. 93, no. 7, pp. 538–545, 2001.

[21] N. N. Bulayeva and C. S. Watson, "Xenoestrogen-induced ERK-1 and ERK-2 activation via multiple membrane-initiated signaling pathways," *Environmental Health Perspectives*, vol. 112, no. 15, pp. 1481–1487, 2001.

[22] M. Maggiolini, A. Vivacqua, G. Fasanella et al., "The G protein-coupled receptor GPR30 Mediates c-fos up-regulation by 17β-estradiol and phytoestrogens in breast cancer cells," *Journal of Biological Chemistry*, vol. 279, no. 26, pp. 27008–27016, 2004.

[23] D. W. Singleton, Y. Feng, C. J. Burd, and S. A. Khan, "Nongenomic activity and subsequent c-fos induction by estrogen receptor ligands are not sufficient to promote deoxyribonucleic acid synthesis in human endometrial adenocarcinoma cells," *Endocrinology*, vol. 144, no. 1, pp. 121–128, 2003.

[24] E. Shaulian and M. Karin, "AP-1 as a regulator of cell life and death," *Nature Cell Biology*, vol. 4, no. 5, pp. E131–E136, 2002.

[25] D. M. Hockenbery, "Bcl-2, a novel regulator of cell death," *BioEssays*, vol. 17, no. 7, pp. 631–638, 1995.

[26] G. Kroemer, "The proto-oncogene Bcl-2 and its role in regulating apoptosis," *Nature Medicine*, vol. 3, no. 6, pp. 614–620, 1997.

[27] A. M. Miermont, A. R. Parrish, and P. A. Furth, "Role of ERα in the differential response of Stat5a loss in susceptibility to mammary preneoplasia and DMBA-induced carcinogenesis," *Carcinogenesis*, vol. 31, no. 6, pp. 1124–1131, 2010.

[28] K. Yoshidome, M. A. Shibata, C. Couldrey, K. S. Korach, and J. E. Green, "Estrogen promotes mammary tumor development in C3(1)/SV40 large T-antigen transgenic mice: paradoxical loss of estrogen receptoralpha expression during tumor progression," *Cancer Research*, vol. 60, no. 24, pp. 6901–6910, 2000.

[29] S. J. Ellem and G. P. Risbridger, "Treating prostate cancer: a rationale for targeting local oestrogens," *Nature Reviews Cancer*, vol. 7, no. 8, pp. 621–627, 2007.

[30] L. A. Helguero, M. H. Faulds, J.-Å. Gustafsson, and L.-A. Haldosén, "Estrogen receptors alfa (ERα) and beta (ERβ) differentially regulate proliferation and apoptosis of the normal murine mammary epithelial cell line HC11," *Oncogene*, vol. 24, no. 44, pp. 6605–6616, 2005.

[31] J. Yang, Y. Wang, Y. Gao, J. Shao, X. J. Zhang, and Z. Yao, "Reciprocal regulation of 17β-estradiol, interleukin-6 and interleukin-8 during growth and progression of epithelial ovarian cancer," *Cytokine*, vol. 46, no. 3, pp. 382–391, 2009.

[32] B. Schleipen, T. Hertrampf, K. H. Fritzemeier et al., "ERβ-specific agonists and genistein inhibit proliferation and induce apoptosis in the large and small intestine," *Carcinogenesis*, vol. 32, no. 11, pp. 1675–1683, 2011.

[33] G. Pinton, W. Thomas, P. Bellini et al., "Estrogen receptor β exerts tumor repressive functions in human malignant pleural mesothelioma via EGFR inactivation and affects response to Gefitinib," *PLoS ONE*, vol. 5, no. 11, Article ID e14110, 2010.

[34] A. Vivacqua, D. Bonofiglio, L. Albanito et al., "17β-Estradiol, genistein, and 4-hydroxytamoxifen induce the proliferation of thyroid cancer cells through the G protein-coupled receptor GPR30," *Molecular Pharmacology*, vol. 70, no. 4, pp. 1414–1423, 2006.

[35] H. O. Smith, H. Arias-Pulido, D. Y. Kuo et al., "GPR30 predicts poor survival for ovarian cancer," *Gynecologic Oncology*, vol. 114, no. 3, pp. 465–471, 2009.

[36] E. J. Filardo and P. Thomas, "GPR30: a seven-transmembrane-spanning estrogen receptor that triggers EGF release," *Trends in Endocrinology & Metabolism*, vol. 16, no. 8, pp. 362–367, 2005.

[37] C. S. Watson, R. A. Alyea, Y.-J. Jeng, and M. Y. Kochukov, "Nongenomic actions of low concentration estrogens and xenoestrogens on multiple tissues," *Molecular and Cellular Endocrinology*, vol. 274, no. 1-2, pp. 1–7, 2007.

[38] J.-H. Kim, I.-Y. Jeong, Y. Lim, Y. H. Lee, and S. Y. Shin, "Estrogen receptor β stimulates Egr-1 transcription via MEK1/Erk/Elk-1 cascade in C6 glioma cells," *BMB Reports*, vol. 44, no. 7, pp. 452–457, 2011.

[39] C. J. Sherr and J. M. Roberts, "Living with or without cyclins and cyclin-dependent kinases," *Genes and Development*, vol. 18, no. 22, pp. 2699–2711, 2004.

[40] T. Barkhem, S. Nilsson, and J.-Å. Gustafsson, "Molecular mechanisms, physiological consequences and pharmacological implications of estrogen receptor action," *American Journal of PharmacoGenomics*, vol. 4, no. 1, pp. 19–28, 2004.

Hindawi Publishing Corporation
BioMed Research International
Volume 2015, Article ID 827462, 10 pages
http://dx.doi.org/10.1155/2015/827462

Research Article

Cosuppression of Sprouty and Sprouty-Related Negative Regulators of FGF Signalling in Prostate Cancer: A Working Hypothesis

Stephen J. Assinder,[1] Daniella Beniamen,[1] and Frank J. Lovicu[2]

[1]*Disciplines of Physiology, School of Medical Sciences and Bosch Institute, University of Sydney, Sydney, NSW 2006, Australia*
[2]*Anatomy and Histology, School of Medical Sciences and Bosch Institute, University of Sydney, Sydney, NSW 2006, Australia*

Correspondence should be addressed to Stephen J. Assinder; stephen.assinder@sydney.edu.au

Received 11 July 2014; Accepted 14 November 2014

Academic Editor: Tarunveer S. Ahluwalia

Deregulation of FGF receptor tyrosine kinase (RTK) signalling is common in prostate cancer. Normally, to moderate RTK signalling, induction of Sprouty (SPRY) and Sprouty-related (SPRED) antagonists occurs. Whilst decreased SPRY and SPRED has been described in some cancers, their role in prostate cancer is poorly understood. Therefore, we hypothesise that due to the need for tight regulation of RTK signalling, SPRY and SPRED negative regulators provide a degree of redundancy which ensures that a suppression of one or more family member does not lead to disease. Contrary to this, our analyses of prostates from 24-week-old *Spry1*- or *Spry2*-deficientmice, either *hemizygous* (+/−) or *homozygous* (−/−) for the null allele, revealed a significantly greater incidence of PIN compared to wild-type littermates. We further investigated redundancy of negative regulators in the clinical setting in a preliminary analysis of Gene Expression Omnibus and Oncomine human prostate cancer datasets. Consistent with our hypothesis, in two datasets analysed a significant cosuppression of SPRYs and SPREDs is evident. These findings demonstrate the importance of negative regulators of receptor tyrosine signalling, such as Spry, in the clinical setting, and highlight their importance for future pharmacopeia.

1. Introduction

Worldwide, prostate cancer accounts for one death every 4 minutes. It is the most commonly diagnosed cancer and the second leading cause of cancer death in men. The economic impact of prostate cancer is substantial. In 2010, prostate cancer is estimated to have cost AU$204,136,795 in Australia alone [1]. With estimated increases in the elderly population and increased survival rates [1], the burden of this disease will escalate significantly. The limited treatment options available result in significant morbidity to the individual. Side effects include lost libido, impotence, and incontinence. Most cases of advanced prostate cancer become resistant to treatment and inevitably result in death. In their analysis of the economic burden of prostate cancer, Roehrborn and Black [1] conclude that "Costs of prostate cancer treatment are only likely to increase in the future unless new strategies are devised to reduce the number of diagnoses and/or focus treatment where it is clinically most appropriate." There is an urgent need for (i) better treatments of prostate cancer; (ii) prognostic markers that inform patient care; and (iii) individualised therapies. Essential to the discovery of novel pharmacological agents for individualised cancer therapy is an understanding of how disruption of intracellular signalling pathways leads to the formation of cancer.

Hyperactivation of FGF signalling is evident in 80% of prostate cancers [2]. Several mechanisms result in hyperactivation, including increased FGF expression that correlates with increased Gleason score [3], increased FGF availability from extracellular matrix [4], and sensitisation to FGF due to increased receptor levels [4, 5]. Indeed, in a prostate epithelium-specific FGFR1 knock-in mouse model, activation of expression results in adenocarcinoma [6], whilst in the clinical setting, a single nucleotide polymorphism in the

FGFR4 gene is associated with poor prognosis of prostate cancer [7, 8].

Normally, increased FGF signalling is counteracted by feedback inhibitors. Sprouty was one of the first negative feedback regulators of the FGF pathway to be identified, initially shown to be important for regulation of FGF-induced tracheal branching in *Drosophila* [9, 10]. Mammalian Sproutys are expressed in a highly restricted pattern that correlate with FGF signalling [11]. Spry is recognised in many physiological and developmental processes as an antagonist of receptor tyrosine kinase (RTK) signalling. Its overexpression mimics the functional loss of RTKs, including those activated by FGF [12, 13]. Overexpression of *Spry* in the developing chick limb bud inhibits cell differentiation, displaying a comparable phenotype to that reported in FGF null mutants [14]. Consistent with this, transfected cells overexpressing *Spry* have a reduced responsiveness to growth factors [15]. The exact nature of the inhibitory activity of Spry is unclear. Specific functions are exerted through multiple mechanisms, dependent on the growth factor stimulation and/or cell type [16]. For example, Spry can function as a decoy site, binding intracellular docking proteins, preventing the activation of intracellular signalling molecules, such as the MAPK/ERK1/2 pathway [17, 18]. Spry is selective for ERK1/2 signalling, with members exhibiting slightly different activities as they interact with different signalling proteins [18]. Each Spry protein has a conserved tyrosine residue (Tyr55/*Spry2*, Tyr53/*Spry1* and *Spry4*) that functions as a binding site for the SH2 domain of Grb2 [15]. In the case of FGF signalling, phosphorylated Tyr55 of Spry2 associates with Grb2, blocking the interaction of Grb2 with the FGF receptor adaptor molecule, FRS2, which bridges the FGF receptor to the ERK/MAPK pathway [18]. Hence, Spry can uncouple FGF-induced signal transduction leading to a block in ERK1/2 activation (Figure 1).

Spreds are also negative regulators of ERK/MAPK activation. Spred proteins primarily consist of three domains that (i) bind proline-rich sequences targeting Spreds to specific cellular sites where they function; (ii) allow tyrosine kinase interaction; and (iii) interact with cRaf to suppress ERK phosphorylation and negate FGF signalling (Figure 1).

Loss of SPRY has been reported in breast [19], liver [20], and lung [21] cancers. Functional studies have shown that suppression of SPRYs promotes a malignant phenotype in an *in vitro* model of breast cancer [19]. Direct injection of a dominant negative SPRY2 into mouse livers, with overexpression of β-catenin, induced neoplastic transformation [22]. Ectopic expression of *SPRY2* in cell lines derived from non-small cell lung carcinoma tissues significantly reduced proliferation and tumour formation of subsequent xenografts [21]. Lung tumourigenesis is unable to be induced by the carcinogen urethane in *SPRY2* overexpressing transgenic mice [23]. Similarly, loss of SPREDs in cancer is also evident. In hepatocellular carcinoma, both *SPRED1* and *2* are downregulated, with an associated increase in invasion and metastasis [15, 24].

The role of SPRYs and SPREDs in prostate cancer is, however, poorly defined. There are limited reports of SPRY1 and SPRY2 suppression in clinical samples of prostate cancer

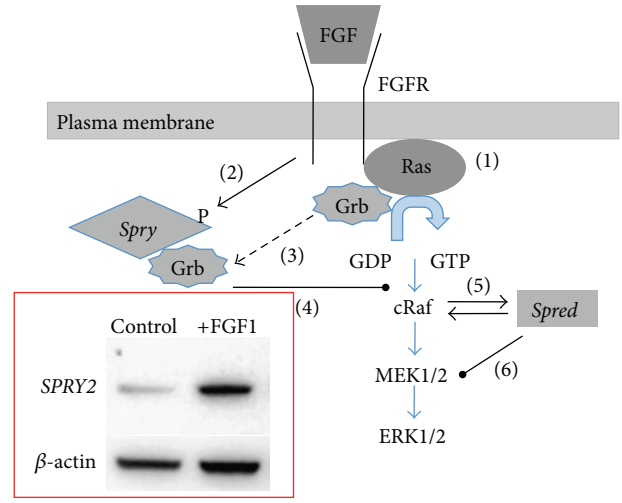

Figure 1: A stepwise overview of the mechanisms of sprouty and SPRED negative regulation of FGF signalling. Activation of the tyrosine kinase receptor (FGFR) results in (1) phosphorylation of Ras and subsequent activation of the MAPK signalling cascade (blue arrows); (2) FGFR activation also results in the direct activation by of Sprys by phosphorylation and increased expression via Ras-MAPK pathway (see inset: western blot of increased SPRY2 following FGF1 (10 ng·mL^{-1}) treatment of normal prostate epithelial cells); subsequent sequestration of the FGFR signalling molecule Grb (3) by pSPRY results in (4) suppression of FGF signalling. Similarly, activation of FGFR results in Spred heterodimerisation and subsequent complexing with Raf (5) resulting in inhibition of MEK activation (6).

[25, 26]. In support of a role for Sprouty as a tumour suppressor, proliferation of prostate cancer cell lines (LNCaP and PC3) is suppressed by *SPRY1* overexpression [25]. Recently, it was demonstrated that concomitant prostate-specific deletion of *Spry1* and *Spry2* in mice resulted in prostatic intraepithelial neoplasia (PIN), while deletion of either *Spry 1* or *Spry 2* in hemizygous *Pten* null mice resulted in invasive carcinoma [27]. Only one report exists with regard to SPREDs in prostate cancer, describing evidence for a loss of *SPRED2* expression in high Gleason grade lesions [28]. Given this, we hypothesise that, due to the need for tight regulation of receptor tyrosine kinase signalling, having a family of SPRY and SPRED negative regulators provides a degree of redundancy where loss of one family member is not significant to disease formation. Until now, this has not been considered in the context of prostate cancer. Hence, in this study, we aimed to determine whether deletion of either *Spry 1 or Spry 2* alone could induce neoplastic changes in the mouse prostate, whilst also assessing public gene expression datasets to test the hypothesis that cosuppression of SPRYs and SPREDs is associated with aggressive prostate cancers.

2. Material and Methods

2.1. Animals and Tissues. This study was approved by the University of Sydney Animal Ethics Committee under protocol number K03/5-2012/3/5763 and the tissue sharing scheme.

Inbred male mice with germline deletions of either *Spry1* [29] or *Spry2* [30] were housed under controlled temperature and 12 hr light/dark regime with food and water provided *ad libitum*. Mice with either homozygous allelic deletions of *Spry1* ($Spry1^{-/-}$; $n = 5$) or *Spry2* ($Spry2^{-/-}$; $n = 2$) or hemizygous allelic deletions of *Spry1* ($Spry1^{+/-}$; $n = 5$) or *Spry2* ($Spry2^{+/-}$; $n = 5$) and their wild-type (WT; $n = 5$) littermates were euthanized at 24 weeks postpartum by CO_2 asphyxiation. Ventral prostates were removed and fixed in neutral-buffered formalin (NBF: 25 mmol·L^{-1} NaH_2PO_4; 50 mmol·L^{-1} Na_2HPO_4; 4% (w/v) formaldehyde). Following fixation, tissue samples were dehydrated and embedded in paraffin wax.

2.2. Histological Examination. Five μm thin sections were cut and stained with haematoxylin and eosin. Stained tissue sections were observed by bright field microscopy by an observer blinded to the genotype. Tissue sections were assessed for normal acinar architecture and pathologies of low grade prostatic intraepithelial neoplasia (LGPIN) and high grade prostatic intraepithelial neoplasia (HGPIN) according to the Bar Harbor Classification of Mouse Prostate Pathologies [31]. At least 200 acini were scored for wild type, hemizygous, and homozygous prostates. The incidence of normal, LGPIN, and HGPIN acini was determined as a percentage of the total number of acini scored for each genotype and differences were determined by $R \times C$ test of independence and *post hoc* Pearson chi-square test.

2.3. Determination of Proliferative Index. Five μm thin sections were assayed for immunoreactive proliferative cell nuclear antigen (PCNA) as a marker of proliferating prostatic epithelium. Briefly, sections were dewaxed in HistoChoice (Sigma-Aldrich) and rehydrated through graded alcohol before washing in phosphate buffered saline (PBS; pH 7.4) 3 times for 5 min each. High temperature antigen retrieval was then performed by immersion in preheated citrate/Tween-20 buffer (10 mMol·L^{-1} $Na_3C_6H_5O_7$; 0.05% (v/v) Tween-20; pH 6.0) and microwaving twice for 5 min at high power (600 W). Sections were left to cool for 35 min before washing 3 times for 5 mins each in PBS. A PCNA staining kit (Zymed Laboratories, Inc., South San Francisco, CA) was then employed according to manufacturers' instructions. In negative controls, the primary monoclonal anti-mouse PCNA antibody was replaced with 10% (v/v) normal mouse serum (Sigma-Aldrich, St Louis, MO, USA) or PBS (no antibody). As a positive control, 5 μm thin sections of mouse testes were included. Following chromogen formation, sections were counterstained with haematoxylin, dehydrated, and coverslipped with dibutyl phthalate xylene. Sections were viewed by bright field microscopy at high magnification under oil immersion. The number of total and immunopositive nuclei was counted in at least 4 fields of view for each animal by an observer blinded to the genotype. Proliferative index was determined as the proportion of PCNA-positive nuclei and a mean index determined. Any significant differences between mean proliferative indices for each of the *Spry1* and *Spry2* genotypes were determined by one-way ANOVA and Tukey's HSD *post hoc* test.

2.4. SPRY and SPRED Gene Expression Analysis of Human Prostate Cancer cDNA Libraries. Two separate gene expression datasets lodged at the Gene Expression Omnibus, NCBI gene expression and hybridisation array data repository (http://www.ncbi.nlm.nih.gov/geo/), and on the Oncomine database (http://www.oncomine.org/), were assessed for *SPRY1, SPRY2, SPRED1, and SPRED2* expression. The GEO dataset (GDS1439: [32]) compares samples of benign prostatic hyperplasia (BPH) tissue with clinically localised primary prostate cancer tissue and with metastatic prostate cancer. The Oncomine dataset (Vanaja_Prostate; [33]) compares normal prostate with clinically localised primary prostate cancer tissue and with metastatic prostate cancer. Each gene was analysed for relative expression according to database output score. Coexpression was compared according to pathology and sum of ranks, where each gene's expression was assigned a rank score (where greater rank score indicates greater expression). Ranks of all 4 genes for each sample were summed and the sum of ranks was analysed for association by rank correlation.

3. Results

3.1. Single Germline Deletions of Either Spry1 Or Spry2 Result in PIN. Histological analysis of prostates from $Spry1^{+/-}$ or $Spry1^{-/-}$ mice determined the presence of normal acini, as well as acini displaying pathologies consistent with LGPIN and HGPIN (Figure 2). All $Spry1^{+/-}$ mice assayed had PIN pathology, whilst four of the 5 $Spry1^{-/-}$ mice were determined as having PIN. No pathology other than ductal hyperplasia was apparent in wild-type mice prostates. The incidence of PIN pathologies, expressed as a percentage of all acini scored, was 29% for both genotypes and significantly greater than in wild-type littermates ($P < 0.0001$). Indeed, both $Spry1^{-/-}$ (14%; $P < 0.0001$) and $Spry1^{-/-}$ (25%; $P < 0.0001$) had significantly greater incidence of LGPIN than wild-type mice, where $Spry1^{-/-}$ prostates displayed significantly greater occurrence than $Spry1^{-/-}$ ($P < 0.01$). The incidence of HGPIN (15%) was significantly greater in the prostates of $Spry1^{-/-}$ mice than in either wild-type ($P < 0.0001$) or $Spry1^{-/-}$ ($P < 0.05$) mice. Whilst 5% of $Spry1^{-/-}$ acini were determined to have HGPIN, this was not significant when compared with wild type.

Similarly, all prostates from $Spry2^{+/-}$ and $Spry2^{-/-}$ mice displayed pathologies of normal, LGPIN, and HGPIN (Figure 3). The sum of the incidences for these pathologies, expressed as a percentage of all acini scored, was 33% and 46% for $Spry2^{+/-}$ and $Spry2^{-/-}$, respectively, significantly greater ($P < 0.001$) than for prostates of wild-type mice that did not exhibit PIN. There was a significantly greater proportion of acini with LGPIN in both $Spry2^{+/-}$ (26%; $P < 0.0001$) and $Spry2^{-/-}$ (21%; $P < 0.0001$) prostates than in wild-type mice. Whilst the incidence of high grade PIN in the prostates

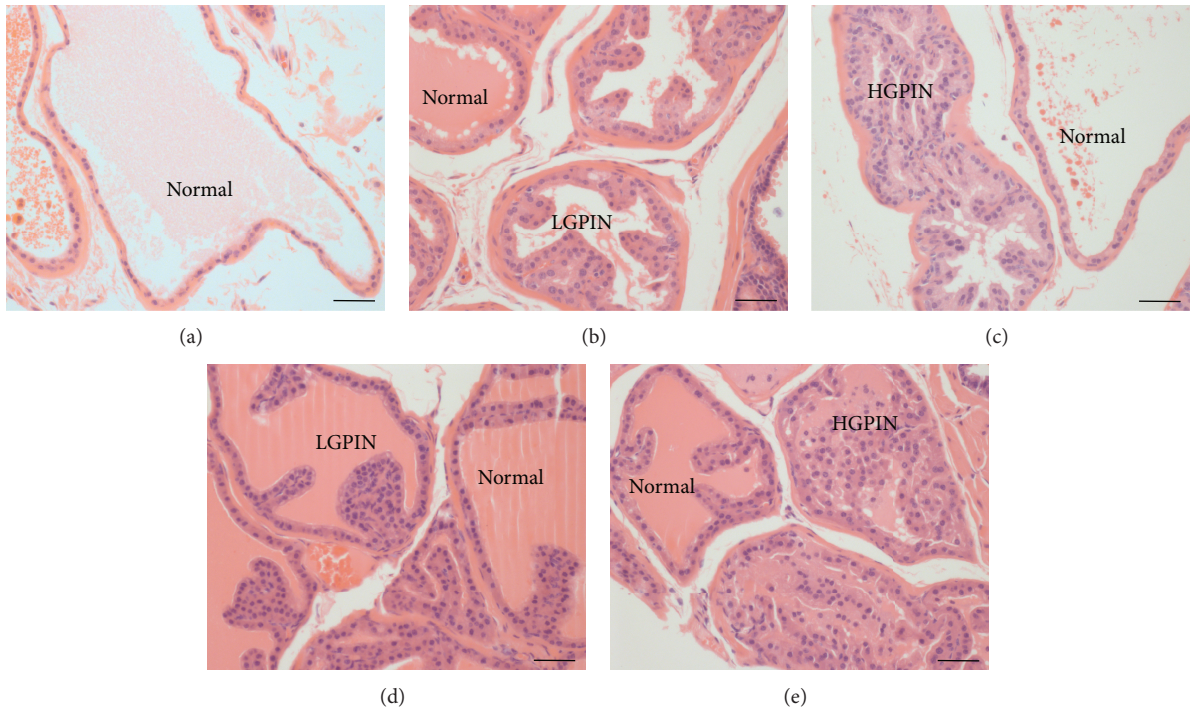

Figure 2: Histology of prostates from 24-week-old wild-type (a), hemizygous (b, c), and homozygous (d, e) null *Spry1* mice. Five μm thin sections were stained with haematoxylin and eosin and assessed for normal acinar architecture and pathologies of low grade prostatic intraepithelial neoplasia (LGPIN) and high grade prostatic intraepithelial neoplasia (HGPIN) according to the Bar Harbor Classification of Mouse Prostate Pathologies [31]. Scale bar = 50 μm.

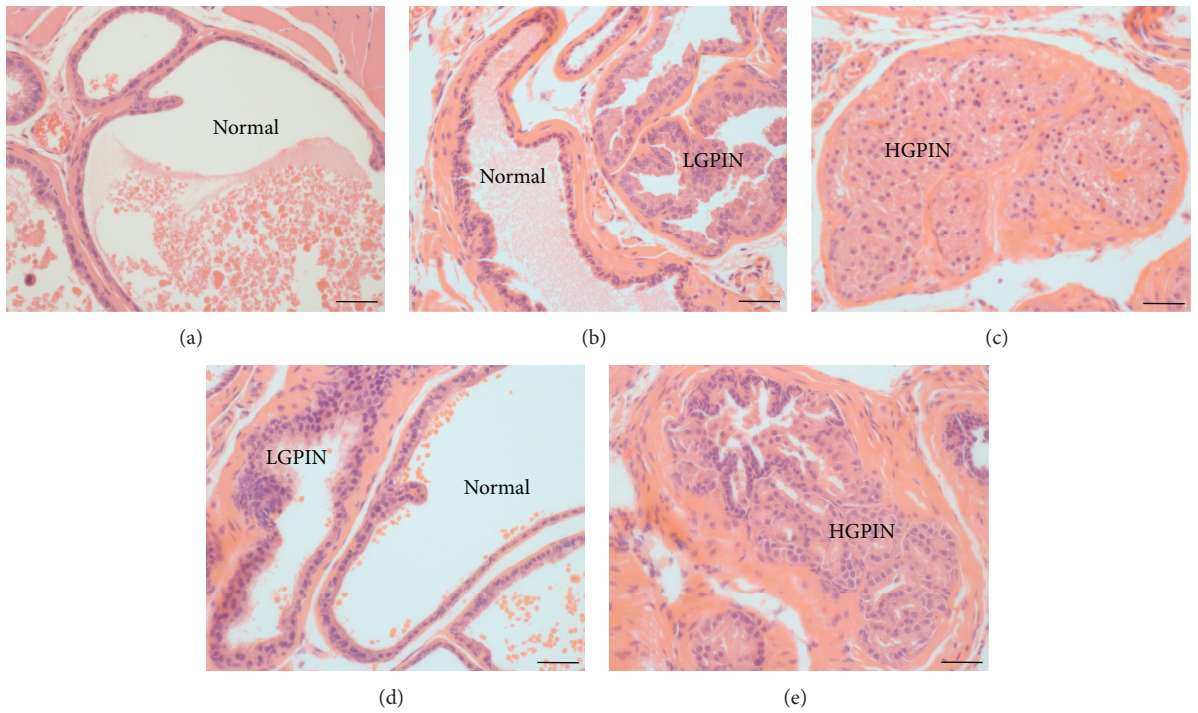

Figure 3: Histology of prostates from 24-week-old wild-type (a), hemizygous (b, c), and homozygous (d, e) null *Spry2* mice. Five μm thin sections were stained with haematoxylin and eosin and assessed for normal acinar architecture and pathologies of low grade prostatic intraepithelial neoplasia (LGPIN) and high grade prostatic intraepithelial neoplasia (HGPIN) according to the Bar Harbor Classification of Mouse Prostate Pathologies [31]. Scale bar = 50 μm.

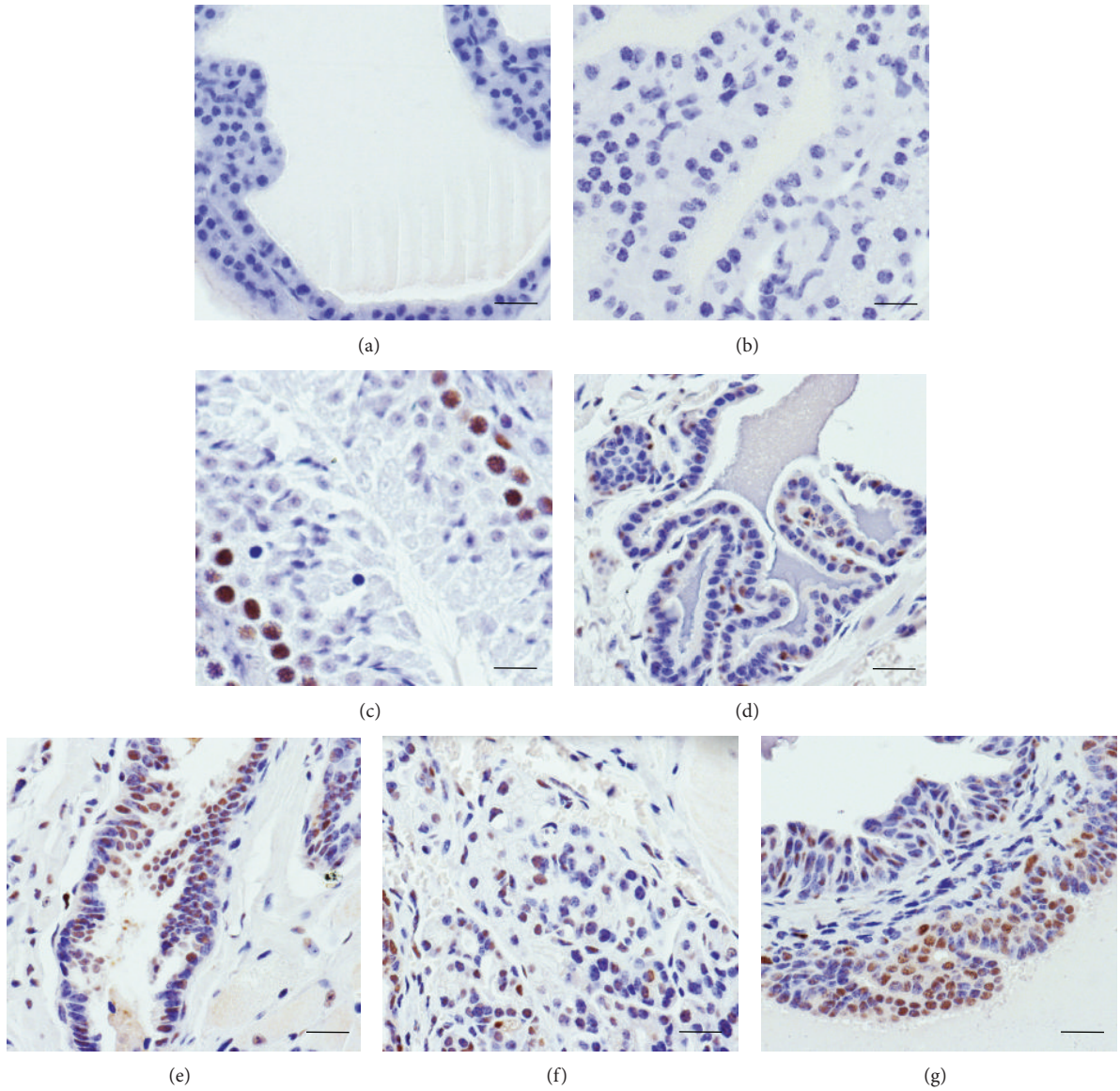

Figure 4: Immunocytochemical analysis of proliferating cell nuclear antigen (PCNA) protein in prostates of hemizygous and homozygous null *Spry* mice. Representative 5 μm thin sections of (a) prostate, whole serum negative control; (b) prostate, no primary antibody negative control; (c) positive control of mouse testis showing immunopositive (brown) proliferating spermatogonia but immunonegative haematoxylin counterstained (blue) developing spermatids; immunopositive nuclei in (d) $Spry1^{+/-}$, (e) $Spry1^{-/-}$, (f) $Spry2^{+/-}$, and (g) $Spry2^{-/-}$ prostates. Scale bar = 25 μm.

of $Spry2^{-/-}$ mice (25%) was significantly greater than in $Spry2^{+/-}$ mice ($P < 0.01$) and wild-type mice ($P < 0.0001$), the incidence of HGPIN in $Spry2^{+/-}$ (7%) was not significant when compared with wild type.

3.2. Single Germline Deletions of Either Spry1 Or Spry2 Increase Prostatic Epithelial Cell Proliferation. Consistent with an increased incidence of PIN pathologies in *Spry1 and Spry2* hemizygous and homozygous mice was an increase in the number of PCNA-immunopositive ductal epithelial cells in the prostates of these mice. Whilst all animals exhibited proliferating cells, as determined by the presence of PCNA immunopositive nuclei (Figure 4), there were significantly ($P < 0.001$) greater proportions of immunopositive prostatic epithelia in $Spry1^{+/-}$ (26 ± 3%); $Spry1^{-/-}$ (31 ± 2%); $Spry2^{+/-}$ (16 ± 2%); and $Spry2^{-/-}$ (39 ± 3%) when compared with wild type (3.1 ± 0.5%). There was, however, no significant difference between the proportions of PCNA-immunopositive nuclei of $Spry1^{+/-}$ and $Spry1^{-/-}$ prostate epithelium. In contrast, $Spry2^{-/-}$ mice prostates had a significantly ($P < 0.001$) greater number of PCNA-immunopositive epithelia than $Spry2^{+/-}$ prostates.

3.3. Cosuppression of SPRY and SPRED Gene Expression Occurs in Human Prostate Cancers. No significant differences in *SPRY1* expression between noncancerous (benign

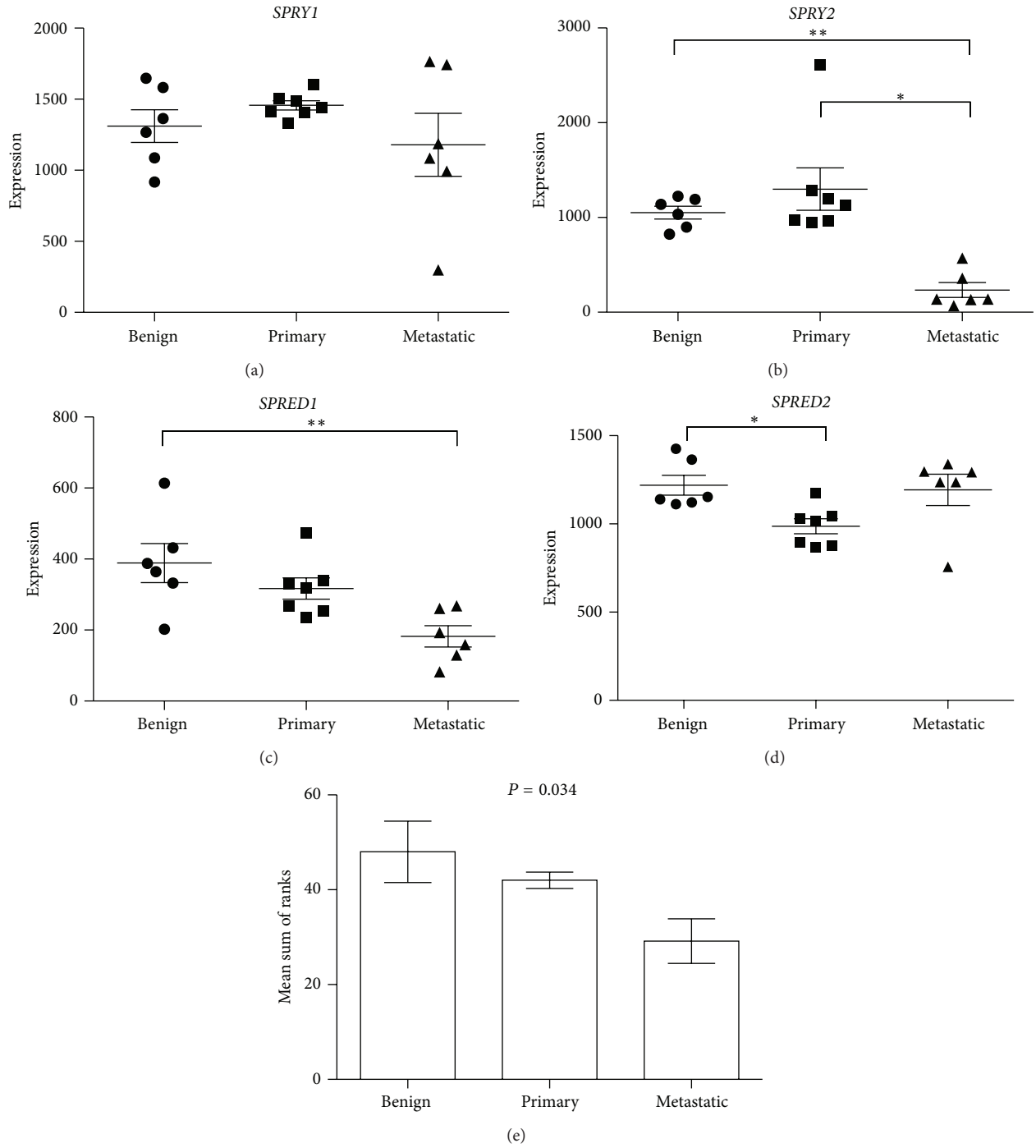

Figure 5: Analysis of (a) *SPRY1*, (b) *SPRY2*, (c) *SPRED1*, and (d) *SPRED2* gene expression in Affymetrix gene chip hybridisation of mRNA (GEO dataset GDS1439; [33]) from benign prostatic hyperplasia (benign, $n = 6$), primary prostate carcinoma tissue (primary, $n = 7$), and metastatic prostate cancer (metastatic, $n = 6$). Individual data points are given with means (±sem) indicated by bar and whiskers of the MAS5-calculated signal intensity where the greater intensity indicates greater expression. Significant differences between means determined by one way ANOVA and Tukey's HSD *post hoc* test, where $^{*}P < 0.05$ and $^{**}P < 0.01$. (e) Analysis of mean (±sem) sums of each gene rank score for individual samples, according to pathology, for association by rank correlation.

prostatic hyperplasia, Figure 5(a); normal, Figure 6(a)) and prostate cancer tissues were evident. In contrast, both datasets displayed significantly decreased *SPRY2* expression, with metastatic tissues having significantly suppressed expression compared with benign and primary carcinoma (Figure 5(b)) and with normal tissue (Figure 6(b)), respectively. *SPRED1* expression was significantly reduced in metastatic prostate cancers in the Varambally Gene Expression Omnibus dataset

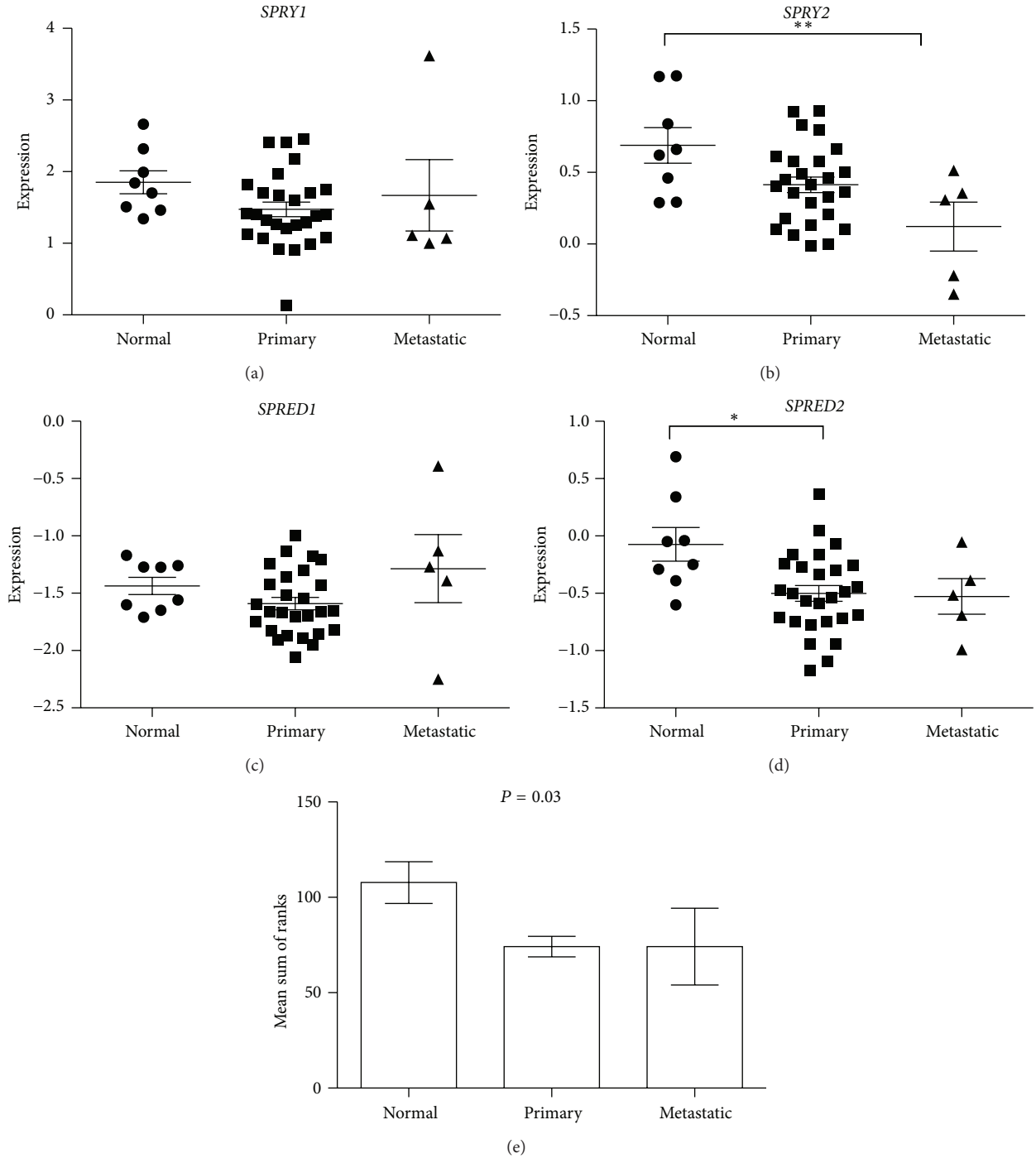

Figure 6: Analysis of (a) *SPRY1*, (b) *SPRY2*, (c) *SPRED1*, and (d) *SPRED2* gene expression in Oncomine dataset Vanaja_Prostate [34] from normal human prostate tissue (normal, $n = 8$), primary prostate carcinoma tissue (primary, $n = 27$), and metastatic prostate cancer (metastatic, $n = 5$) where individual data points are given with means (±sem) indicated by bar and whiskers of the log 2 median-centered signal intensity where the greater intensity indicates greater expression. Significant differences between means determined by one way ANOVA and Tukey's HSD *post hoc* test, where $^{*}P < 0.05$ and $^{**}P < 0.01$. (e) Analysis of mean (±sem) sums of each gene rank score for individual samples, according to pathology, for association by rank correlation.

when compared with benign tissue (Figure 5(c)) but no significant differences in *SPRED1* expression were evident between any tissue sites of the Vanaja dataset (Figure 6(c)). *SPRED2* was significantly decreased in primary prostate carcinomas in both datasets (Figures 5(d) and 6(d)). Analysis of coexpression by comparing the sum of rank scores of each gene for each individual sample in a dataset demonstrated a significant correlation for both datasets, where a decrease in

rank score was associated with disease state (Figures 5(e) and 6(e)).

4. Discussion

A decrease in *SPRY* expression has been reported in cancers including those of the prostate [25, 26] and breast [19]. Their role in antagonising receptor tyrosine kinase signalling and an expanding list of tumours in which they are apparently downregulated has led to them being considered as tumour suppressors. Further evidence of their role as important tumour suppressors comes from a recent study of *Spry1* null mice thyroids which demonstrated that Sprouty can act, independently of the ERK pathway, in hyperproliferative cells to induce senescence via NFκB signalling [34].

The results presented here provide further evidence to support Sprouty as a tumour suppressor. Surprisingly, we have demonstrated that single germline deletions of either *Spry1* or *Spry2* result in the development of prostatic intraepithelial neoplasias, the generally accepted precursor of prostate cancer [35]. Moreover, this was associated with significant increases in proliferative cells, as determined by PCNA analysis in both hemi- and homozygous Spry null mice. These findings were contrary to our original hypothesis that single gene deletions would not result in significant pathologies, based on the study of Schutzman and Martin [27]. It is important to note that in that study a prostate-specific deletion of both *Spry1* and *Spry2* induced LGPIN only. This is in stark contrast to our study where hemizygous mice had HGPIN. It is unclear as to why this difference, and we cannot discount off target effects in our germline deletions that affect other cell types that are important in the development of prostate cancer, such as neuroendocrine cells or stromal cells. These cell types are important in the development of prostate cancer, not least the reactive stroma. A feature of reactive stroma is the induced myodifferentiation of fibroblasts associated with TGF-β [36]. Deregulation of TGF-β signalling in the stroma is known to be associated with prostate cancer development. Suppression of TGF-β signalling in mouse prostatic stroma has been shown to induce PIN formation, whilst hyperstimulation of stromal cells by TGF-β induces tumorigenesis [37]. Both Spry1 and Spry2 have recently been shown to be negative regulators of TGF-β signalling [38]. It is likely then that reduced sprouty in stroma may result in increased TGF-β signalling. As TGF-β stimulates bFGF secretion by stroma [39], we suggest that in our model there is a compound effect of greater FGF present, with decreased attenuation of signalling, resulting in the formation of PIN in both $Spry1^{+/-}$ and $Spry2^{+/-}$ prostates.

Whilst prostates of $Spry1^{-/-}$ mice had a similar total PIN incidence as $Spry1^{+/-}$ mice, they displayed a significantly lower incidence of HGPIN. This suggests a degree of redundancy in the sprouty tumour suppressors, with Spry2 possibly being compensatory in this context. This might also explain why PIN pathology was not seen in one of the $Spry1^{-/-}$ mice. As all $Spry1^{+/-}$ mice assessed had PIN pathology, it is possible that a dose effect is seen such that *Spry2* is increased in *Spry1* null mice to compensate where *Spry2* is the most important of the sprouty family negative regulators of FGF signalling. That all $Spry2^{+/-}$ and $Spry2^{-/-}$ prostates assessed displayed PIN pathology with $Spry2^{-/-}$ mice prostates having the greatest total PIN incidence, the highest levels of HGPIN, and the most proliferative epithelial cells than all other mice studied supports this. Indeed, concomitant loss of Spry1 and Spry2 function results in tumorigenesis [27] with significant PIN and invasive tumours only induced by codeletion of *Spry1* and *Spry2* in haploinsufficient phosphatase and tensin (Pten) mice. Significantly, *Pten* null mice develop prostate cancer [40]. PTEN activity is necessary for the activity of SPRY2 in HeLa cells where silencing PTEN diminished SPRY2-mediated inhibition of cell proliferation [41]. Overexpression of *SPRY2* increased total PTEN and increased the amount of the more active dephosphorylated PTEN [41]. Such crosstalk between cytokine signalling pathways and evidence for sprouty suppression/activation of urokinase and NFκB [35] is a classic example of redundancy in regulation of signalling pathways.

Another possibility is that more specific inhibitors of the ERK/MAPK pathway are involved. One family that could provide this role is the sprouty-related (SPRED) family of proteins. We investigated this further in a preliminary study of publicly available datasets of human prostate cancer. Consistent with our hypothesis, in both datasets analysed, a significant cosuppression of SPRYs and SPREDs is evident. This is the first description of such cosuppression of the Sprouty and Sprouty-related negative regulators to our knowledge. Only one report exists with regard to SPREDs in prostate cancer, describing evidence for a loss of *SPRED2* expression in high Gleason grade lesions [28]. Similarly, in both datasets assessed here, *SPRED2* expression is significantly suppressed in prostate cancer tissues. However, this is only evident in primary tissues, with no further decrease in expression evident in metastatic cancers. *SPRED1* expression whilst suppressed in one dataset did not show any significant change in another. Hence, no clear conclusion with regard to its role in prostate cancer development can be drawn, and this warrants further extensive study in the clinical setting. Of note is our finding that *SPRY1* expression does not appear to be significantly reduced in prostate carcinomas. This is in contrast to a previous study that suggested there was a reduction in *SPRY1* at the gene level, albeit in a smaller sample size, where 16 of 20 tissue samples showed reduced mRNA compared to the normal [25]. Our description of reduced *SPRY2* expression is consistent with other studies of clinical samples of prostate cancer [25, 26].

In conclusion, loss of a single allele of either *Spry1* or *Spry2* results in the development of prostate intraepithelial neoplasia in mice. These findings demonstrate the importance of negative regulators of receptor tyrosine signalling, such as Spry, in the clinical setting. Our observation that there is a concomitant loss of *SPRY2* with *SPREDs 1* and *2* in human prostate cancers supports this hypothesis and suggests that a loss of both Sprouty and Spreds is important in prostate cancer development. As such, these negative regulators of receptor tyrosine kinase signalling provide interesting targets for future pharmacopeia.

Conflict of Interests

The authors declare no conflict of interests that could be perceived as prejudicing the impartiality of the research reported.

Acknowledgments

The authors wish to thank Ms Jessica Boros for her invaluable technical assistance. Maintenance of mice colonies was funded by an NHMRC Project Grant APP1024799 awarded to Frank J. Lovicu.

References

[1] C. G. Roehrborn and L. K. Black, "The economic burden of prostate cancer," *BJU International*, vol. 108, no. 6, pp. 806–813, 2011.

[2] B. Kwabi-Addo, M. Ozen, and M. Ittmann, "The role of fibroblast growth factors and their receptors in prostate cancer," *Endocrine-Related Cancer*, vol. 11, no. 4, pp. 709–724, 2004.

[3] D. Giri, F. Ropiquet, and M. Ittmann, "Alterations in expression of basic fibroblast growth factor (FGF) 2 and its receptor FGFR-1 in human prostate cancer," *Clinical Cancer Research*, vol. 5, no. 5, pp. 1063–1071, 1999.

[4] A. Aigner, M. Butscheid, P. Kunkel et al., "An FGF-binding protein (FGF-BP) exerts its biological function by parallel paracrine stimulation of tumor cell and endothelial cell proliferation through FGF-2 release," *International Journal of Cancer*, vol. 92, no. 4, pp. 510–517, 2001.

[5] K. Sahadevan, S. Darby, H. Y. Leung, M. E. Mathers, C. N. Robson, and V. J. Gnanapragasam, "Selective over-expression of fibroblast growth factor receptors 1 and 4 in clinical prostate cancer," *The Journal of Pathology*, vol. 213, no. 1, pp. 82–90, 2007.

[6] V. D. Acevedo, R. D. Gangula, K. W. Freeman et al., "Inducible FGFR-1 activation leads to irreversible prostate adenocarcinoma and an epithelial-to- mesenchymal transition," *Cancer Cell*, vol. 12, no. 6, pp. 559–571, 2007.

[7] J. Wang, W. Yu, Y. Cai, C. Ren, and M. M. Ittmann, "Altered fibroblast growth factor receptor 4 stability promotes prostate cancer progression," *Neoplasia*, vol. 10, no. 8, pp. 847–856, 2008.

[8] N. Sugiyama, M. Varjosalo, P. Meller et al., "Fibroblast growth factor receptor 4 regulates tumor invasion by coupling fibroblast growth factor signaling to extracellular matrix degradation," *Cancer Research*, vol. 70, no. 20, pp. 7851–7861, 2010.

[9] N. Hacohen, S. Kramer, D. Sutherland, Y. Hiromi, and M. Krasnow, "Sprouty encodes an antagonist of FGF signalling that patterns apical branching of Drosophila airways," *Cell*, vol. 9, pp. 219–222, 1998.

[10] J. D. Tefft, L. Matt, S. Smith et al., "Conserved function of *mSpry-2*, a murine homolog of *Drosophila sprouty*, which negatively modulates respiratory organogenesis," *Current Biology*, vol. 9, no. 4, pp. 219–222, 1999.

[11] D. Chambers and I. Mason, "Expression of sprouty 2 during early development of the chick embryo is coincident with known sites of FGF signalling," *Mechanisms of Development*, vol. 91, no. 1-2, pp. 361–364, 2000.

[12] T. Casci, J. Vinós, and M. Freeman, "Sprouty, an intracellular inhibitor of Ras signaling," *Cell*, vol. 96, no. 5, pp. 655–665, 1999.

[13] G. Minowada, L. A. Jarvis, C. L. Chi et al., "Vertebrate sprouty genes are induced by FGF signaling and can cause chondrodysplasia when overexpressed," *Development*, vol. 126, no. 20, pp. 4465–4475, 1999.

[14] M. Fürthauer, F. Reifers, M. Brand, B. Thisse, and C. Thisse, "Sprouty 4 acts in vivo as a feedback-induced antagonist of FGF signalling in Zebrafish," *Development*, vol. 128, no. 12, pp. 2175–2186, 2001.

[15] H. Hanafusa, S. Torii, T. Yasunaga, and E. Nishida, "Sprouty1 and Sprouty2 provide a control mechanism for the Ras/MAPK signalling pathway," *Nature Cell Biology*, vol. 4, no. 11, pp. 850–858, 2002.

[16] A. Sasaki, T. Taketomi, R. Kato et al., "Mammalian Sprouty4 suppresses Ras-independent ERK activation by binding to Raf1," *Nature Cell Biology*, vol. 5, no. 5, pp. 427–432, 2003.

[17] P. Yusoff, D. H. Lao, S. H. Ong et al., "Sprouty2 inhibits the Ras/MAP kinase pathway by inhibiting the activation of Raf," *Journal of Biological Chemistry*, vol. 277, no. 5, pp. 3195–3201, 2002.

[18] D. Kovalenko, X. Yang, R. J. Nadeau, L. K. Harkins, and R. Friesel, "Sef inhibits fibroblast growth factor signaling by inhibiting FGFR1 tyrosine phosphorylation and subsequent ERK activation," *The Journal of Biological Chemistry*, vol. 278, no. 16, pp. 14087–14091, 2003.

[19] T. L. Lo, P. Yusoff, C. W. Fong et al., "The ras/mitogen-activated protein kinase pathway inhibitor and likely tumor suppressor proteins, sprouty 1 and sprouty 2 are deregulated in breast cancer," *Cancer Research*, vol. 64, no. 17, pp. 6127–6136, 2004.

[20] C. W. Fong, M.-S. Chua, A. B. McKie et al., "Sprouty 2, an inhibitor of mitogen-activated protein kinase signaling, is down-regulated in hepatocellular carcinoma," *Cancer Research*, vol. 66, no. 4, pp. 2048–2058, 2006.

[21] H. Sutterlüty, C.-E. Mayer, U. Setinek et al., "Down-regulation of Sprouty2 in non-small cell lung cancer contributes to tumor malignancy via extracellular signal-regulated kinase pathway-dependent and -independent mechanisms," *Molecular Cancer Research*, vol. 5, no. 5, pp. 509–520, 2007.

[22] S. A. Lee, C. Ho, R. Roy et al., "Integration of genomic analysis and in vivo transfection to identify sprouty 2 as a candidate tumor suppressor in liver cancer," *Hepatology*, vol. 47, no. 4, pp. 1200–1210, 2008.

[23] G. Minowada and Y. E. Miller, "Overexpression of *Sprouty 2* in mouse lung epithelium inhibits urethane-induced tumorigenesis," *American Journal of Respiratory Cell and Molecular Biology*, vol. 40, no. 1, pp. 31–37, 2009.

[24] T. Yoshida, T. Hisamoto, J. Akiba et al., "Spreds, inhibitors of the Ras/ERK signal transduction, are dysregulated in human hepatocellular carcinoma and linked to the malignant phenotype of tumors," *Oncogene*, vol. 25, no. 45, pp. 6056–6066, 2006.

[25] B. Kwabi-Addo, J. Wang, H. Erdem et al., "The expression of Sprouty1, an inhibitor of fibroblast growth factor signal transduction, is decreased in human prostate cancer," *Cancer Research*, vol. 64, no. 14, pp. 4728–4735, 2004.

[26] S. Fritzsche, M. Kenzelmann, M. J. Hoffmann et al., "Concomitant down-regulation of *SPRY1* and *SPRY2* in prostate carcinoma," *Endocrine-Related Cancer*, vol. 13, no. 3, pp. 839–849, 2006.

[27] J. L. Schutzman and G. R. Martin, "Sprouty genes function in suppression of prostate tumorigenesis," *Proceedings of the National Academy of Sciences of the United States of America*, vol. 109, no. 49, pp. 20023–20028, 2012.

[28] N. Kachroo, T. Valencia, A. Y. Warren, and V. J. Gnanapragasam, "Evidence for downregulation of the negative regulator SPRED2 in clinical prostate cancer," *British Journal of Cancer*, vol. 108, no. 3, pp. 597–601, 2013.

[29] M. A. Basson, S. Akbulut, J. Watson-Johnson et al., "Sprouty1 is a critical regulator of GDNF/RET-mediated kidney induction," *Developmental Cell*, vol. 8, no. 2, pp. 229–239, 2005.

[30] K. Shim, G. Minowada, D. E. Coling, and G. R. Martin, "Sprouty2, a mouse deafness gene, regulates cell fate decisions in the auditory sensory epithelium by antagonizing FGF signaling," *Developmental Cell*, vol. 8, no. 4, pp. 553–564, 2005.

[31] S. B. Shappell, G. V. Thomas, R. L. Roberts et al., "Prostate pathology of genetically engineered mice: definitions and classification. The consensus report from the Bar Harbor meeting of the mouse models of human cancer consortium prostate pathology committee," *Cancer Research*, vol. 64, no. 6, pp. 2270–2305, 2004.

[32] S. Varambally, J. Yu, B. Laxman et al., "Integrative genomic and proteomic analysis of prostate cancer reveals signatures of metastatic progression," *Cancer Cell*, vol. 8, no. 5, pp. 393–406, 2005.

[33] D. K. Vanaja, J. C. Cheville, S. J. Iturria, and C. Y. F. Young, "Transcriptional silencing of zinc finger protein 185 identified by expression profiling is associated with prostate cancer progression," *Cancer Research*, vol. 63, no. 14, pp. 3877–3882, 2003.

[34] A. MacIà, M. Vaquero, M. Gou-Fàbregas et al., "Sprouty1 induces a senescence-associated secretory phenotype by regulating NFκB activity: implications for tumorigenesis," *Cell Death & Differentiation*, vol. 21, no. 2, pp. 333–343, 2014.

[35] A. M. De Marzo, A. K. Meeker, S. Zha et al., "Human prostate cancer precursors and pathobiology," *Urology*, vol. 62, no. 5, pp. 55–62, 2003.

[36] M. J. Gerdes, M. Larsen, T. D. Dang, S. J. Ressler, J. A. Tuxhorn, and D. R. Rowley, "Regulation of rat prostate stromal cell myodifferentiation by androgen and TGF-β1," *Prostate*, vol. 58, no. 3, pp. 299–307, 2004.

[37] F. Yang, J. A. Tuxhorn, S. J. Ressler, S. J. McAlhany, T. D. Dang, and D. R. Rowley, "Stromal expression of connective tissue growth factor promotes angiogenesis and prostate cancer tumorigenesis," *Cancer Research*, vol. 65, no. 19, pp. 8887–8895, 2005.

[38] E. H. H. Shin, M. A. Basson, M. L. Robinson, J. W. McAvoy, and F. J. Lovicu, "Sprouty is a negative regulator of transforming growth factor β-induced epithelial-to-mesenchymal transition and cataract," *Molecular Medicine*, vol. 18, pp. 861–873, 2012.

[39] F. Yang, D. W. Strand, and D. R. Rowley, "Fibroblast growth factor-2 mediates transforming growth factor-β action in prostate cancer reactive stroma," *Oncogene*, vol. 27, no. 4, pp. 450–459, 2008.

[40] S. Wang, A. J. Garcia, M. Wu, D. A. Lawson, O. N. Witte, and H. Wu, "Pten deletion leads to the expansion of a prostatic stem/progenitor cell subpopulation and tumor initiation," *Proceedings of the National Academy of Sciences of the United States of America*, vol. 103, no. 5, pp. 1480–1485, 2006.

[41] F. Edwin, R. Singh, R. Endersby, S. J. Baker, and T. B. Patel, "The tumor suppressor PTEN is necessary for human sprouty 2-mediated inhibition of cell proliferation," *The Journal of Biological Chemistry*, vol. 281, no. 8, pp. 4816–4822, 2006.

Hindawi Publishing Corporation
BioMed Research International
Volume 2015, Article ID 657179, 9 pages
http://dx.doi.org/10.1155/2015/657179

Research Article

Deguelin Induces Apoptosis by Targeting Both EGFR-Akt and IGF1R-Akt Pathways in Head and Neck Squamous Cell Cancer Cell Lines

Yuh Baba,[1] Masato Fujii,[2] Toyonobu Maeda,[3] Atsuko Suzuki,[3] Satoshi Yuzawa,[3] and Yasumasa Kato[3]

[1] *Department of General Clinical Medicine, Ohu University School of Dentistry, 31-1 Mitsumido, Tomiya-machi, Koriyama City, Fukushima 963-8611, Japan*
[2] *National Institute of Sensory Organs, National Tokyo Medical Center, 2-5-1 Higashigaoka, Meguro, Tokyo 152-8902, Japan*
[3] *Department of Oral Function and Molecular Biology, Ohu University School of Dentistry, 31-1 Mitsumido, Tomiya-machi, Koriyama City, Fukushima 963-8611, Japan*

Correspondence should be addressed to Yuh Baba; y-baba@den.ohu-u.ac.jp and Yasumasa Kato; yasumasa-kato@umin.ac.jp

Received 6 August 2014; Revised 7 November 2014; Accepted 7 November 2014

Academic Editor: Sandeep Singh

Deguelin, a rotenoid compound from the African plant *Mundulea sericea* (Leguminosae), has been shown to possess antitumor activities but the exact role for the growth factor receptor mediated signaling pathway in head and neck squamous cell carcinoma (HNSCC) is currently still unclear. In the present study, we investigated the effect of deguelin on epidermal growth factor receptor (EGFR) and insulin-like growth factor-1 receptor (IGF1R) pathways in HNSCC cell lines. Flowcytometric analysis revealed accumulation of annexin V positivity in deguelin-treated cells, showing that deguelin induced apoptosis. The deguelin-induced apoptosis was accompanied by the reduction of constitutive phosphorylated levels of IGF1R, Akt, and extracellular signal-regulated kinase1/2 (ERK1/2). LY294002-mediated inhibition of phosphatidylinositol-3 kinase, which is an upstream effector for Akt activation, increased cleavage of poly(ADP-ribosyl) polymerase (PARP) but ERK inhibition by U0126 did not. Deguelin inhibited both IGF-1- and EGF-induced Akt activation. These results showed that deguelin possessed antitumor effect by targeting Akt in dual axis such as EGFR and IGF1R signaling pathways and suggested that it provides an applicable therapeutic strategy for HNSCC patients.

1. Introduction

Head and neck squamous cell carcinoma (HNSCC) is the sixth most common neoplasm worldwide, with approximately 600,000 patients newly diagnosed each year [1]. Over the past 30 years, patients with recurrent and/or metastatic HNSCC have had a poor prognosis [2, 3]. A total of 30–50% of patients develop local or regional recurrence, with more patients developing distant metastases [4, 5]. Therefore, research focused on gaining a better understanding of this disease and on the development of novel treatment strategies is required.

Epidermal growth factor receptor (EGFR) is a ubiquitously expressed transmembrane glycoprotein belonging to the ErbB/HER family of receptor tyrosine kinases (TK). Activation of EGFR leads to autophosphorylation and activation of intracellular signaling pathways including the phosphatidylinositol 3-kinase (PI3K)/Akt pathway (as a survival signal) and extracellular signal-regulated kinase 1/2 (ERK1/2) pathway (as a proliferation signal). EGFR is abundantly expressed in squamous cell carcinomas including head and neck region [6]. Because elevated expression of EGFR in HNSCC correlates with poor prognosis and EGFR plays critical roles in cell survival and proliferation, EGFR signaling had been thought to be the most important target as the anticancer treatment strategy [7]. Therefore, the use of EGFR inhibitors such as gefitinib and erlotinib was expected to be applicable strategy for HNSCC therapy. However, clinical

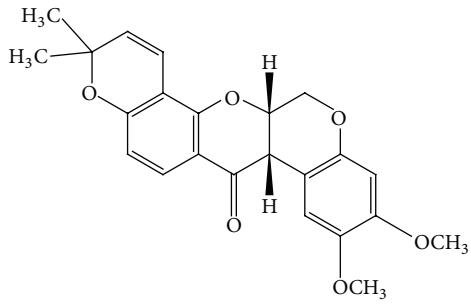

Figure 1: The chemical structure of deguelin.

study showed disappointing results; that is, respective overall response rate for gefitinib and erlotinib was 11% [8] and 4% [9] in the patients with recurrent and/or metastatic HNSCC. As we have previously postulated that crosstalk between EGFR-Akt and IGF1R-Akt pathways is thought of as one mechanism of low response rate of EGFR inhibitor alone for HNSCC patients [10], management for both signaling pathways should be considered for the patients with HNSCC.

Deguelin, which is a rotenoid isolated from the African plant *Mundulea sericea* (Leguminosae), is a potent chemopreventive agent for some kinds of cancers. Using it in mouse chemical carcinogenesis assay, it has been shown that deguelin suppresses formation of not only aberrant crypt foci in colons [11], skin papilloma [12, 13], and lung tumor [14] but also carcinoma formation such as mammary grand adenocarcinoma [13].

In recent years, molecular mechanism of deguelin's function has been uncovered. Many functions of deguelin have been reported by Yang et al. [15]; that is, deguelin has an inhibitory activity for Akt signaling, and deguelin disrupts association between heat shock protein (HSP) 90 with survivin and cyclin-dependent kinase 4, while inducing ubiquitination followed by the degradation. They also reported that deguelin induces ceramide production which results in apoptosis by autophagy through the ceramide-AMP-activated protein kinase-Ulk1 axis [15]. Although deguelin could be reduced by both EGFR-Akt [16] and IGF1R-Akt pathways [17] in breast cancer model, the potential effect of deguelin on those pathways in HNSCC is still unknown. Therefore, we determined whether deguelin has inhibitory activity for both EGFR-Akt and IGF1R-Akt pathways to induce apoptosis in HNSCC.

2. Methods

2.1. Reagents. Dulbecco's modified Eagle's medium (DMEM) was from Nissui (Tokyo, Japan). Fetal bovine serum (FBS) was from Hyclone (South Logan, UT, USA). Deguelin (Figure 1), purchased from Wako (Osaka, Japan), was dissolved in DMSO as a 50 mM stock solution, stored as small aliquots at −20°C. U0126 (ERK kinase (MEK) inhibitor), LY294002 (phosphatidylinositol 3-kinase (PI3K) inhibitor), and rabbit monoclonal antibodies against p-Akt (Ser^{73}), total-p44/42 MAPK (ERK1/2), total-IGF1R, and phosphorylated-EGFR (p-EGFR; Tyr^{1068}) and rabbit polyclonal antibodies against total-Akt and poly(ADP-ribosyl) polymerase (PARP) were purchased from Cell Signaling Technology (Beverly, MA, USA). Rabbit polyclonal antibodies against glyceraldehyde 3-phosphate dehydrogenase (GAPDH) were from GeneTex (Irvine, CA, USA). Mouse monoclonal antibody against phosphorylated-ERK1/2 (p-ERK1/2) and rabbit polyclonal antibody against total EGFR were from Santa Cruz Biotechnology (Dallas, TX, USA). Rabbit recombinant oligoclonal antibodies against phosphorylated IGF1R (p-IGF1R; Tyr^{1135}/Tyr^{1136}) were from Invitrogen (Carlsbad, CA, USA), and mouse monoclonal antibody against p-EGFR (Tyr^{1173}) was from Millipore (Billerica, MA, USA). Anti-annexin V antibody, conjugated with a fluoroisothiocynate fluorescence dye, was from Bio-Rad (Hercules, CA, USA). Biotin-conjugated goat anti-mouse IgG (H+L) and biotin-conjugated goat anti-rabbit IgG (H+L) were from Jackson ImmunoResearch (West Grove, PA, USA). Blocking Reagent N102 was from NOF Corp. (Tokyo, Japan). Chemiluminescence reagent was from Amersham (Buckinghamshire, UK). Protein assay kit was from Bio-Rad. Bovine serum albumin was from Sigma-Aldrich (St. Louis, MO, USA).

2.2. Cell Lines and Culture. SCC-4 cells and HSC-4 cells, cell lines derived from human tongue carcinoma, were provided from the Human Science Research Resources Bank (HSRRB) (Osaka, Japan). They were maintained in DMEM supplemented with 10% FBS and 100 U/ml penicillin G and 100 μg/ml streptomycin. Cells were incubated at 37°C in a humidified atmosphere containing 5% CO_2 and 95% air.

2.3. Cell Viability Assay. SCC-4 cells (2×10^5 cells/ml) and HSC-4 cells (1×10^6 cells/ml) were cultured in complete DMEM medium in the presence of 0 and 100 μM deguelin in 6-well tissue-culture plate (Thermo Fisher Scientific, Hudson, NH, USA). After 24 h of culture, the cell numbers were determined by the trypan-blue dye exclusion method.

2.4. Analysis of Cell Cycle. After incubation period, cells were collected by the trypsin treatment and fixed with 70% ethanol. The cellular DNA was stained for 30 min with 0.1 mg/ml propidium iodide solution. Finally, the cells were analyzed via flow cytometry (Epics Elite, Coulter, Hialeah, FL, USA).

2.5. Annexin V Assay. To identify apoptosis, we detected annexin V positivity by flow cytometry. Cells (5×10^5) were incubated with 100 μM deguelin and then stained. They were washed twice in PBS, resuspended in 100 μL of a binding buffer containing a fluoroisothiocynate-conjugated anti-annexin V antibody and propidium iodide, and then analyzed by the flow cytometry (FACS Calibur; BD Biosciences, San Jose, CA, USA).

2.6. Western Blot Analysis. Protein level was compared by Western blot analysis which was described elsewhere [18].

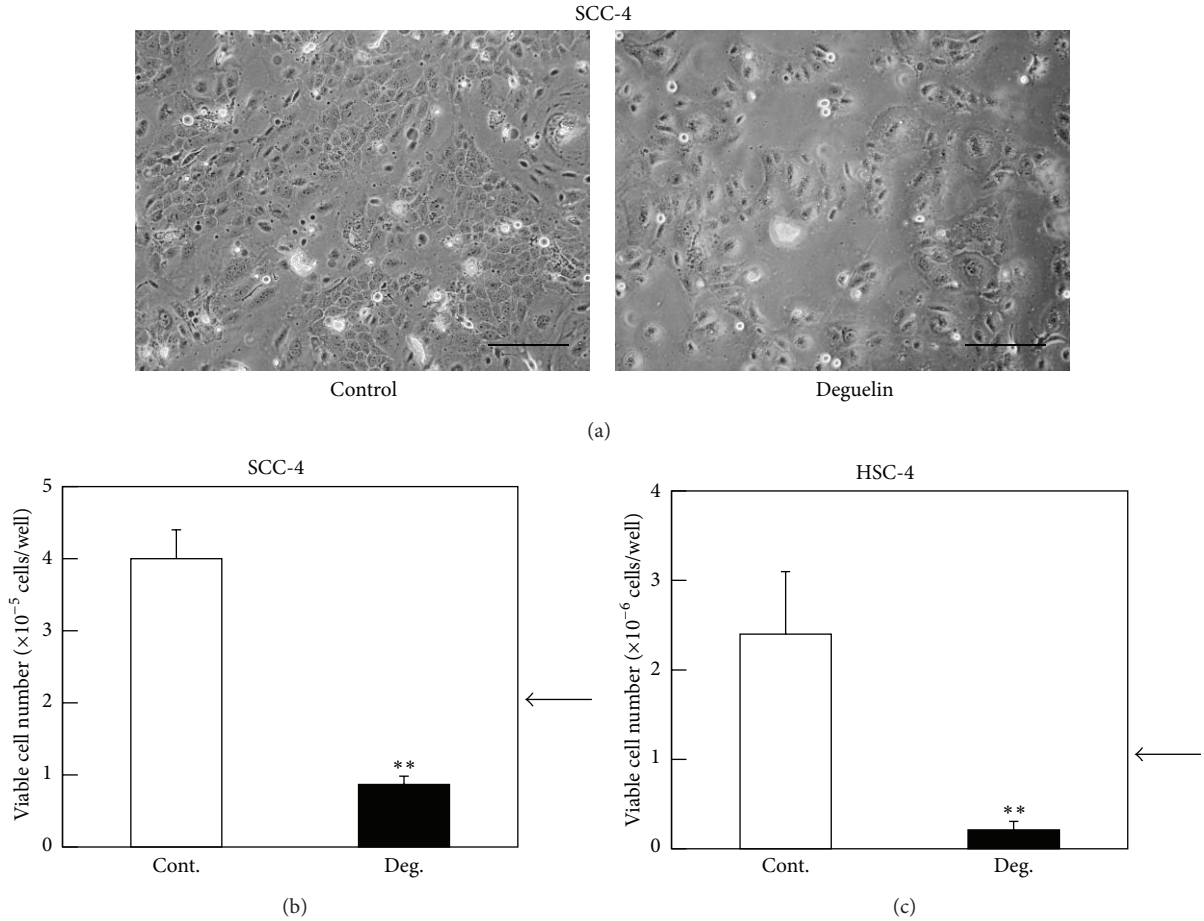

Figure 2: Deguelin induced cell death in SCC-4 and HSC-4 cell lines. Phase-contrast microscopic analysis. SCC-4 cells were treated with 0 or 100 μM deguelin in DMEM + 10% FBS. After 24 h incubation, photographs were taken under phase-contrast microscopy. Representative phase-contrast micrographs are shown (a). Bar: 50 μm. Trypan-blue dye exclusion assay was performed to measure cell viability of SCC-4 cells (b) and HSC-4 cells (c) at 24 h after 100 μM deguelin treatment. Arrows indicate initial cell numbers. Each point represents the mean ± SD from triplicate assay ($^{**}P < 0.01$).

In brief, proteins in whole-cell lysates were electrophoresed on sodium dodecyl sulfate containing 7.5% polyacrylamide gel and they were electrotransferred onto polyvinylidene fluoride (PVDF) membranes. After blocking with 20% Blocking Reagent N102, the membrane was treated with first antibody of interest, followed by treatment with biotin-conjugated secondary antibody. Signals were detected with chemiluminescence reagent. The blots were stripped and reprobed with anti-GAPDH antibodies to show equal protein loading. Intensity of immunoreacted bands was quantified by Scion Image (Scion Corp., Frederick, MD, USA).

2.7. Protein Assay. The protein content in the lysates was measured according to Lowry method using Bio-Rad protein assay kit with bovine serum albumin as the standard.

2.8. Statistical Analysis. Statistical significance was calculated using Student's t-test. P values less than 0.05 were considered significant.

3. Results

3.1. Deguelin Induced Cell Death in SCC-4 and HSC-4 Cell Lines. We examined whether deguelin suppresses the proliferation of human tongue squamous cell carcinoma cell lines, using trypan blue dye exclusion method. As shown in Figure 2, deguelin treatment inhibited proliferation of SCC-4 and HSC-4 cells. Viable cell numbers after deguelin treatment were less than initial cell numbers (Figures 2(b) and 2(c)), suggesting that deguelin induced cell death in both SCC-4 and HSC-4 cell lines.

3.2. Deguelin Induced Apoptosis. Cell cycle analysis was performed using flow cytometry. Deguelin-treated SCC-4 cells accumulated in the sub G1 phase (27.0%) by 24 h treatment as compared with its vehicle control (7.38%) (Figure 3(a)). Then, annexin V positivity in deguelin-treated cells was evaluated using flow cytometric analysis (Figures 3(b) and 3(c)). Deguelin-induced apoptotic cell population in early stage (annexin V^+/propidium $iodide^-$) increased to 13.30% from

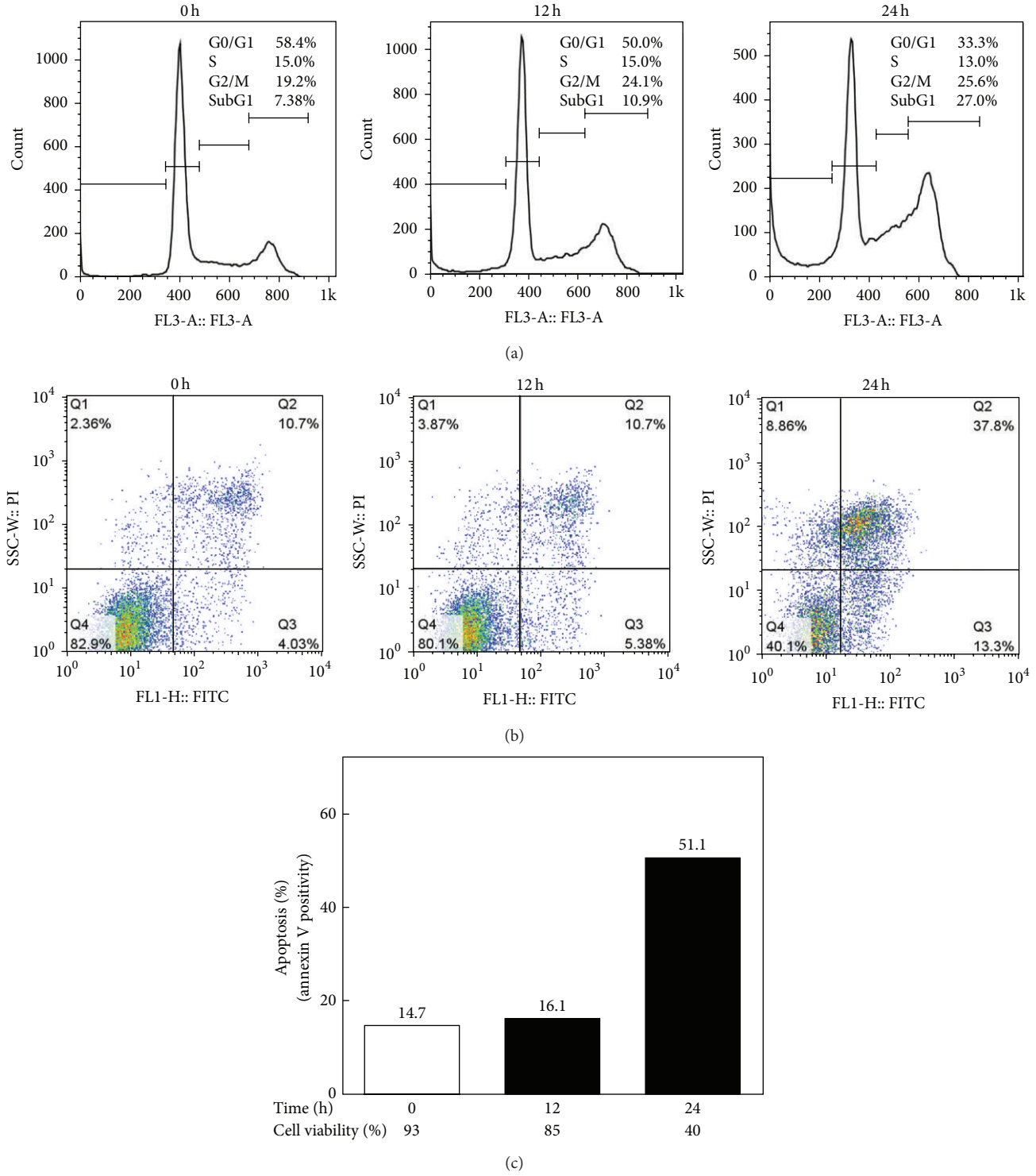

Figure 3: Deguelin induced apoptosis in SCC-4 cell lines. SCC-4 cells were incubated in the absence or presence of 100 μM deguelin for different times. Thereafter, the cells were washed and fixed. They were further stained with propidium iodide (PI, x-axis) to detect accumulation of cell cycle phase (a) and treated with anti-annexin V antibody conjugated with FITC (FITC, y-axis) to analyze apoptosis (b) by flow cytometry.

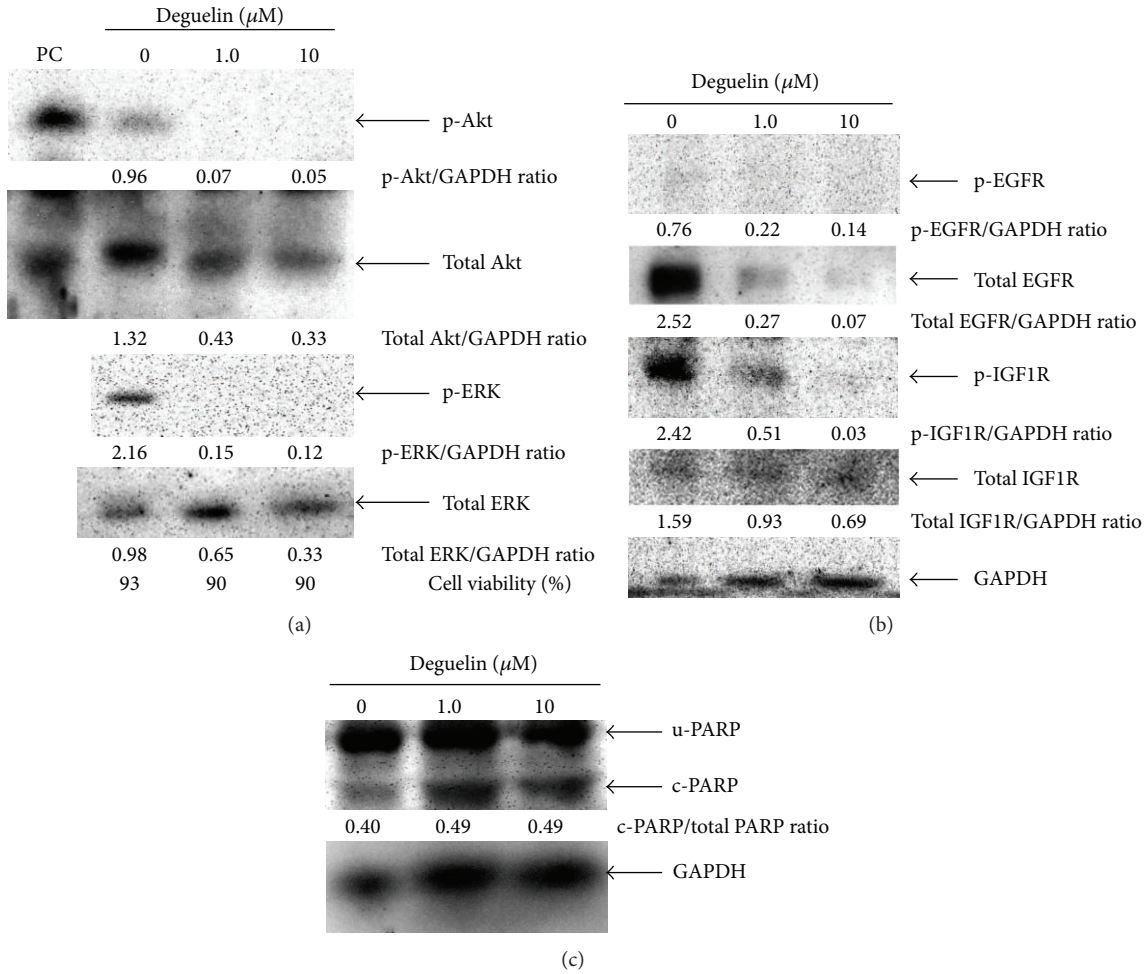

Figure 4: Deguelin reduced the expression of phosphorylated IGF1R, p-Akt, and p-ERK and induced apoptosis in SCC-4 cell lines. Subconfluent culture was treated with deguelin at different concentrations for 24 h. Whole-cell extracts were prepared and analyzed by Western blot using antibodies against p-Akt, Akt, p-ERK, and ERK (a); p-EGFR, EGFR, p-IGF1R, and IGF1R (b); and PARP (c-PARP, cleaved PARP; u-PARP, uncleaved PARP; total PARP, sum of cleaved and uncleaved PARP) (c). Total cell extracts from Jurkat cells: serum starved overnight and then treated with Calyculin A was used as positive control (PC) for p-Akt and Akt.

4.03% (basal level) after 24 h treatment while those in late stage (annexin V^+/propidium $iodide^+$) reached 37.8% from 10.7% (basal level) after 24 h treatment. Overall apoptotic cell population by deguelin was increased from 14.7% to 51.1% in a time-dependent manner.

3.3. Deguelin Reduced the Expression of p-IGF1R, p-Akt, and p-ERK. The majority of the HNSCC cells show overexpression of EGFR, whose activation leads to activation of intracellular signaling including the PI3K/Akt and ERK pathways. Although deguelin has been shown to inhibit Akt activation, the effect of deguelin on EGFR signaling cascade is still not known in HNSCC. As shown in Figure 4, deguelin reduced the expression of total EGFR, p-Akt, and p-ERK in SCC-4 cells. We could not detect constitutive level of p-EGFR in the standard culture condition, suggesting that Akt and ERK are not a downstream target of EGFR but possibly IGF1R which was examined later. Expectedly, IGF1R has been constitutively phosphorylated as the basal level and deguelin reduced its phosphorylation concordance with the elevation of PARP cleavage (Figures 4(b) and 4(c)). These results suggested that deguelin induced apoptosis with the suppression of both IGF1R-Akt and IGF1R-ERK pathways.

3.4. Deguelin-Induced Downregulation of p-IGF1R, p-Akt, and p-ERK Is Not due to Its Effects on Cell Viability. To exclude the possibility that the downregulation of p-IGF1R, p-Akt, and p-ERK is due to the cytotoxic effects of deguelin, SCC-4 cells were exposed to different concentrations of deguelin for 24 h and then examined for cell viability by trypan blue dye-exclusion method. Cell viability remained about 90% at 10 μM or less for 24 h and it decreased by 60% at 100 μM (Figure 4(a)). Since a decrease in p-IGF1R, p-Akt, and p-ERK was seen in the cells 24 h after deguelin treatment at either 1.0 or 10 μM (see Figures 4(a) and 4(b)), it was suggested that deguelin-mediated decreases in p-IGF1R, p-Akt, and p-ERK levels are not due to its cytotoxic effects.

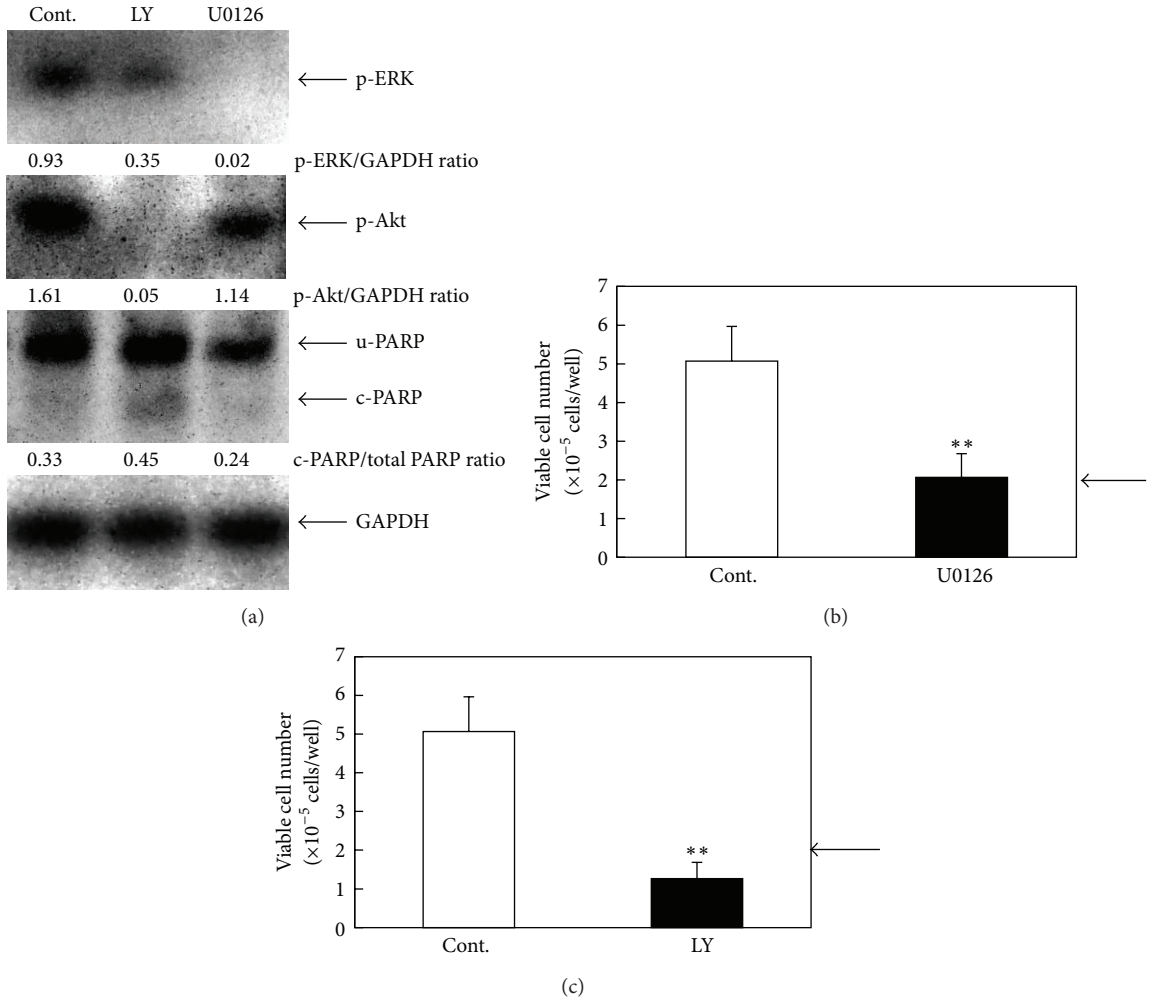

Figure 5: Inhibition of activated Akt rather than inhibition of activated ERK is associated with deguelin-induced apoptosis in SCC-4 cells. (a) Subconfluent culture was incubated for 24 h in serum-free medium. After the starvation, cells were treated with U0126 (10 μM) or LY294002 (50 μM) for 1 h, and cells were incubated for 15 min in 10% FBS-containing medium. Whole-cell lysates were extracted and analyzed by Western blot using antibodies against p-Akt, p-ERK, and PARP (c-PARP, cleaved PARP; u-PARP, uncleaved PARP; total PARP, sum of cleaved and uncleaved PARP). Trypan-blue dye exclusion assay was performed to measure cell viability of SCC-4 cells at 24 h after U0126 (10 μM) (b) or LY294002 (50 μM) (c) treatment. Arrows indicate inoculated cell numbers. Each point represents the mean ± SD from triplicate assay ($^{**}P < 0.01$).

3.5. Inhibition of p-Akt rather than Inhibition of p-ERK Is Associated with Deguelin-Induced Apoptosis in SCC-4 Cell Line. As general understanding, Akt signaling and ERK signaling are important as survival and proliferation, respectively. In addition, in fibroblast cells, ERK signaling is considered to be survival signal [19]. Therefore, in order to confirm that the apoptotic effect of deguelin is mediated by interacting with Akt signaling or ERK signaling in SCC-4 cells, we examined the effects of ERK inhibitor U0126 and PI-3 kinase/Akt inhibitor LY294002. As expected, U0126 inhibited phosphorylation of ERK while it did not affect PARP cleavage (Figure 5(a)). Furthermore, U0126 suppressed the proliferation of SCC-4 cells without any cytotoxicity because viable cell number after U0126 treatment remained unchanged with the vehicle control (Figure 5(b)). On the contrary, LY294002 reduced p-Akt while it cleaved PARP (Figure 5(a)). LY294002 also suppressed the cell viability of SCC-4 and viable cell number after LY294002 treatment was less than the vehicle control (Figure 5(c)). These results strongly suggest the involvement of the inhibition of the PI-3 kinase/Akt pathway rather than the inhibition of the MEK/ERK pathway in the deguelin-induced apoptosis.

3.6. Deguelin Induced Apoptosis by Reducing IGF-Stimulated Akt Activation in SCC-4 Cells. Next, we examined whether deguelin induced apoptosis by reducing IGF1-Akt signaling in SCC-4 cells. As shown in Figure 6(a), p-Akt was elevated by IGF1 treatment for 15 min and this induction was suppressed by deguelin accompanied with increase in the cleaved PARP. These results clearly indicated that deguelin induced apoptosis by targeting IGF1R-Akt pathway in SCC-4 cells.

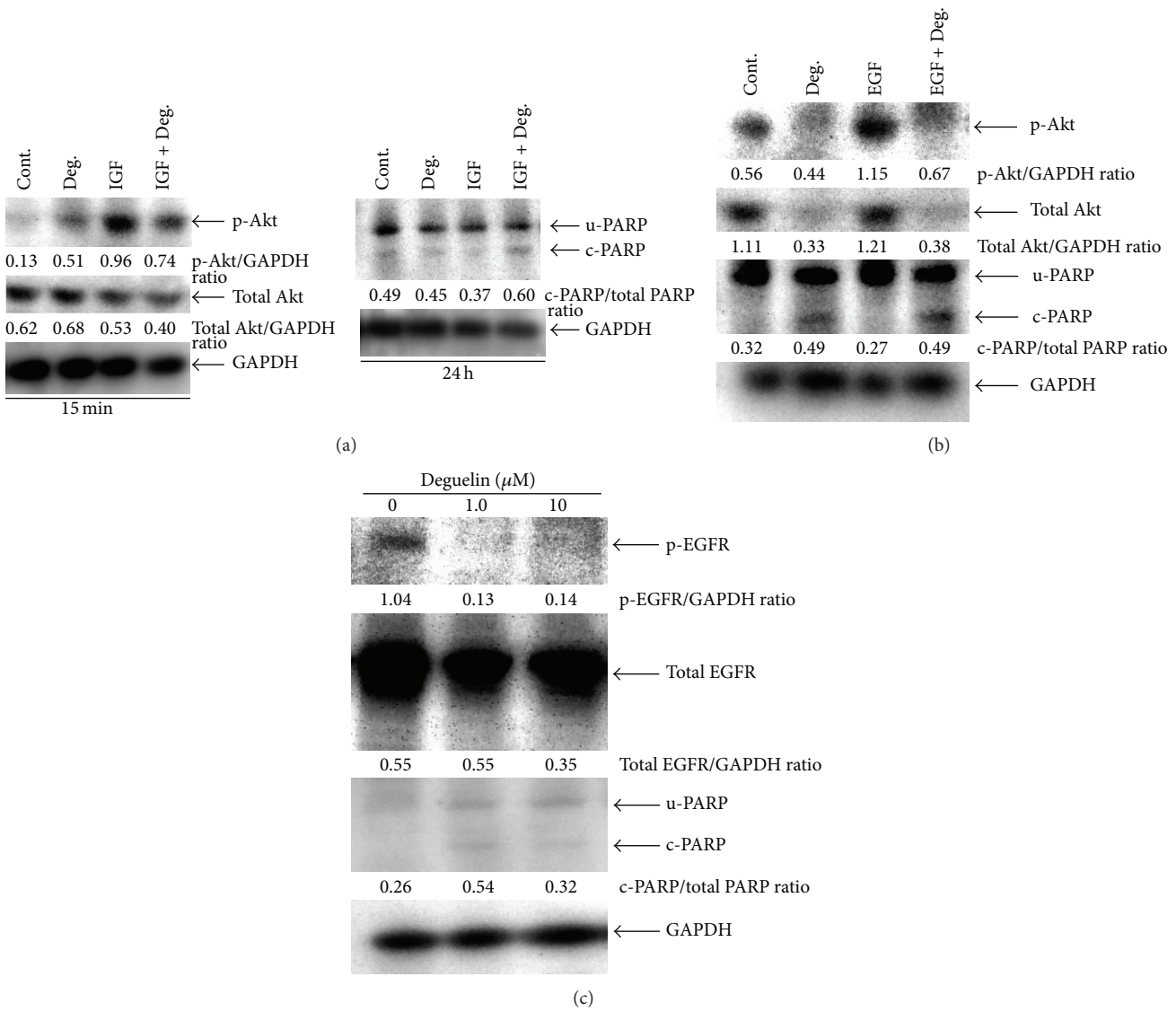

Figure 6: Deguelin induced apoptosis by targeting both EGFR-Akt and IGF1R-Akt pathways in HNSCC cell lines. Subconfluent cultures were incubated for 24 h in serum-free medium. After the starvation, cells were treated with 10 μM deguelin for 1 h. (a) The deguelin-treated SCC-4 cells were incubated for 15 min and 24 h with or without 10 ng/ml of IGF, respectively. (b) The deguelin-treated HSC-4 cells were incubated for 24 h with or without 10 ng/ml of EGF. Whole-cell extracts were analyzed by Western blot using antibodies against p-Akt, Akt, and PARP. (c) HSC-4 cells were treated with deguelin at different concentrations for 24 h in 10% FBS-containing medium. Whole-cell extracts were analyzed by Western blot using antibodies against p-EGFR, EGFR, and PARP (c-PARP, cleaved PARP; u-PARP, uncleaved PARP; total PARP, sum of cleaved and uncleaved PARP).

3.7. Deguelin Induced Apoptosis Accompanied with the Reduction of Constitutive and EGF-Stimulated Akt Activation in HSC-4 Cell Line. Finally, we examined whether deguelin induced apoptosis accompanied with the reduction of constitutive and EGF-stimulated Akt activation in HSC-4 cells. As shown in Figure 6(b), deguelin increased in the levels of cleaved-PARP accompanied with the reduction of both constitutive and EGF-stimulated p-Akt protein levels. Furthermore, deguelin induced apoptosis by reducing p-EGFR expression in HSC-4 cells, as shown in Figure 6(c). These results clearly suggested that deguelin induced apoptosis by targeting EGFR-Akt pathway in HSC-4 cells.

4. Discussion

We showed that deguelin induced cell death in HNSCC cell lines. To better understand the action mechanisms of deguelin, we further examined intracellular signaling. We found that deguelin induced apoptosis by targeting IGF1R-Akt and targeting EGFR-Akt pathways in HNSCC cell lines. To the best of our knowledge, this is the first report that deguelin can target both EGFR-Akt and IGF1R-Akt pathways in HNSCC cell lines. Previously, deguelin was reported to induce apoptosis by autophagy through AMPK-Ulk signaling, inhibition of Akt signaling, and degradation

of CDK4/Survivin in HNSCC [15]. Another report indicated that deguelin suppressed NF-κB in SCC-4 cells [20]. Therefore, many signaling pathways may work together to exert the antitumor effect of deguelin, and our studies extended the fact that deguelin has an applicable potential for HNSCC therapy.

Inhibition of activated Akt rather than inhibition of activated ERK is associated with deguelin-induced apoptosis in HNSCC. Recent study has suggested crosstalk between Akt signaling and ERK signaling: for example, feedback from the PI3K-Akt-mTORC1 (mammalian target of rapamycin complex 1) to the Ras-MEK-ERK pathway [21] and ERK activates Akt signaling at the mTOR level [22]. However, in SCC-4 cells, we indicated that inhibition of activated Akt rather than inhibition of activated ERK is associated with deguelin-induced apoptosis because U0126 showed cytostatic effect without changes of PARP cleavage level and LY294002 had cytotoxic effect with increase in PARP cleavage. Probably, crosstalk between two signalings seems to be cell type specific.

Deguelin was proposed as an inhibitor of Hsp90 [23]. The client protein of HSP 90 includes Akt, EGFR, and IGF1R. EGFR is expressed at high levels in the majority of epithelial malignancies including HNSCC [6]. Elevated expression of EGFR in HNSCC correlates with poor prognosis, and EGFR has been a target of anticancer treatments due to its critical roles in cell survival and proliferation [7]. Therefore, cetuximab, antibody of EGFR, is an applicable strategy for HNSCC therapy [24]. However, Jameson et al. [25] postulated that IGF1R-Akt signaling underlies cetuximab resistance for HNSCC. Therefore, deguelin should be applicable for HNSCC as combination with EGFR inhibitors such as cetuximab and erlotinib.

5. Conclusion

Deguelin possessed antitumor effect in HNSCC by targeting both EGFR-Akt and IGF1R-Akt pathways. Because deguelin is reported to be nontoxic and tolerable in the animal model [26], deguelin should be an applicable strategy for HNSCC therapy.

Conflict of Interests

The authors declare that there is no conflict of interests regarding the publication of this paper.

Acknowledgment

This study was supported in part by a Grant-in-Aid for Scientific Research (C): 23592546 to Yuh Baba.

References

[1] C. Cripps, E. Winquist, M. C. Devries, D. Stys-Norman, and R. Gilbert, "Epidermal growth factor receptor targeted therapy in stages III and IV head and neck cancer," *Current Oncology*, vol. 17, no. 3, pp. 37–48, 2010.

[2] F. R. Khuri, D. M. Shin, B. S. Glisson, S. M. Lippman, and W. K. Hong, "Treatment of patients with recurrent or metastatic squamous cell carcinoma of the head and neck: current status and future directions," *Seminars in Oncology*, vol. 27, supplement 8, no. 4, pp. 25–33, 2000.

[3] A. Forastiere, W. Koch, A. Trotti, and D. Sidransky, "Head and neck cancer," *The New England Journal of Medicine*, vol. 345, no. 26, pp. 1890–1900, 2001.

[4] S. Aggarwal, Y. Takada, S. Singh, J. N. Myers, and B. B. Aggarwal, "Inhibition of growth and survival of human head and neck squamous cell carcinoma cells by curcumin via modulation of nuclear factor-κB signaling," *International Journal of Cancer*, vol. 111, no. 5, pp. 679–692, 2004.

[5] P. M. Stell, "Time to recurrence of squamous cell carcinoma of the head and neck," *Head and Neck*, vol. 13, no. 4, pp. 277–281, 1991.

[6] D. Saranath, R. G. Panchal, R. Nair, A. R. Mehta, V. D. Sanghavi, and M. G. Deo, "Amplification and overexpression of epidermal growth factor receptor gene in human oropharyngeal cancer," *European Journal of Cancer Part B: Oral Oncology*, vol. 28, no. 2, pp. 139–143, 1992.

[7] B. Burtness, "The role of cetuximab in the treatment of squamous cell cancer of the head and neck," *Expert Opinion on Biological Therapy*, vol. 5, no. 8, pp. 1085–1093, 2005.

[8] E. E. W. Cohen, F. Rosen, W. M. Stadler et al., "Phase II trial of ZD1839 in recurrent or metastatic squamous cell carcinoma of the head and neck," *Journal of Clinical Oncology*, vol. 21, no. 10, pp. 1980–1987, 2003.

[9] D. Soulieres, N. N. Senzer, E. E. Vokes, M. Hidalgo, S. S. Agarvala, and L. L. Siu, "Multicenter phase II study of erlotinib, an oral epidermal growth factor receptor tyrosine kinase inhibitor, in patients with recurrent or metastatic squamous cell cancer of the head and neck," *Journal of Clinical Oncology*, vol. 22, no. 1, pp. 77–85, 2004.

[10] Y. Baba, M. Fujii, Y. Tokumaru, and Y. Kato, "Present and future of EGFR inhibitors for head and neck squamous cell cancer," *Journal of Oncology*, vol. 2012, Article ID 986725, 9 pages, 2012.

[11] G. Murillo, J. W. Kosmeder II, J. M. Pezzuto, and R. G. Mehta, "Deguelin suppresses the formation of carcinogen-induced aberrant crypt foci in the colon of CF-1 mice," *International Journal of Cancer*, vol. 104, no. 1, pp. 7–11, 2003.

[12] C. Gerhauser, W. Mar, N. Suh et al., "Rotenoids mediate potent cancer chemopreventive activity through transcriptional regulation of ornithine decarboxylase," *Nature Medicine*, vol. 1, no. 3, pp. 260–266, 1995.

[13] G. O. Udeani, C. Gerhäuser, C. F. Thomas et al., "Cancer chemopreventive activity mediated by deguelin, a naturally occurring rotenoid," *Cancer Research*, vol. 57, no. 16, pp. 3424–3428, 1997.

[14] H.-Y. Lee, S.-H. Oh, J. K. Woo et al., "Chemopreventive effects of deguelin, a novel Akt inhibitor, on tobacco-induced lung tumorigenesis," *Journal of the National Cancer Institute*, vol. 97, no. 22, pp. 1695–1699, 2005.

[15] Y.-L. Yang, C. Ji, Z.-G. Bi et al., "Deguelin induces both apoptosis and autophagy in cultured head and neck squamous cell carcinoma cells," *PLoS ONE*, vol. 8, no. 1, Article ID e54736, 2013.

[16] R. Mehta, H. Katta, F. Alimirah et al., "Deguelin action involves c-Met and EGFR signaling pathways in triple negative breast cancer cells," *PLoS ONE*, vol. 8, no. 6, Article ID e65113, 2013.

[17] Y.-A. Suh, J.-H. Kim, M. A. Sung et al., "A novel antitumor activity of deguelin targeting the insulin-like growth factor (IGF)

receptor pathway via up-regulation of IGF-binding protein-3 expression in breast cancer," *Cancer Letters*, vol. 332, no. 1, pp. 102–109, 2013.

[18] Y. Baba, Y. Kato, I. Mochimatsu et al., "Inostamycin suppresses vascular endothelial growth factor-stimulated growth and migration of human umbilical vein endothelial cells," *Clinical and Experimental Metastasis*, vol. 21, no. 5, pp. 419–425, 2004.

[19] P. Erhardt, E. J. Schremser, and G. M. Cooper, "B-Raf inhibits programmed cell death downstream of cytochrome c release from mitochondria by activating the MEK/Erk pathway," *Molecular and Cellular Biology*, vol. 19, no. 8, pp. 5308–5315, 1999.

[20] A. S. Nair, S. Shishodia, K. S. Ahn, A. B. Kunnumakkara, G. Sethi, and B. B. Aggarwal, "Deguelin, an Akt inhibitor, suppresses IκBα kinase activation leading to suppression of NF-κB-regulated gene expression, potentiation of apoptosis, and inhibition of cellular invasion," *The Journal of Immunology*, vol. 177, no. 8, pp. 5612–5622, 2006.

[21] H.-F. Yuen, O. Abramczykd, G. Montgomery et al., "Impact of oncogenic driver mutations on feedback between the PI3K and MEK pathways in cancer cells," *Bioscience Reports*, vol. 32, no. 4, pp. 413–422, 2012.

[22] V. Ramakrishnan, T. Kimlinger, J. Haug et al., "Anti-myeloma activity of Akt inhibition is linked to the activation status of PI3K/ Akt and MEK/ERK pathway," *PLoS ONE*, vol. 7, no. 11, Article ID e50005, 2012.

[23] S. H. Oh, J. K. Woo, Y. D. Yazici et al., "Structural basis for depletion of heat shock protein 90 client proteins by deguelin," *Journal of the National Cancer Institute*, vol. 99, no. 12, pp. 949–961, 2007.

[24] A. Ye, J. Hay, J. Laskin, J. Wu, and C. Ho, "Toxicity and outcomes in combined modality treatment of head and neck squamous cell carcinoma: cisplatin versus cetuximab," *Journal of Cancer Research and Therapeutics*, vol. 9, no. 4, pp. 607–612, 2013.

[25] M. J. Jameson, A. D. Beckler, L. E. Taniguchi et al., "Activation of the insulin-like growth factor-1 receptor induces resistance to epidermal growth factor receptor antagonism in head and neck squamous carcinoma cells," *Molecular Cancer Therapeutics*, vol. 10, no. 11, pp. 2124–2134, 2011.

[26] Y. Yan, Y. Wang, Q. Tan, R. A. Lubet, and M. You, "Efficacy of deguelin and silibinin on Benzo(a)pyrene-induced lung tumorigenesis in A/J Mice," *Neoplasia*, vol. 7, no. 12, pp. 1053–1057, 2005.

Hindawi Publishing Corporation
BioMed Research International
Volume 2015, Article ID 426429, 14 pages
http://dx.doi.org/10.1155/2015/426429

Research Article

Progesterone and Src Family Inhibitor PP1 Synergistically Inhibit Cell Migration and Invasion of Human Basal Phenotype Breast Cancer Cells

Mingxuan Xie,[1,2,3] Li Zhou,[3,4] Xi Chen,[2] Lindsey O. Gainey,[3] Jian Xiao,[1,2] Mark S. Nanes,[5] Anji Hou,[4] Shaojin You,[3] and Qiong Chen[1,2]

[1]*Department of Geriatrics, Xiangya Hospital, Central South University, 87 Xiangya Road, Changsha, Hunan 410008, China*
[2]*Department of Respiratory, Xiangya Hospital, Central South University, 87 Xiangya Road, Changsha, Hunan 410008, China*
[3]*Laboratory of Cancer Experimental Therapy, Atlanta Research & Educational Foundation (151F), Atlanta VA Medical Center, 1670 Clairmont Road, Decatur, GA 30033, USA*
[4]*Department of Oncology, Shanghai Seventh People's Hospital, 358 Datong Road, Pudong New District, Shanghai 200137, China*
[5]*Medical Service, Atlanta VA Medical Center and Division of Endocrinology, Metabolism, and Lipids, Department of Medicine, Emory University School of Medicine, Decatur, GA 30033, USA*

Correspondence should be addressed to Shaojin You; shaojin.you@va.gov and Qiong Chen; qiongch@163.com

Received 10 July 2014; Accepted 19 November 2014

Academic Editor: Sandeep Singh

Basal phenotype breast cancer is one of the most aggressive breast cancers that frequently metastasize to brain. The role of sex hormones and their receptors in development of this disease is largely unclear. We demonstrated that mPRα was expressed at a moderate level in a brain metastatic BPBC cell line MB231Br, which was derived from the parent mPRα undetectable MB231 cells. It functioned as an essential mediator for progesterone induced inhibitory effects on cell migration of MB231Br and, when coincubated with PP1, synergistically enhanced the progesterone's inhibitory effect on cell migration and invasion *in vitro*. Progesterone and PP1 cotreatment induced a cascade of molecular signaling events, such as dephosphorylation of FAK, downregulation of MMP9, VEGF, and KCNMA1 expressions. Our *in vitro* study demonstrated that mPRα was expressed and functioned as an essential mediator for progesterone induced inhibitory effects on cell migration and invasion in BPBC cells. This inhibitory effect was enhanced by PP1 via FAK dephosphorylation, MMP9, VEGF, and KCNMA1 downregulation mechanisms. Our study provides a new clue toward the development of novel promising agents and pathways for inhibiting nuclear hormonal receptor-negative and endocrine-resistant breast cancers.

1. Introduction

Current antihormonal therapies are frequently used for the treatment of hormone receptor positive breast cancers (i.e., estrogen receptor alpha and/or nuclear progesterone receptors, ER+ and/or PR+). For ER+ breast cancers, antiestrogen therapies (such as tamoxifen and anastrozole) are often effective, both in primary and in metastatic settings. The status of PR expression is used with ER to indicate potential effectiveness of antiestrogen therapies since the majority of breast cancers express ER and PR concurrently, even though PR may have independent predictive value for breast cancer [1, 2]. Previous studies with large-scale data sets found that ER+/PR− breast cancers do not respond as well as ER+/PR+ cancers to selective ER modulators [2]. It was proposed that patients with PR− breast cancer may receive a substantially better response from anastrozole rather than tamoxifen (compared to those with PR+ breast cancer) [1]. Synthetic progestin has been listed as a second line anticancer agent in "The NCCN Guidelines" (Version 1.2012 Breast Cancer, page 113). For example, megestrol acetate (MA) is used as an optional therapeutic agent for postmenopausal patients [3, 4] and medroxyprogesterone acetate (MPA) is often prescribed for treatment of metastatic breast cancer

[5]. In clinical practice, cases of successful combination of MPA and chemotherapy are frequently reported in breast cancer patients with various distant metastases, including bones [6, 7], liver [8, 9], and lung [10]. For treatment of human basal phenotype breast cancer (BPBC) or triple negative breast cancer (TNBC), however, current hormonal therapies may not be appropriated since these cancers are resistant to commonly used antihormonal agents [11, 12]. Great attention has been focused on discovering new molecular targets for development of novel therapeutic tools against these cancers.

The role of progesterone (P4) on breast cancer development remains controversial. In premenopausal patients, the sex hormonal milieu in the late stage of menstrual cycle has been associated with the lowest metastatic potential, both in human breast cancer [13, 14] and in rodent mammary tumors [15, 16]. Sivaraman and Medina demonstrated that P4, when used with estrogen (E2), has a protective role against mammary tumorigenesis *in vivo* [17, 18]. The Multiethnic Cohort and Women's Health Initiative Trials, however, reported that postmenopausal women receiving estroprogestin therapy are at an increased risk of breast cancer compared with those receiving estrogen alone, supporting the concept that P4 may contribute to the development of breast cancer [19, 20]. Differing results have also been reported for the effect of P4 on breast cancer cells *in vitro*. Depending upon the experimental cell model, cell context, and duration of treatment, P4 can elicit either cancer promotion or cancer protective effects on breast cancer cells [21]. For example, P4 induced cell growth and migration of T47D cells, an ER+ and PR+ human breast cancer cell line [22], but it inhibited proliferation of MDA-MB468 (MB468) cells, a human BPBC cell line with strong membrane progesterone receptor alpha (mPRα) expression [23]. In another human BPBC cell line MDA-MB231 (MB231), which was negative for both PR and mPRα receptors, P4 induced no response in cell proliferation. Introduction of mPRα cDNA into these cells rescued inhibition of cell proliferation by P4 [23], indicating that the P4 $\rightarrow$ mPRα signaling pathway played an essential role in controlling cell proliferation of human BPBC cells [23].

Progesterone exerts rapid nongenomic actions and these nonclassical actions usually take several minutes to half an hour to act [24, 25]. Extranuclear activity has been demonstrated for nuclear PR, especially PR-B, which involves the binding of the SH3 domain of Src and rapidly activates downstream MAPK/Erk1/2 [26]. P4 also exerts actions in cells and tissues naturally devoid of PR, such as T-lymphocytes, platelets, and rat corpus luteum [27–29]. Furthermore, potent PR agonist (i.e., R5020) and PR antagonist (i.e., RU486) showed little or no effect on P4's nongenomic actions [24, 30, 31]. This evidence lends strong support to the existence of membrane-bounded progesterone receptors. Recently, cell membrane hormonal receptors, such as mPR family (α, β, γ) and progesterone membrane receptor component-1 (PGMRC1), were demonstrated to be functional in breast cancer [32, 33]. It was reported that rapid responses are triggered by P4 binding to membrane receptors (i.e., mPRα) [34–36], subsequently inducing a series of alterations in secondary messenger pathways through activation of pertussis toxin-sensitive inhibitory G-proteins, to activate MAPK/Erk 1/2 pathway [32, 33, 37, 38]. We recently reported that the signaling cascade of P4 induced mesenchymal repression is mediated through caveolae bound signaling molecules, namely, Cav-1, EGFR, and PI3K. We also observed that one of the Src family kinase inhibitors [39–41] (4-amino-5-(4-methylphenyl)-7-(t-butyl)pyrazolo[3,4-d]-pyrimidine, or PP1) blocked the P4's action on expression of occludin and E-cadherin (epithelial phenotypes) but not on the expression of snail and fibronectin (one of the mesenchymal phenotypes) [23]. The roles of Src pathway in the P4/mPRα induced epithelial to mesenchymal transition (EMT) relevant signaling pathways remain to be explored in human BPBC cells.

Basal phenotype breast cancer (BPBC) is one of the most malignant breast cancers accounting for 15% of all breast cancers, and recent studies show that these cancers are often associated with brain metastasis [42, 43]. Unfortunately there is no well accepted mechanism that can explain how this brain metastatic potential is being developed in human BPBC cancers, and understanding this mechanism is essential for development of novel therapeutic tools for treatment of BPBC. MB231 is classified as a basal phenotype breast cancer cell line [44]. By a series of *in vivo* selections in mice, the populations with distinct brain metastatic tropisms were isolated [45, 46]. The brain metastatic derivative MB231 cell line (MB231Br) develops brain metastasis in 100% of mice and has served as the mainstay of most brain metastasis studies [47, 48]. It was reported that MB231Br cells have increased invasiveness through both Matrigel and blood-brain barrier (BBB) but decreased proliferation rate when compared with parental MB231 cells [49]. Genome-wide expression analysis suggested alternations in the gene expression profile of 243 genes in MB231Br cells as compared with the parent line [50]. In this study, we found that the expression of mPRα was upregulated in MB231Br cells and thus wondered if the upregulated mPRα is functional and can be used as a molecular target for modulating cell biological behavior of human BPBC cancers.

2. Material and Methods

2.1. Antibodies and Pathway Inhibitors. RU486 (MIF), AG1498, wortmannin, rapamycin, and pyrazolopyrimidine compound (PP1) were purchased from EMD Chemicals (Gibbstown, NJ, USA). BpV (phen) was from Thermo Fisher Scientific (Pittsburgh, PA, USA). Anti-mPRα goat polyclonal IgG, anti-MMP9 goat polyclonal IgG, anti-GAPDH goat polyclonal IgG, anti-mPRα blocking peptide, donkey anti-goat IgG-HRP, goat anti-rabbit IgG-HRP, and anti-mouse IgG were purchased from Santa Cruz Biotechnology (CA, USA). Anti-VEGF polyclonal antibody was from Abcom (Cambridge, MA, USA). Anti-KCNMA1 rabbit polyclonal antibody was from Millipore (Billerica, MA, USA). Anti-FAK rabbit polyclonal and anti-p-FAK rabbit polyclonal IgG were from Cell Signaling (Danvers, MA, USA). P4-BSA-FITC conjugate and anti-α-tubulin mouse monoclonal IgM were purchased from Sigma (St. Louis, MO, USA).

2.2. Cell Culture. The human breast cancer cell lines MDA-MB468 (MB468) and MDA-MB231 (MB231) were obtained

from the American Type Culture Collection (Rockville, MD, USA). These cell lines are negative for ER, PR, and Her-2 and are classified as "basal phenotype A" breast cancer cells [15]. The brain seeking MB231 cell line (MB231Br) was a gift from Dr. Yoneda, which was established by six successive rounds of *in vivo* selection and *ex vivo* culture from parental MB231 cells [47]. These breast cancer cells were cultured in DMEM (Mediatech, VA, USA) containing 10% FBS, 100 U/mL penicillin, and 100 μg/mL streptomycin (Gibco, Carlsbad, CA, USA) in a humidified incubator at 37°C with 5% CO_2.

2.3. Transfection of mPRα cDNA Plasmid. Transfection was performed as previously described [23]. Briefly, MB231 cells were cultured and split when the cell confluence reached approximately 90%. The human mPRα cDNA constructed in a pUC-based plasmid with CMV promoter (pBK-CMV) vector [30] was purified and then transfected into the cells using Lipofectamine 2000 reagent following the manufacturer's instructions (Invitrogen, Carlsbad, CA, USA).

2.4. RT-PCR Assay. Total RNA was extracted using TRIzol (Invitrogen, Carlsbad, CA, USA) and concentrations of RNA were determined using a NanoDrop2000 Spectrophotometer (Thermo Scientific, USA). Reverse transcription for synthesizing cDNA was carried out using the Quantitect Reverse Transcription Kit (Qiagen, Valencia, CA, USA). PCR amplification (35 cycles of 95°C for 20 sec, 58°C for 30 sec, and 72°C for 20 sec) was conducted in a total volume of 25 μL using the GoTaq Hot Start Green Master Mix (Promega, Madison, WI, USA). Following PCR amplification, 25 μL of the samples was separated via electrophoresis on a 1.5% agarose gel. The primers used for PCR amplification were mPRα-(5′-CCT GCTGTGTGATCTTAG-3′ and 5′-CGGAAATAGAAGCGCCAG-3′) [31], 18-S-(5′-GTTGGTTTTCGGAACTGAGGC-3′ and 5′-GTCGGCATCGTTTATGGTCG-3′) [51].

2.5. Immunoblotting Assay. Western blot assays were performed as described previously [23]. After treatment with or without P4 and/or diverse pathway inhibitors, the growth-arrested cells were lysed with 500 μL ice-cold lysis buffer (50 mM HEPES, 5 mM EDTA, 50 mM sodium chloride, pH 7.4), 1% Triton X-100, protease inhibitors (10 μg/mL aprotinin, 1 mM phenylmethylsulfonyl fluoride, and 10 μg/mL leupeptin), and phosphatase inhibitors (50 mM sodium fluoride, 1 mM sodium orthovanadate, and 10 mM sodium pyrophosphate). Cell lysates (30 μg) were separated using SDS-PAGE and transferred to nitrocellulose membranes, blocked for one hour in TBS buffer containing 5% nonfat dry milk and 0.1% Tween 20, and incubated overnight with primary antibodies at proper dilutions. After incubation with secondary antibodies, proteins of interests were detected by ECL chemiluminescence. Image J (http://rsb.info.nih.gov/ij/) was used for image analysis and quantitative data was normalized with the reference proteins (i.e., GAPDH or α-tubulin) or calculated as ratios of phosphor protein/total protein when the reference proteins were the same.

2.6. Localization of P4-BSA-FITC Binding Sites on MB231Br Cells. Breast cancer cells were cultured in chamber slides and exposed to 100 nM P4-3-(O-carboxymethyl) oxime-BSA-FITC (P4-BSA-FITC) for 30 min in serum-depleted medium [24]. Cells were then washed with PBS buffer, fixed by 10% buffered formalin, counterstained with DAPI, and observed under a confocal microscope (Olympus FV1000, Tokyo, Japan) using an oil objective lens (×60).

2.7. Cell Proliferation Assay. Cell proliferation assay was performed using MTT kit (Invitrogen, CA, USA) [52]. Cells were seeded in a 96-well plate in 100 μL of culture medium with or without the compounds to be tested and incubated for 16 hrs at 37°C. MTT labeling reagent (1 μL of stock solution) was added to the designated wells and continually incubated for 4 hrs. The supernatant was removed and then 50 μL dimethyl sulfoxide (DMSO) was added. After shaking for 10 min at 37°C, the absorbance of each well was measured at a wavelength of 595 nm with a Bio-Tek microplate reader (Winooski, VT, USA). Experiments were designed in a triplicate format and cell proliferation rates were expressed as percentage proliferation compared to controls.

2.8. Wound Closure Migration Assay. Cells (5×10^5/well) were seeded in a 24-well plate and cultured to reach confluence and then scraped with a sterile micropipette tip to create a denuded zone (gap) with a constant width (T_0). After removing cell debris with repeated PBS rinses, fresh serum-free DMEM medium with or without P4 (30 ng/mL) and/or other testing reagents were supplemented. Anti-mPRα antibody (1 : 200) and/or anti-mPRα blocking peptide (1 : 100) were added two hours before P4 treatment. PP1 (10 μM), AG 1478 (1 μM), wortmannin (0.1 μM), rapamycin (10 nM), and BpV (phen) (1 μM) were added one hour before P4 treatment. The cells migrated at various speeds toward the middle axis from both edges of the scraped gaps, depending upon the treatment of aforementioned testing reagents, when they were incubated continually for 16 hours. After incubation, the width of the gap ($T_{16\,\mathrm{hrs}}$) was measured by Image J. The rate of wound closure (WC) was calculated by the following equation: $\mathrm{WC} = 1 - (T_{16\,\mathrm{hrs}}/T_0) * 100\%$ [53]; as referring control cells, migration inhibiting rate of treated cells (MIR) $= 1 - (\mathrm{WC}_{\mathrm{treatment}}/\mathrm{WC}_{\mathrm{control}}) * 100\%$.

2.9. Invasion Assay. Cell invasion was assayed using the BD BioCoat Matrigel Invasion Chamber (BD Biosciences, MD, USA) [54]. Cells (4×10^4 cells/well) were seeded in the upper chamber of a 24-well BD transwell coated with Matrigel and cultured with DMEM medium containing 1% FBS. After treatment with P4 at 30 ng/mL for 24 hrs with or without PP1 treatment at 10 μM for one hour, the complete medium was applied to the lower chamber as chemoattractant. Cells were washed by PBS and then incubated for additional 16 hrs and the cells in the upper surface of the chamber membrane were then carefully removed with a cotton swab. Cells that invaded into the lower surface of the membrane were fixed with 10% buffered formalin and stained with hematoxylin solution. The number of invading cells (IC)

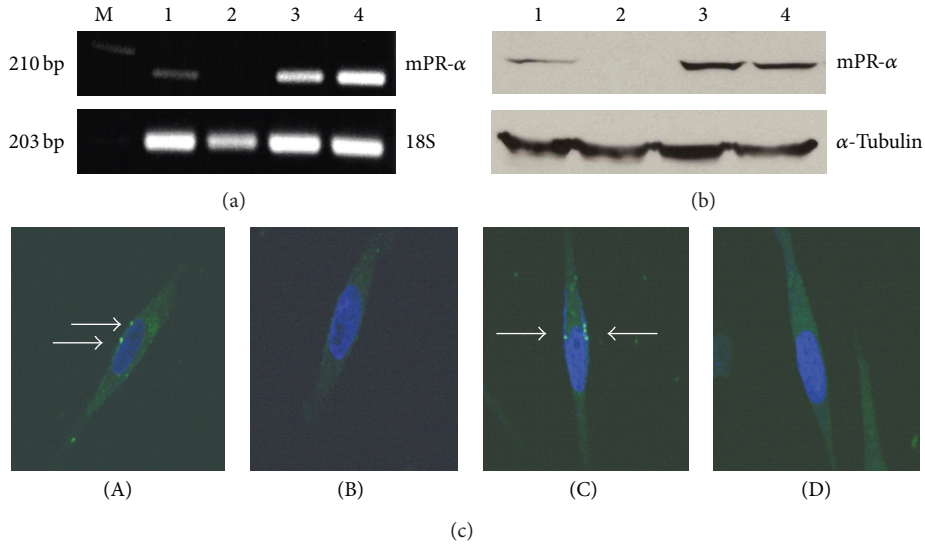

FIGURE 1: MPRα mRNA (a) and protein (b) expressions and receptor distribution (c) in various human BPBC cells. As shown in (a) and (b), the samples of mPRα mRNA and protein are indicated as "1–4," representing MB231Br, MB231, mPRα cDNA transfected MB231 (231 w/mPRα), and MB468 breast cancer cells, respectively. The expressions of 18S and α-tubulin are used as references. (c)(A)–(c)(C) show the results of incubating the cells with P4-BSA-FITC conjugates (white arrows indicate the specific binding sites), MB231Br cells, MB231 cells, and MB231 cells w/mPRα, respectively; (c)(D) shows the result of incubating MB231Br cells with P4-BSA-FITC conjugates and excessive free P4. Images were taken under confocal microscope using ×60 oil objective lens.

from twenty random microscopic fields (×200 magnification) was counted. Invasion inhibition rate (IIR) was calculated as follows: $\text{IIR} = 1 - (\text{IC}_{\text{treatment}}/\text{IC}_{\text{control}}) * 100\%$.

2.10. Statistical Analysis. The data was expressed as mean ± standard error (SE) and statistical differences between mean values were determined by Student's paired two-tailed t-test, followed by Fisher's protected least significance difference (PLSD). $P < 0.05$ was considered significant.

3. Results

3.1. Upregulation of mPRα Expression in the Brain Seeking MB231Br Cells. The brain seeking MB231Br cell line is increasingly used as a work horse model in brain metastatic studies, even though the molecular basis for its brain metastatic tropism is largely unknown [47, 48]. It was suggested that these cancer cells acquire the capacity to colonize brain *in vivo* following alternations in gene expression [47, 48]. In this study, we found that the expression of mPRα was upregulated from underdetectable to moderately positive at both the transcriptional and translational levels. As shown in Figure 1(a), the designated PCR band for mPRα in MB231Br cells was clearly seen at a moderate level (line 1), while there was no band for the parent MB231 cells (line 2) and there were very strong bands for the mPRα cDNA transfected MB231 cells and MB468 cells (lines 3 and 4). Using cell lysates isolated from those cells, an identical pattern of mPRα protein expression was documented by Western blot assays (Figure 1(b)). To determine if mPRα protein in MB231Br cells is translocated to the membrane compartment, we performed *in vitro* binding tests using a cell impermeable P4 conjugate (P4-BSA-FITC). After a short incubation (30 min), we observed clear fluorescent signals in the membrane of MB231Br cells (white arrows, Figure 1(c)(A)). Similar fluorescent signals were also seen in the membrane of the mPRα transfected MB231 cells (Figure 1(c)(C)), but not in the parent MB231 cells (Figure 1(c)(B)). To further demonstrate the binding specificity, we coincubated MB231Br cells with P4-BSA-FITC conjugate and excessive unconjugated free P4. As shown in Figure 1(c)(D), no fluorescent signals were shown in MB231Br cells. Binding studies with the fluorescent probe P4-BSA-FITC, which cannot enter cells because of the bulk moiety of BSA, confirms the presence of progestin-binding sites on the surface of cell membranes. This binding is specific because only free P4 was able to displace P4-BSA-FITC from breast cancer cells. This specificity was also confirmed by other studies that only unlabeled P4 human was able to substitute P4-BSA-FITC in pregnant myometrial cells *in vitro* whereas E2 and 11-deoxycortisone were ineffective [24, 25]. To study the function of mPRα receptor in MB231Br cells, we treated the cells with P4 at a series of concentrations (0, 30, and 60 ng/mL) for 48 hrs and demonstrated that the cell proliferation was inhibited in a dose dependent manner (Figure 2(a)). Cell morphological study showed that MB231Br cells without P4 incubation showed apparent mesenchymal phenotypes (Figures 2(b) and 2(c)), characterized by diverse sizes and spindle or elongated shapes, while, with P4 treatment, most of the cells showed epithelial-like phenotypes, featured by large and polygonal shapes or small oval shapes (Figures 2(d) and 2(e)).

3.2. Cell Migration of Human BPBC Cells in Response to Treatment of P4 and/or PPI. Further experiments were done

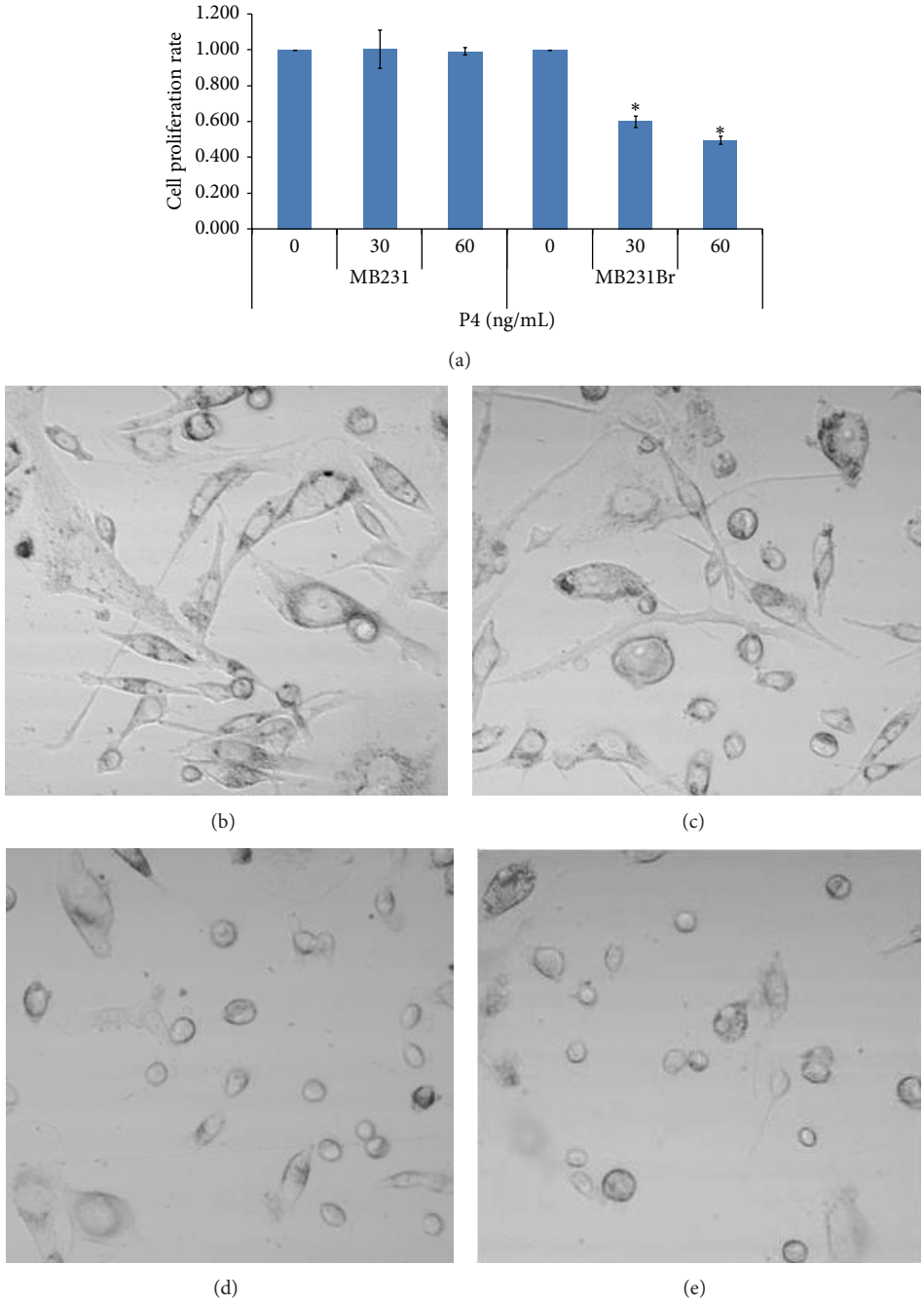

FIGURE 2: Effect of P4 on cell morphology and proliferation of MB231Br. (a) shows the results of cell proliferation assay of MB231Br and MB231 cells ($^{*}0.05 > P > 0.01$). (b) and (c) show the cell morphology of MB231Br without P4 treatment; (d) and (e) show the cells treated by P4 (30 ng/mL and 60 ng/mL). Images were taken under confocal microscope (DIC) using ×40 oil objective lens.

to determine the effect of P4 treatment on cell migration. Using a wound closure assay, we found that the wound closure (WC) of MB231Br cells was slower (even though only marginally significant) when the cells were treated with P4 (30 ng/mL) for 16 hrs as compared to the cells without P4 treatment (40.6 ± 2.7% versus 50.0 ± 0.6%, MIR 18.9%, $P_{WC} = 0.06$, Figure 3). To explore the pathways that may be associated with P4's effect, the cells were coincubated with P4 and/or a number of pathway inhibitors. As shown in Figure 3, the WC rate for cells treated by Src1 inhibitor (PP1) alone was minimally inhibited (MB231Br cells 35.7 ± 8.9% versus 50.0 ± 0.6%, MIR 28.5%, $P_{WC} = 0.11$), which was comparable to cells treated with P4 alone (P4 versus PP1 $P = 0.46$). Coincubation of P4 and PP1 resulted in a significant lower WC rate, as compared to the control (9.7 ± 4.5% versus 50.0 ± 0.6%, MIR 80.6%, $P_{WC} = 0.01$) or to P4 or PP1 treatment alone ($P_{WC} = 0.007$ or 0.02). In addition, coincubation of P4 and PP1 also caused the lowest WC rates in MB468 cells (16.7 ± 1.5%

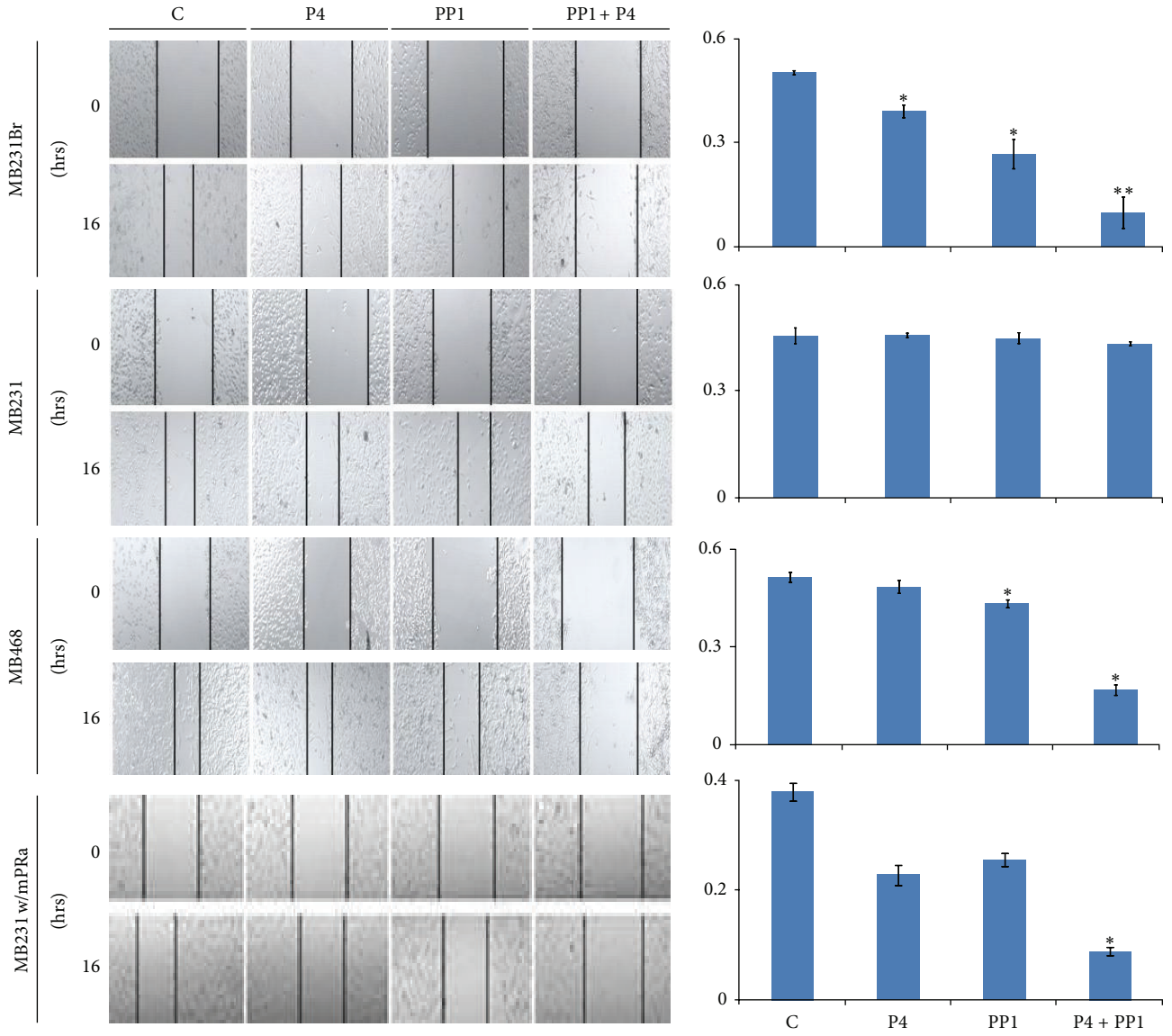

Figure 3: Effect of P4 + PP1 on cell migration of human BPBC cells. The left panel shows the wound closure assays of MB231Br, MB231, MB468, and mPRα transfected MB231 cells (231 w/mPRα), with or without P4 and/or PP1 treatments. Images were taken under confocal microscope using ×10 objective lens. The right panel shows the summarized data from four independent assays ($^{*}0.05 > P > 0.01$ and $^{**}P < 0.01$).

versus 51.1 ± 1.5%, MIR 67.3%, P_{WC} = 0.001) and mPRα cDNA transfected MB231 cells (11.5 ± 0.6% versus 37.9 ± 2.9%, MIR 69.6%, P_{WC} value 0.009, Figure 3). In parental MB231 cells, neither P4 alone nor P4 in combination with PP1 treatment showed significant changes in wound closure rates as compared to that of control (P4, PP1, and P4 + PP1 versus control = 45.7 ± 0.6%, 44.8 ± 1.5%, and 43.3 ± 0.6% versus 45.6 ± 2.3%, all P values > 0.05, Figure 3). These results indicated that P4 + PP1 synergistically inhibit cell migration of mPRα+ human BPBC cells, namely, MB231Br, MB468, and mPRα cDNA transfected MB231 cells.

The mPRα expressing MB231Br cells were also treated with P4 and other pathway inhibitors, such as the EGFR inhibitor AG 1478 (51.7 ± 1.9%), PI3K inhibitor wortmannin (48.6 ± 0.5%), the mTOR inhibitor rapamycin (49.6 ± 1.2%), and the PTEN inhibitor (BpV (phen)) (47.8 ± 3.7%). There were no obvious WC differences observed as compared to controls (MIR were 2.2%, 3.8%, 1.7%, and 5.4%, P values were 0.80, 0.66, 0.84, and 0.63, respectively, Figure S1) (see Supplementary Material available online at http://dx.doi.org/10.1155/2014/426429).

3.3. MPRα and Its Role in Cell Migration of the Brain Seeking MB231Br Cells. In order to clarify the role of P4 → mPRα signaling in cell migration, we preincubated MB231Br cells with anti-mPRα antibody to block the binding of P4 to mPRα receptor one hour before P4 + PP1 cotreatment. The inhibitory effects of P4 + PP1 on cell migration were abrogated (WC 46.8 ± 3.3% versus 47.5 ± 3.7%, MIR1.5%, P_{WC} = 0.82), indicating that mPRα receptor plays a key role

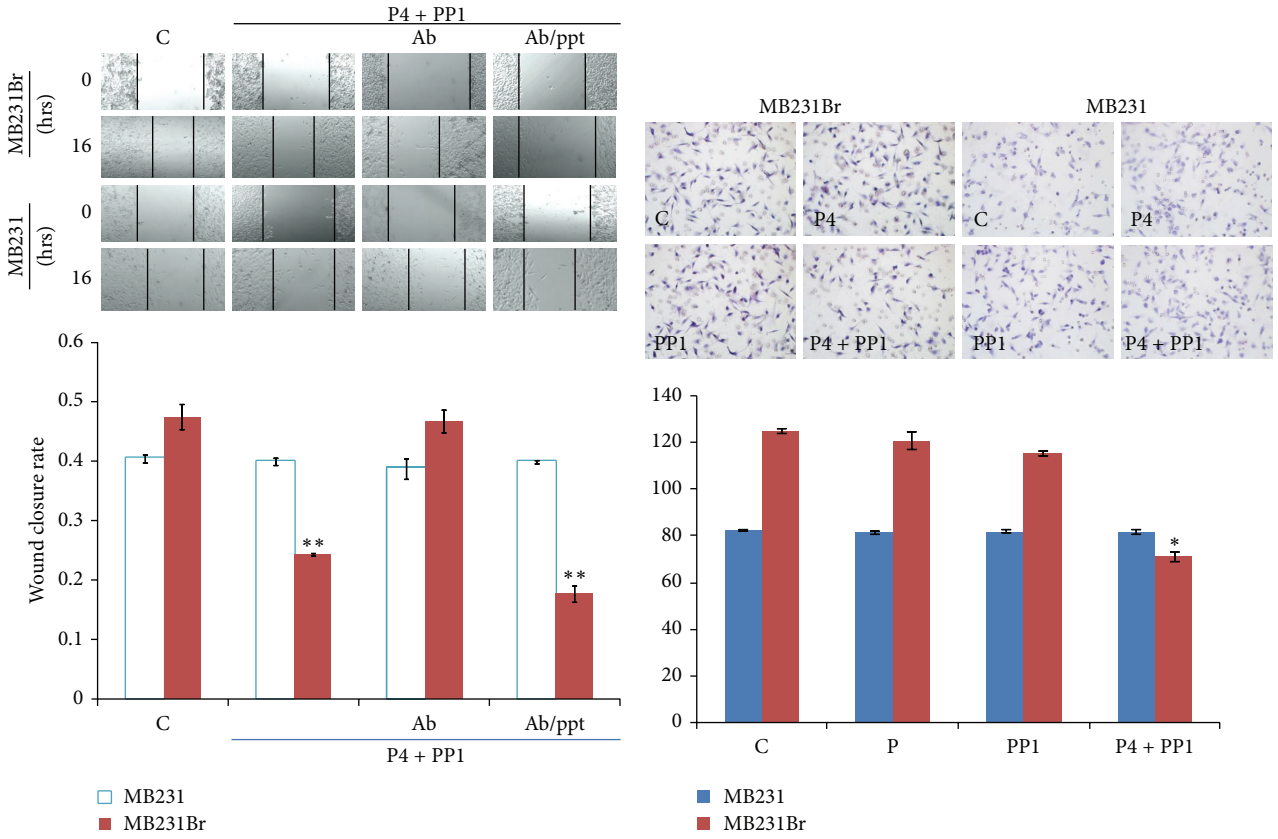

FIGURE 4: (a) Effect of P4 + PP1 on cell migration of MB231Br in presence of anti-mPRα antibody and mPRα blocking peptide. (Ab/ppt: anti-mPRα antibody and mPRα blocking peptide.) The up panels of (a) show the wound closure assays of MB231Br and MB231 cells with or without treatments as indicated. Images were taken using confocal microscope (×10 objective lens). The low panel of (a) shows the summarized data from two independent assays ($^{**}P < 0.01$). (b) Effect of P4 + PP1 on cell invasion of MB231Br. The left panel of (b) shows the cell invasion assays of MB231Br and MB231 cells with or without P4 and/or PP1 treatments as indicated. The right panel of (b) shows the summarized data from two independent experiments ($^{**}P < 0.01$).

in P4 + PP1 induced cell migratory inhibition. When the cells were preincubated with anti-mPRα antibody and excess anti-mPRα blocking peptide, the inhibitory effects of P4 + PP1 on cell migration of MB231Br cells were restored (17.7 ± 2.3% versus 47.5 ± 3.7%, MIR 62.7%, $P_{WC} = 0.001$, Figure 4(a)).

3.4. Cell Invasion of the Brain Seeking MB231Br Cells in Response to P4 and/or PP1 Treatment. As cancer invasion *in vivo* is a three-dimensional process involving transendothelial migration and penetration through extracellular matrix, a 3D cell invasion model could further delineate the role of P4 and/or PP1 on metastatic potential of MB231Br cells [55]. To assess the role of P4 and PP1 on cell invasion of MB231Br cells, a cell invasion assay was performed. After P4 and/or PP1 treatment for 16 hrs, the number of cells that invaded into the lower chamber of Matrigel (IC) was decreased as compared to control (71 ± 2 versus 125 ± 1 cells, IIR 43.2%, $P < 0.001$), but treatment with either P4 or PP1 alone was ineffective (121 ± 4 and 116 ± 1 cells, IIR were 3.2% and 7.2%; P_{IC} values were 0.61 and 0.22). In parent MB231 cells, there were no obvious IC changes with or without P4 and/or PP1 treatment, as expected (Figure 4(b)).

3.5. Neither Nuclear PR Nor PGRMC1 Plays a Key Role in Mediating P4 + PP1's Inhibitory Effects on Cell Migration of MB231Br Cells. The expression of PR in basal phenotype breast cancer cells (i.e., MB468 cells) may be induced by P4 treatment, even though the extent of induction is very low [23]. To clarify if induction of endogenous PR expression has a role in the P4 induced cell migratory inhibition, we preincubated MB231Br cells with MIF, a PR antagonist, before P4 and/or PP1 treatment. It was found that wound closure rates were not affected after P4 and/or PP1 treatment (P4 versus MIF + P4, PP1 versus MIF + PP1, and P4 + PP1 versus MIF + P4 + PP1 were 38.9±1.8% versus 35.3±5.1%, 26.6±4.2% versus 36.1 ± 5.6%, and 9.7 ± 4.5% versus 14.2 ± 4.9%; all P_{WC} values > 0.05, Figure 5(a)).

In addition to mPRα, PGRMC1 has been implicated in membrane-initiated progesterone signaling [56]. It is unclear whether mPRα functions alone or requires PGRMC1 as a comediator. In a Western blot assay, the protein expression of PGRMC1was observed noticeably in MB231Br cells but showed minimal changes with P4 and/or PP1 treatment (Figure 5(b)). We then preincubated MB231Br cells with PGRMC1 antibody to block or interfere with the function of

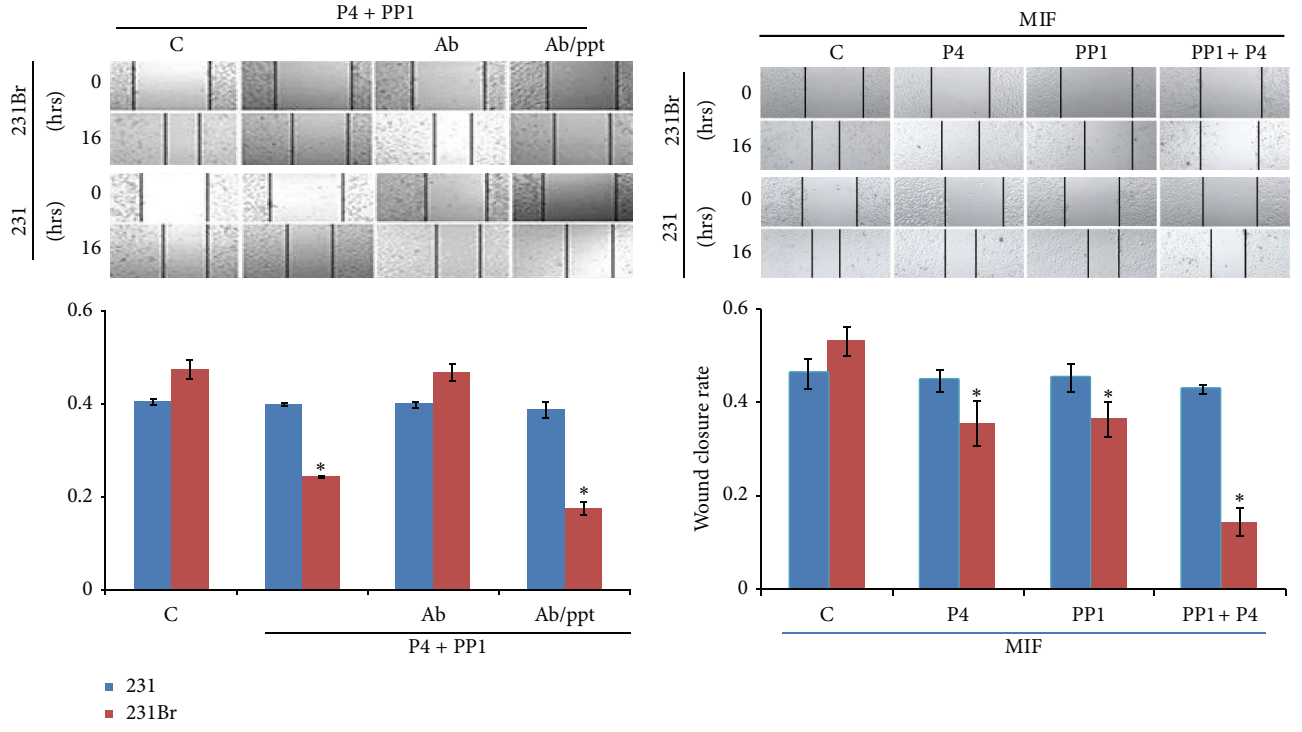

(a)

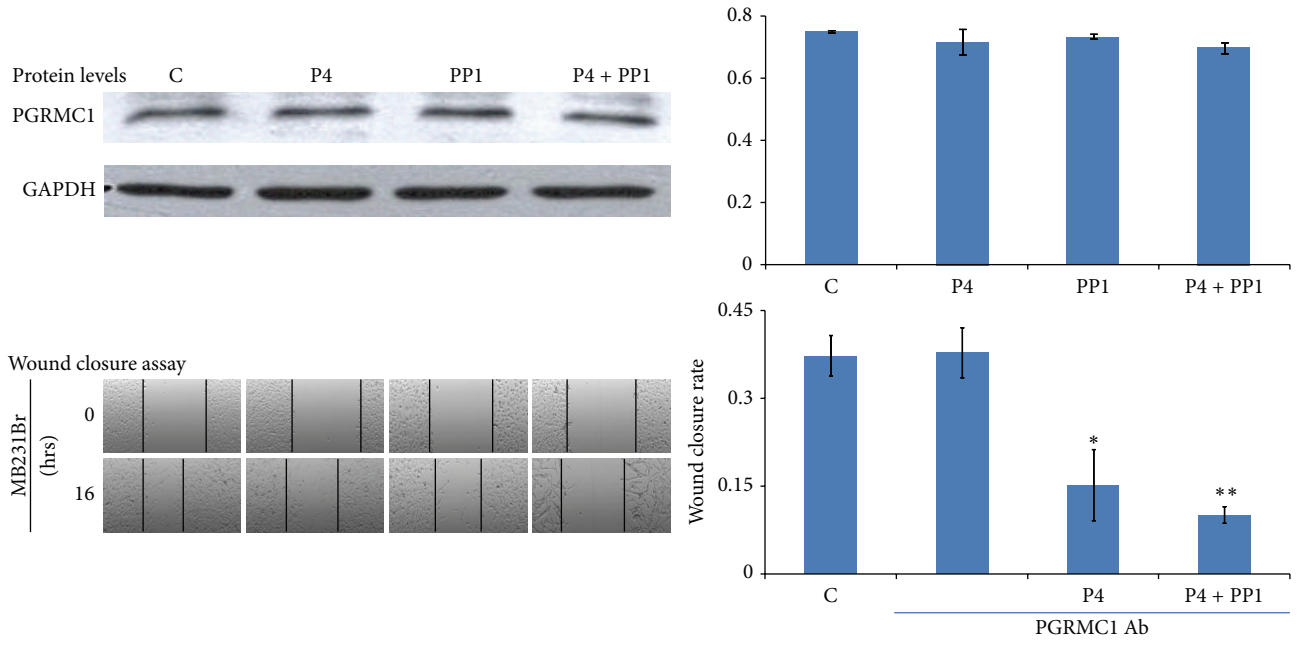

(b)

Figure 5: (a) Effect of P4 + PP1 on cell migration of MB231Br in presence of MIF. The up panels of (a) show the wound closure assays of MB231Br and MB231 cells with or without P4 and/or PP1 treatments as indicated. All of the cells were preincubated with MIF. Images were taken under confocal microscope using ×10 objective lens. The lower panel of (a) shows the summarized data from two independent assays ($^{*}0.05 > P > 0.01$). (b) Effect of P4 + PP1 on cell migration of MB231Br in presence of anti-PGRMC1 antibody. Growth-arrested MB231Br and MB231 cells were treated with or without P4 and/or PP1 treatment as indicated. Western blot assays for evaluating PGRMC1 expression were performed. The up panel of (b) shows the representative image from three Western blot assays. The middle panel of (b) shows the wound closure assays of MB231Br cells with or without P4 and/or PP1 treatments as indicated. Images were taken under confocal microscope using ×10 objective lens. The graph in the bottom of (b) shows the summarized data from four independent assays ($^{*}0.05 > P > 0.01$, $^{**}P < 0.01$).

PGRMC1 protein one hour before P4 and/or PP1 treatment. The wound closure rates, in the presence of anti-PGRMC1 antibody, demonstrated no change on cell migration pattern as compared to those induced by P4 alone or by P4 + PP1 (WC 15.2 ± 6.1% and 10.2 ± 1.4% versus 37.3 ± 3.4%, P values were 0.047 and 0.008, resp.). Treatment of anti-PGRMC1 antibody alone had no effect on cell migration (37.8 ± 4.3% versus 37.3 ± 3.4%, $P = 0.93$).

3.6. Molecular Pathways Involved in the P4 + PP1 Inhibited Cell Migration of MB231Br Cells. Based upon the results of cell migration assays, synergistic effect of P4 and PP1 on cell migration and invasion of MB231Br cells was suggested. Moreover, P4 has been reported to signal via Src family kinases for the formation of focal adhesion complex via focal adhesion kinase (FAK, a key component for tumor metastasis) phosphorylation at Tyr (397) [57]. To confirm the molecular mechanisms underlying P4 + PP1's action, we evaluated the phosphorylation of Src and FAK using Western blot assay. It was found that the level of phosphor-FAK in MB231Br cells was inhibited by P4 + PP1 treatment significantly (as compare to that of control, 43.6% versus 100%, $P = 0.009$), while the status of Src phosphorylation was not changed by P4 + PP1 cotreatment. P4 or PP1 treatment alone did not change the levels of phosphor-FAK in MB231Br cells (94.68%, 81.1% versus 100%, all P values > 0.05) (Figure 6(a)). We also investigated the effect of P4 and/or PP1 on expression of other selected cancer metastasis relevant proteins, such as MMP9, VEGF, and KCNMA1 [58]. The expression levels of MMP9 (79.3% versus 100%, $P = 0.009$), VEGF (33.2% versus 100%, $P = 0.04$), and KCNMA1 (77.6% versus 100%, $P = 0.02$) were reduced by P4 + PP1 cotreatment in MB231Br cells remarkably but again not by P4 or PP1 individual treatments as compared to controls (All P values > 0.05, Figure 6(b)).

4. Discussion

4.1. Upregulation of MPRα May Contribute to the Brain Metastatic Tropism of MB231Br Cells. The role of progesterone (P4) in breast cancer development has attracted substantial interest. It is believed that the physiological action of P4 is mediated through either nuclear PR or membrane-bound receptors. In this study, using RT-PCR and Western blotting assays, we first showed the expression of mPRα in the membrane of MB231Br cells, a functional site of this hormonal receptor. To study the function of mPRα in MB231Br cells, we demonstrated that P4 treatment inhibits cell proliferation (Figure 2(a)) and reverses cell morphology from mesenchymal phenotypes to epithelial-like phenotypes (Figures 2(b)–2(d)), while in mPRα negative MB231 cells P4 treatment had no effect. These results were consistent with our previous results on MB468 cells [23]. Khan et al. performed a genowide expression profiling on two human BPBC cell lines—parental MB231 and brain seeking MB231Br cells [59]. They found elevated levels of genes that promote cell motility and invasion, while genes that prevent cancer metastasis were downregulated in MB231Br cells (compared to parental MB231 cells) [60–62]. Bos et al. compared the gene expression profiles of the brain seeking cells from MDA-MB-231 and CN34 cells from the tumor of an ER-patient [50]. They found 243 genes differentially expressed between the brain metastasis and parental cell lines. Of those, the expression of 17 genes was correlated with brain relapse in patient samples without association with bone, liver, or lymph node metastasis [63]. It was assumed that these altered gene expression profiles acquainted from a series of *in vivo/ex vivo* selections may facilitate the successful colonization in brain.

4.2. MPRα May Serve as a Key Mediator for P4's Action on Cell Migratory and Invasion Inhibition in MB231Br Cells. Progesterone is known to play a profound role in breast cancer cell migration. In this study, we showed that P4 treatment alone can slightly inhibit, rather than enhance, the cell migration of MB231Br cells; more interestingly, treatment of P4 plus PP1 can significantly inhibit cell migration of MB231Br cells. Since PP1 treatment alone inhibited cell migration only at a moderate level, which was comparable to P4, we assumed that combinational treatment with both can synergize the molecular signal magnitude and vigorously inhibit cell migration *in vitro*. Similarly, in cell invasion assay, synergistic results were also obtained from the cells which were treated by P4 + PP1 (IIR 43.2%) but not by P4 or PP1 alone (IIR = 3.2% and 7.2%), while Fu et al. found that cell migration and invasion were both enhanced by all the P4 and its derivatives tested in T47-D cells (ER+/PR+) [64, 65]. Different results may be due to various cell lines with different PR and ER expression.

Since parent MB231 cells do not contain full-length or C-terminus PRs [66], we assumed that the acquired expression of mPRα may serve as a key mediator for P4's action in MB231Br cells. This assumption was supported by the following findings. (1) Block the binding of P4 to mPRα receptor by preincubating MB231Br cells with anti-mPRα antibody, which abrogated the inhibitory effects of P4 + PP1 on cell migration. Preincubating the cells with anti-mPRα antibody and excess anti-mPRα blocking peptide, the inhibitory effects of P4 + PP1 on cell migration were unaffected. These results indicated that the role of mPRα in cell migration and regulation is essential. (2) P4 treatment may upregulate PR expression in human BPBC cells (e.g., MB231 cells) [23, 67], which could mediate the effect of P4. To exclude the potential role of PR in this study, we preincubated the cells with MIF, a P4 antagonist, and found that it did not affect P4's and/or PP1's effects on MB231Br cell migration. (3) PGRMC1 is required for some aspects of P4 signaling in estrogen receptor-negative breast tumors through an unidentified mechanism [68, 69]. Thomas et al. demonstrated that overexpression of human PGRMC1 in nuclear PR negative breast cancer cell lines causes increased expression of mPRα on cell membranes and increased specific P4 binding [70]. To exclude the potential role of PGRMC1 in this study, we demonstrated that P4 and/or PP1 treatment had no effect on PGRMC1 expression in MB231Br cells, as compared to that in vehicle treated control cells. In addition, coincubating the MB231Br cells with anti-PGRMC1 antibody and P4 and/or PP1 did not affect the cell migration patterns. These results suggested that PGRMC1 and its signaling pathways

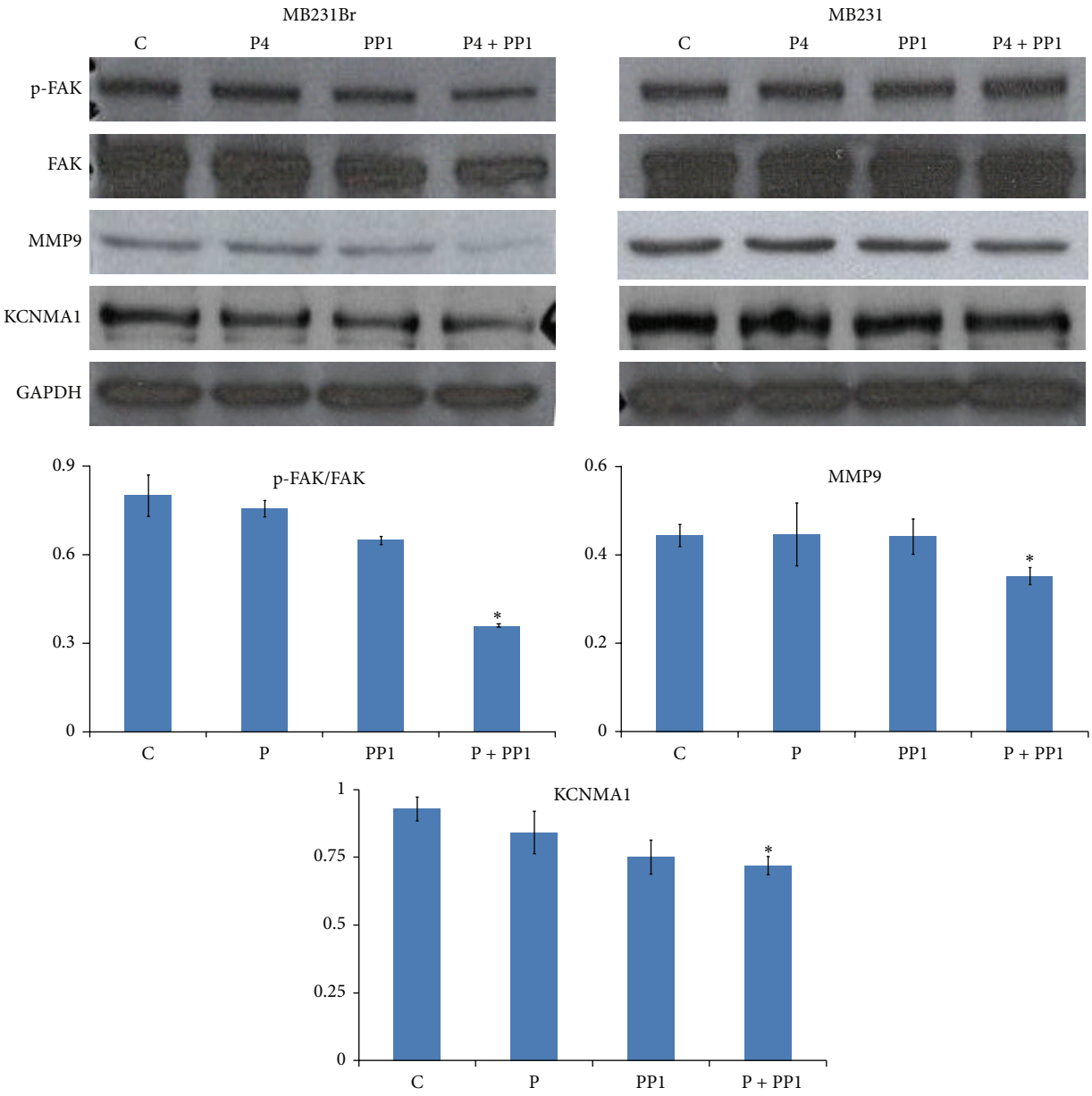

Figure 6: Effect of P4 + PP1 on FAK phosphorylation and expression of MMP-9 and KCNMA1 in MB231Br cells. Growth-arrested MB231Br and MB231 cells were treated with or without P4 and/or PP1 treatment as indicated. Western blot assays for evaluating the status of Src and FAK phosphorylation and expression of MMP-9, VEGF, and KCNMA1 were performed with proper antibodies. The up panel shows the representative image from three Western blot assays. The graph in the bottom shows the summarized data from three independent assays ($^{*}0.05 > P > 0.01$).

may not be involved in the roles of P4 and PP1 on cell migration.

4.3. Molecular Pathways Involved in P4 + PP1/mPRα Signaling. Progesterone exerts rapid nongenomic actions which are triggered by P4 binding to mPRα [34–36] and subsequently induces a series of alterations in secondary messenger pathways through activation of pertussis toxin-sensitive inhibitory G-proteins, to activate MAPK/Erk 1/2 pathway [32, 33, 37, 38]. We recently reported that the signaling cascade of P4 induced mesenchymal repression of human BPBC cells through caveolae bound signaling molecules, namely, Cav-1, EGFR, and PI3K. We also observed that the Src family kinase inhibitor (PP1) blocked the P4's action on proteins that control cell epithelial differentiation but not on the proteins that control cell mesenchymal differentiation. Src has been reported to be a starting point for many biochemical cascades and exerts a profound effect on focal adhesion systems and cytoskeleton reorganization and thereby influences cancer cell migration and invasion as well as other tumor progression-related events [71]. In this report, we showed that P4 + PP1 (a Src family inhibitor [72, 73]) synergistically inhibited the cell migration of the mPRα expressing MB231Br cells significantly. Focal adhesion

kinase (FAK) is a downstream component of Src signaling pathway controlling cell motility [74]. Through multifaceted molecular connections, FAK controls cell movement by regulating the cytoskeleton structures, cell adhesion sites, and membrane protrusions [74, 75]. In presence of PR, P4 could induce the phosphorylation and activation of FAK [76]. For example, MB231 breast cancer cells transfected with PR were exposed to P4 and displayed an increased expression of phosphorylated FAK and formation of FA complexes, which led to an enhanced cell migration and invasion [76]. In human BPBC cell models, which are depleted of nuclear PR but mPRα positive, P4 and PP1 cotreatment induced significant FAK dephosphorylation (rather than phosphorylation), while P4 or PP1 individual treatment did not affect the status of FAK. This may explain the diverse roles of P4 in different human BPBC and non-BPBC cancer cells. Also, the roles of other pathway inhibitors on cell migration of MB231Br cells were also tested. Cotreatment of these cells with P4 and EGFR inhibitor (AG 1478) or PI3K inhibitor (wortmannin) or mTOR inhibitor (rapamycin) and/or PTEN inhibitor (BpV (phen)) had no obvious WC differences observed as compared to controls (Figure S1).

To determine the downstream effector protein molecules of Src/FAK pathway, we studied metastatic relevant protein expression profiles. Matrix metalloproteinases (MMPs) and VEGF have been implicated in several aspects of tumor progression, such as invasion through basement membrane and interstitial matrices, angiogenesis, and tumor cell growth. In the present study, we found that MB231Br cells express MMP-9 and VEGF at comparable levels as that of MB231 cells. In response to P4 or PP1 treatment alone, the expression of MMP9 and VEGF in MB231Br cells exhibited minimal changes; however, combination treatment with both induced significant reduction in MMP9 and VEGF expression, a similar pattern as that of FAK dephosphorylation, supporting these prometastatic proteins as the downstream effectors of Src/FAK pathway. KCNMA1 (large conductive calcium-activated potassium channel, subfamily M, alpha member 1) is a pore forming α-subunit of the large-conductance calcium- and voltage-activated potassium channel (BK_{Ca}) [77]. KCNMA1 expression was reported in metastatic breast cancer cells and increased BKCa channel activity might associate with greater invasiveness and transendothelial migration [58]. It was assumed that the relative abundance of BKCa channel expression in brain metastatic breast cancer may provide a unique opportunity to identify breast tumors that are at high risk for brain metastasis [58]. In this study, we found that KCNMA1 expression was also inhibited in MB231Br cells in a similar pattern as compared with that of FAK dephosphorylation and MMP9 expression in response to P4 and/or PP1 treatment. We assumed that MMP-9 and KCNMA1 serve as terminal effects of the Src/FAK signal pathway.

5. Conclusions

In summary, using brain seeking MB231Br cells and other human BPBC cell lines as models, we identified an mPRα mediated pathway that involves Src/FAK and a chain of downstream cell signaling components. This molecular pathway could be inhibited by incubating MB231Br cells with P4 and PP1 concurrently. It was assumed that PP1 enhances the P4's effect on FAK dephosphorylation, MMP9, VEGF, and KCNMA1 downregulation and eventually inhibits cell migration synergistically. Our study has provided a mechanistic view on the effects of P4 as a promising physiological anticancer agent, through mPRα $\rightarrow$ Src/FAK relevant signal transduction pathways in human BPBC cells.

Abbreviations

BPBC: Basal phenotype breast cancers
P4: Progesterone
MB468: MDA-MB468 cells
EMT: Epithelial-mesenchymal transition
mPRα: Membrane progesterone receptor α
MB231: MDA-MB231 cells
PRs: Progesterone receptors
ATCC: American Type Culture Collection
IHC: Immunohistochemistry
TNBC: Triple negative cancers.

Conflict of Interests

The authors declare that they have no competing interests.

Acknowledgments

The authors thank Dr. Peter Thomas (Marine Science Institute, University of Texas at Austin) for providing mPRα plasmid and kind consultancy and Dr. Hima Bindu Chunduri and Dr. Prem Sharma (Atlanta Research & Educational Foundation, Atlanta VA Medical Center, GA) for their assistance in plasmid DNA isolation. This study was supported by the Emory University Research ACTSI Award (S. You), Atlanta Research and Education Foundation Bridge Fund (S. You), and China Scholarship Council and Central South University (Mingxuan Xie and Qiong Chen).

References

[1] M. T. Weigel and M. Dowsett, "Current and emerging biomarkers in breast cancer: prognosis and prediction," *Endocrine-Related Cancer*, vol. 17, no. 4, pp. R245–R262, 2010.

[2] X. Cui, R. Schiff, G. Arpino, C. K. Osborne, and A. V. Lee, "Biology of progesterone receptor loss in breast cancer and its implications for endocrine therapy," *Journal of Clinical Oncology*, vol. 23, no. 30, pp. 7721–7735, 2005.

[3] J. Alexieva-Figusch, H. A. van Gilse, W. C. J. Hop, C. H. Phoa, J. Blonk-van der Wijst, and R. E. Treurniet, "Progestin therapy in advanced breast cancer: megestrol acetate: an evaluation of 160 treated cases," *Cancer*, vol. 46, no. 11, pp. 2369–2372, 1980.

[4] P. A. Johnson, H. Muss, P. Bonomi et al., "Megestrol acetate as primary hormonal therapy for advanced breast cancer," *Seminars in Oncology*, vol. 15, supplement 1, no. 2, pp. 34–37, 1988.

[5] R. Nishimura, K. Nagao, M. Matsuda et al., "Predictive value of serum medroxyprogesterone acetate concentration for

response in advanced or recurrent breast cancer," *European Journal of Cancer Part A*, vol. 33, no. 9, pp. 1407–1412, 1997.

[6] S. Otani, N. Toyota, K. Nozaka et al., "Successful combination therapy with 5′-DFUR and MPA for breast cancer with spinal and vertebral metastases," *Gan to Kagaku Ryoho*, vol. 31, no. 13, pp. 2151–2153, 2004.

[7] T. Otsuka, Y. Terashima, and S. Tashiro, "A case of long surviving advanced recurrent breast cancer with multiple bone metastases responding to treatment with 5'-DFUR combined with MPA," *Gan To Kagaku Ryoho*, vol. 29, no. 2, pp. 313–316, 2002.

[8] R. Zaucha, K. Sosińska-Mielcarek, and J. Jassem, "Long-term survival of a patient with primarily chemo-resistant metastatic breast cancer treated with medroxyprogesterone acetate," *Breast*, vol. 13, no. 4, pp. 321–324, 2004.

[9] T. Toyama, H. Yamashita, Y. Hara, Y. Hikosaka, S. Kobayashi, and H. Iwase, "Successful management of breast cancer with liver metastases with medroxyprogesterone acetate treatment," *International Journal of Clinical Oncology*, vol. 6, no. 6, pp. 306–309, 2001.

[10] H. Mio, "A case of postoperative recurrent breast cancer with multiple lung metastases that completely responded to combination therapy of docetaxel (TXT) and medroxyprogesterone acetate (MPA)," *Cancer & Chemotherapy*, vol. 30, no. 7, pp. 985–988, 2003.

[11] D. Generali, F. M. Buffa, A. Berruti et al., "Phosphorylated ERα, HIF-1α, and MAPK signaling as predictors of primary endocrine treatment response and resistance in patients with breast cancer," *Journal of Clinical Oncology*, vol. 27, no. 2, pp. 227–234, 2009.

[12] P. Thomas, C. Tubbs, and V. F. Garry, "Progestin functions in vertebrate gametes mediated by membrane progestin receptors (mPRs): Identification of mPRα on human sperm and its association with sperm motility," *Steroids*, vol. 74, no. 7, pp. 614–621, 2009.

[13] L. S. Cooper, C. E. Gillett, N. K. Patel, D. M. Barnes, and I. S. Fentiman, "Survival of premenopausal breast carcinoma patients in relation to menstrual cycle timing of surgery and estrogen receptor/progesterone receptor status of the primary tumor," *Cancer*, vol. 86, no. 10, pp. 2053–2058, 1999.

[14] Z. Saad, V. Bramwell, J. Duff et al., "Timing of surgery in relation to the menstrual cycle in premenopausal women with operable breast cancer," *British Journal of Surgery*, vol. 81, no. 2, pp. 217–220, 1994.

[15] K. Bove, D. W. Lincoln, P. A. Wood, and W. J. M. Hrushesky, "Fertility cycle influence on surgical breast cancer cure," *Breast Cancer Research and Treatment*, vol. 75, no. 1, pp. 65–72, 2002.

[16] W. J. M. Hrushesky, S. A. Gruber, R. B. Sothern et al., "Natural killer cell activity: age, estrous- and circadian-stage dependence and inverse correlation with metastatic potential," *Journal of the National Cancer Institute*, vol. 80, no. 15, pp. 1232–1237, 1988.

[17] L. Sivaraman and D. Medina, "Hormone-induced protection against breast cancer," *Journal of Mammary Gland Biology and Neoplasia*, vol. 7, no. 1, pp. 77–92, 2002.

[18] D. Medina, "Mammary developmental fate and breast cancer risk," *Endocrine-Related Cancer*, vol. 12, no. 3, pp. 483–495, 2005.

[19] J. E. Rossouw, G. L. Anderson, R. L. Prentice et al., "Risks and benefits of estrogen plus progestin in healthy postmenopausal women: principal results from the women's health initiative randomized controlled trial," *Journal of the American Medical Association*, vol. 288, no. 3, pp. 321–333, 2002.

[20] G. L. Anderson, M. Limacher, A. R. Assaf et al., "Effects of conjugated equine estrogen in postmenopausal women with hysterectomy: the Women's Health Initiative randomized controlled trial," *JAMA*, vol. 291, no. 14, pp. 1701–1712, 2004.

[21] C. A. Lange, J. K. Richer, and K. B. Horwitz, "Hypothesis: progesterone primes breast cancer cells for cross-talk with proliferative or antiproliferative signals," *Molecular Endocrinology*, vol. 13, no. 6, pp. 829–836, 1999.

[22] E. M. McGowan, S. Saad, L. J. Bendall, K. F. Bradstock, and C. L. Clarke, "Effect of progesterone receptor A predominance on breast cancer cell migration into bone marrow fibroblasts," *Breast Cancer Research and Treatment*, vol. 83, no. 3, pp. 211–220, 2004.

[23] L. Zuo, W. Li, and S. You, "Progesterone reverses the mesenchymal phenotypes of basal phenotype breast cancer cells via a membrane progesterone receptor mediated pathway," *Breast Cancer Research*, vol. 12, article R34, 2010.

[24] E. Karteris, S. Zervou, Y. Pang et al., "Progesterone signaling in human myometrium through two novel membrane G protein-coupled receptors: potential role in functional progesterone withdrawal at term," *Molecular Endocrinology*, vol. 20, no. 7, pp. 1519–1534, 2006.

[25] C. Tubbs and P. Thomas, "Progestin signaling through an olfactory G protein and membrane progestin receptor-α in Atlantic croaker sperm: potential role in induction of sperm hypermotility," *Endocrinology*, vol. 150, no. 1, pp. 473–484, 2009.

[26] V. Boonyaratanakornkit, E. McGowan, L. Sherman, M. A. Mancini, B. J. Cheskis, and D. P. Edwards, "The role of extranuclear signaling actions of progesterone receptor in mediating progesterone regulation of gene expression and the cell cycle," *Molecular Endocrinology*, vol. 21, no. 2, pp. 359–375, 2007.

[27] G. R. Ehring, H. H. Kerschbaum, C. Eder et al., "A nongenomic mechanism for progesterone-mediated immunosuppression: inhibition of K^+ channels, Ca^{2+} signaling, and gene expression in T lymphocytes," *The Journal of Experimental Medicine*, vol. 188, no. 9, pp. 1593–1602, 1998.

[28] R. Colomer, S. Montero, A. Lluch et al., "Circulating HER2 extracellular domain and resistance to chemotherapy in advanced breast cancer," *Clinical Cancer Research*, vol. 6, no. 6, pp. 2356–2362, 2000.

[29] O.-K. Park-Sarge, T. G. Parmer, Y. Gu, and G. Gibori, "Does the rat corpus luteum express the progesterone receptor gene?" *Endocrinology*, vol. 136, no. 4, pp. 1537–1543, 1995.

[30] P. Thomas, Y. Pang, J. Dong et al., "Steroid and G protein binding characteristics of the seatrout and human progestin membrane receptor α subtypes and their evolutionary origins," *Endocrinology*, vol. 148, no. 2, pp. 705–718, 2007.

[31] C. Dosiou, A. E. Hamilton, Y. Pang et al., "Expression of membrane progesterone receptors on human T lymphocytes and Jurkat cells and activation of G-proteins by progesterone," *Journal of Endocrinology*, vol. 196, no. 1, pp. 67–77, 2008.

[32] P. Thomas, "Characteristics of membrane progestin receptor alpha (mPRalpha) and progesterone membrane receptor component 1 (PGMRC1) and their roles in mediating rapid progestin actions," *Frontiers in Neuroendocrinology*, vol. 29, no. 2, pp. 292–312, 2008.

[33] G. E. Dressing and P. Thomas, "Identification of membrane progestin receptors in human breast cancer cell lines and biopsies and their potential involvement in breast cancer," *Steroids*, vol. 72, no. 2, pp. 111–116, 2007.

[34] E. Falkenstein, H.-C. Tillmann, M. Christ, M. Feuring, and M. Wehling, "Multiple actions of steroid hormones—a focus on rapid, nongenomic effects," *Pharmacological Reviews*, vol. 52, no. 4, pp. 513–555, 2000.

[35] R. Lösel and M. Wehling, "Nongenomic actions of steroid hormones," *Nature Reviews Molecular Cell Biology*, vol. 4, no. 1, pp. 46–56, 2003.

[36] R. Lösel, S. Breiter, M. Seyfert, M. Wehling, and E. Falkenstein, "Classic and non-classic progesterone receptors are both expressed in human spermatozoa," *Hormone and Metabolic Research*, vol. 37, no. 1, pp. 10–14, 2005.

[37] N. Sleiter, Y. Pang, C. Park et al., "Progesterone receptor A (PRA) and PRB-independent effects of progesterone on gonadotropin-releasing hormone release," *Endocrinology*, vol. 150, no. 8, pp. 3833–3844, 2009.

[38] Y. Zhu, C. D. Rice, Y. Pang, M. Pace, and P. Thomas, "Cloning, expression, and characterization of a membrane progestin receptor and evidence it is an intermediary in meiotic maturation of fish oocytes," *Proceedings of the National Academy of Sciences of the United States of America*, vol. 100, no. 5, pp. 2231–2236, 2003.

[39] W. Xu, X. Yuan, Y. J. Jung et al., "The heat shock protein 90 inhibitor geldanamycin and the ErbB inhibitor ZD1839 promote rapid PP1 phosphatase-dependent inactivation of AKT in ErbB2 overexpressing breast cancer cells," *Cancer Research*, vol. 63, no. 22, pp. 7777–7784, 2003.

[40] Y. Hirokawa, A. Levitzki, G. Lessene et al., "Signal therapy of human pancreatic cancer and *NF1*-deficient breast cancer xenograft in mice by a combination of PP1 and GL-2003, anti-PAK1 drugs (Tyr-kinase inhibitors)," *Cancer Letters*, vol. 245, no. 1-2, pp. 242–251, 2007.

[41] A. C. Bishop, C.-Y. Kung, K. Shah, L. Witucki, K. M. Shokat, and Y. Liu, "Generation of monospecific nanomolar tyrosine kinase inhibitors via a chemical genetic approach," *Journal of the American Chemical Society*, vol. 121, no. 4, pp. 627–631, 1999.

[42] S. Cleator, W. Heller, and R. C. Coombes, "Triple-negative breast cancer: therapeutic options," *The Lancet Oncology*, vol. 8, no. 3, pp. 235–244, 2007.

[43] N. U. Lin, E. Claus, J. Sohl, A. R. Razzak, A. Arnaout, and E. P. Winer, "Sites of distant recurrence and clinical outcomes in patients with metastatic triple-negative breast cancer: high incidence of central nervous system metastases," *Cancer*, vol. 113, no. 10, pp. 2638–2645, 2008.

[44] R. M. Neve, K. Chin, J. Fridlyand et al., "A collection of breast cancer cell lines for the study of functionally distinct cancer subtypes," *Cancer Cell*, vol. 10, no. 6, pp. 515–527, 2006.

[45] Y. Kang, P. M. Siegel, W. Shu et al., "A multigenic program mediating breast cancer metastasis to bone," *Cancer Cell*, vol. 3, no. 6, pp. 537–549, 2003.

[46] A. J. Minn, G. P. Gupta, P. M. Siegel et al., "Genes that mediate breast cancer metastasis to lung," *Nature*, vol. 436, no. 7050, pp. 518–524, 2005.

[47] T. Yoneda, P. J. Williams, T. Hiraga, M. Niewolna, and R. Nishimura, "A bone-seeking clone exhibits different biological properties from the MDA-MB-231 parental human breast cancer cells and a brain-seeking clone in vivo and in vitro," *Journal of Bone and Mineral Research*, vol. 16, no. 8, pp. 1486–1495, 2001.

[48] R. J. Weil, D. C. Palmieri, J. L. Bronder, A. M. Stark, and P. S. Steeg, "Breast cancer metastasis to the central nervous system," *The American Journal of Pathology*, vol. 167, no. 4, pp. 913–920, 2005.

[49] E. I. Chen, J. Hewel, J. S. Krueger et al., "Adaptation of energy metabolism in breast cancer brain metastases," *Cancer Research*, vol. 67, no. 4, pp. 1472–1486, 2007.

[50] P. D. Bos, X. H. Zhang, C. Nadal et al., "Genes that mediate breast cancer metastasis to the brain," *Nature*, vol. 459, no. 7249, pp. 1005–1009, 2009.

[51] V. T. Ciavatta, M. Kim, P. Wong et al., "Retinal expression of *Fgf2* in RCS rats with subretinal microphotodiode array," *Investigative Ophthalmology & Visual Science*, vol. 50, no. 10, pp. 4523–4530, 2009.

[52] L. Min, Q. Chen, S. He, S. Liu, and Y. Ma, "Hypoxia-induced increases in A549/CDDP cell drug resistance are reversed," *Molecular Medicine Reports*, vol. 5, no. 1, pp. 228–232, 2012.

[53] N. Dhanesuan, J. A. Sharp, T. Blick, J. T. Price, and E. W. Thompson, "Doxycycline-inducible expression of SPARC/Osteonectin/BM40 in MDA-MB-231 human breast cancer cells results in growth inhibition," *Breast Cancer Research and Treatment*, vol. 75, no. 1, pp. 73–85, 2002.

[54] B. Desai, T. Ma, and M. A. Chellaiah, "Invadopodia and matrix degradation, a new property of prostate cancer cells during migration and invasion," *The Journal of Biological Chemistry*, vol. 283, no. 20, pp. 13856–13866, 2008.

[55] C. Cougoule, V. Le Cabec, R. Poincloux et al., "Three-dimensional migration of macrophages requires Hck for podosome organization and extracellular matrix proteolysis," *Blood*, vol. 115, no. 7, pp. 1444–1452, 2010.

[56] H. Neubauer, Y. Yang, H. Seeger et al., "The presence of a membrane-bound progesterone receptor sensitizes the estradiol-induced effect on the proliferation of human breast cancer cells," *Menopause*, vol. 18, no. 8, pp. 845–850, 2011.

[57] X.-D. Fu, L. Goglia, A. M. Sanchez et al., "Progesterone receptor enhances breast cancer cell motility and invasion via extranuclear activation of focal adhesion kinase," *Endocrine-Related Cancer*, vol. 17, no. 2, pp. 431–443, 2010.

[58] D. Khaitan, U. T. Sankpal, B. Weksler et al., "Role of KCNMA1 gene in breast cancer invasion and metastasis to brain," *BMC Cancer*, vol. 9, article 258, 2009.

[59] J. Khan, L. H. Saal, M. L. Bittner, Y. Chen, J. M. Trent, and P. S. Meltzer, "Expression profiling in cancer using cDNA microarrays," *Electrophoresis*, vol. 20, no. 2, pp. 223–229, 1999.

[60] A. M. Stark, B. Anuszkiewicz, R. Mentlein, T. Yoneda, H. M. Mehdorn, and J. Held-Feindt, "Differential expression of matrix metalloproteinases in brain- and bone-seeking clones of metastatic MDA-MB-231 breast cancer cells," *Journal of Neuro-Oncology*, vol. 81, no. 1, pp. 39–48, 2007.

[61] D. Oxmann, J. Held-Feindt, A. M. Stark, K. Hattermann, T. Yoneda, and R. Mentlein, "Endoglin expression in metastatic breast cancer cells enhances their invasive phenotype," *Oncogene*, vol. 27, no. 25, pp. 3567–3575, 2008.

[62] A. M. Stark, K. Tongers, N. Maass, H. M. Mehdorn, and J. Held-Feindt, "Reduced metastasis-suppressor gene mRNA-expression in breast cancer brain metastases," *Journal of Cancer Research and Clinical Oncology*, vol. 131, no. 3, pp. 191–198, 2005.

[63] A. J. Minn, G. P. Gupta, D. Padua et al., "Lung metastasis genes couple breast tumor size and metastatic spread," *Proceedings of the National Academy of Sciences of the United States of America*, vol. 104, no. 16, pp. 6740–6745, 2007.

[64] X.-D. Fu, M. S. Giretti, L. Goglia et al., "Comparative actions of progesterone, medroxyprogesterone acetate, drospirenone and nestorone on breast cancer cell migration and invasion," *BMC Cancer*, vol. 8, article 166, 2008.

[65] X.-D. Fu, M. S. Giretti, C. Baldacci et al., "Extra-nuclear signaling of progesterone receptor to breast cancer cell movement and invasion through the actin cytoskeleton," *PLoS ONE*, vol. 3, no. 7, Article ID e2790, 2008.

[66] Y. Pang and P. Thomas, "Progesterone signals through membrane progesterone receptors (mPRs) in MDA-MB-468 and mPR-transfected MDA-MB-231 breast cancer cells which lack full-length and N-terminally truncated isoforms of the nuclear progesterone receptor," *Steroids*, vol. 76, no. 9, pp. 921–928, 2011.

[67] K. B. Horwitz, W. W. Dye, J. C. Harrell, P. Kabos, and C. A. Sartorius, "Rare steroid receptor-negative basal-like tumorigenic cells in luminal subtype human breast cancer xenografts," *Proceedings of the National Academy of Sciences of the United States of America*, vol. 105, no. 15, pp. 5774–5779, 2008.

[68] R. J. Craven, "PGRMC1: a new biomarker for the estrogen receptor in breast cancer," *Breast Cancer Research*, vol. 10, no. 6, article 113, 2008.

[69] H. Neubauer, S. E. Clare, W. Wozny et al., "Breast cancer proteomics reveals correlation between estrogen receptor status and differential phosphorylation of PGRMC1," *Breast Cancer Research*, vol. 10, no. 5, article R85, 2008.

[70] P. Thomas, Y. Pang, and J. Dong, "Enhancement of cell surface expression and receptor functions of membrane progestin receptor α (mPRα) by progesterone receptor membrane component 1 (PGRMC1): evidence for a role of PGRMC1 as an adaptor protein for steroid receptors," *Endocrinology*, vol. 155, no. 3, pp. 1107–1119, 2014.

[71] M. Guarino, "Src signaling in cancer invasion," *Journal of Cellular Physiology*, vol. 223, no. 1, pp. 14–26, 2010.

[72] J. H. Hanke, J. P. Gardner, R. L. Dow et al., "Discovery of a novel, potent, and Src family-selective tyrosine kinase inhibitor. Study of Lck- and FynT-dependent T cell activation," *The Journal of Biological Chemistry*, vol. 271, no. 2, pp. 695–701, 1996.

[73] R. Karni, S. Mizrachi, E. Reiss-Sklan, A. Gazit, O. Livnah, and A. Levitzki, "The pp60^{c-Src} inhibitor PP1 is non-competitive against ATP," *FEBS Letters*, vol. 537, no. 1–3, pp. 47–52, 2003.

[74] S. K. Mitra, D. A. Hanson, and D. D. Schlaepfer, "Focal adhesion kinase: in command and control of cell motility," *Nature Reviews Molecular Cell Biology*, vol. 6, no. 1, pp. 56–68, 2005.

[75] J. J. Acosta, R. M. Muñoz, L. González et al., "Src mediates prolactin-dependent proliferation of T47D and MCF7 cells via the activation of focal adhesion kinase/Erk1/2 and phosphatidylinositol 3-kinase pathways," *Molecular Endocrinology*, vol. 17, no. 11, pp. 2268–2282, 2003.

[76] V. C. Lin, E. H. Ng, S. E. Aw, M. G. Tan, E. H. Ng, and B. H. Bay, "Progesterone induces focal adhesion in breast cancer cells MDA-MB-231 transfected with progesterone receptor complementary DNA," *Molecular Endocrinology*, vol. 14, no. 3, pp. 348–358, 2000.

[77] X. Liu, Y. Chang, P. H. Reinhart, and H. Sontheimer, "Cloning and characterization of glioma BK, a novel BK channel isoform highly expressed in human glioma cells," *The Journal of Neuroscience*, vol. 22, no. 5, pp. 1840–1849, 2002.

Hindawi Publishing Corporation
BioMed Research International
Volume 2014, Article ID 568693, 13 pages
http://dx.doi.org/10.1155/2014/568693

Research Article

Biological and Molecular Effects of Small Molecule Kinase Inhibitors on Low-Passage Human Colorectal Cancer Cell Lines

Falko Lange,[1,2] Benjamin Franz,[1] Claudia Maletzki,[3] Michael Linnebacher,[3] Maja Hühns,[4] and Robert Jaster[1]

[1] *Department of Medicine II, Division of Gastroenterology, Rostock University Medical Center, Ernst-Heydemann-Straße 6, 18057 Rostock, Germany*
[2] *Oscar Langendorff Institute of Physiology, Rostock University Medical Center, Gertrudenstraße 9, 18057 Rostock, Germany*
[3] *Molecular Oncology and Immunotherapy, Department of General Surgery, Rostock University Medical Center, Schillingallee 35, 18057 Rostock, Germany*
[4] *Institute of Pathology, Rostock University Medical Center, Strempelstraße 14, 18055 Rostock, Germany*

Correspondence should be addressed to Robert Jaster; jaster@med.uni-rostock.de

Received 27 June 2014; Accepted 26 August 2014; Published 17 September 2014

Academic Editor: Raj Kumar

Low-passage cancer cell lines are versatile tools to study tumor cell biology. Here, we have employed four such cell lines, established from primary tumors of colorectal cancer (CRC) patients, to evaluate effects of the small molecule kinase inhibitors (SMI) vemurafenib, trametinib, perifosine, and regorafenib in an *in vitro* setting. The mutant *BRAF* (V600E/V600K) inhibitor vemurafenib, but also the MEK1/2 inhibitor trametinib efficiently inhibited DNA synthesis, signaling through ERK1/2 and expression of genes downstream of ERK1/2 in *BRAF* mutant cells only. In case of the AKT inhibitor perifosine, three cell lines showed a high or intermediate responsiveness to the drug while one cell line was resistant. The multikinase inhibitor regorafenib inhibited proliferation of all CRC lines with similar efficiency and independent of the presence or absence of *KRAS, BRAF, PIK3CA*, and *TP53* mutations. Regorafenib action was associated with broad-range inhibitory effects at the level of gene expression but not with a general inhibition of AKT or MEK/ERK signaling. In vemurafenib-sensitive cells, the antiproliferative effect of vemurafenib was enhanced by the other SMI. Together, our results provide insights into the determinants of SMI efficiencies in CRC cells and encourage the further use of low-passage CRC cell lines as preclinical models.

1. Introduction

Colorectal carcinoma (CRC) represents the third most common cancer in both sexes and the third leading cause of cancer-related deaths in the United States [1]. Despite considerable achievements in recent years, the therapeutic options in the locally advanced and metastatic stages of the disease still remain quite limited. For this reason, high hopes are associated with the clinical introduction of novel therapeutics that act by targeting protumorigenic mediators and intracellular signaling pathways. While monoclonal antibodies to vascular endothelial growth factor (VEGF) (bevacizumab) and the extracellular domain of epidermal growth factor receptor (EGFR) (cetuximab, panitumumab) are already established in treatment of advanced CRC [2], the application of small molecule kinase inhibitors (SMI) is still largely restricted to clinical trials. An important exception is the multikinase inhibitor regorafenib that blocks various angiogenic (VEGF receptor 1-3, TIE2), stromal (platelet-derived growth factor receptor-beta, fibroblast growth factor receptor), and oncogenic kinases (KIT, RET, and RAF) [3]. Regorafenib increases the overall survival of patients with metastatic CRC [4] and has been approved by the United States Food and Drug Administration in 2012. Various other SMI, many of them with more restricted targets than regorafenib, are currently in different phases of clinical testing.

In the transduction of proliferative and antiapoptotic signals in CRC cells, the signaling cascades RAS/RAF/MEK/ERK (extracellular signal regulated kinase) and PTEN

(phosphatase and tensin homolog)/PI3K (phosphatidylinositol 3-kinase)/AKT/mTOR play pivotal roles [5, 6]. Both signaling pathways are activated by numerous growth factor receptors and mediate intracellular signals by the consecutive activation of downstream proteins. Upon activation by GTP-bound RAS, the serine/threonine kinase RAF triggers downstream signaling by phosphorylating MEK1 and MEK2, which in turn phosphorylate and activate ERK1 and ERK2. Activated ERKs may translocate into the nucleus where they phosphorylate transcription factors with key functions in the induction of cell proliferation and suppression of apoptosis [7, 8]. In CRC, activating mutations of the oncogenes *KRAS* and *BRAF* are observed in 30–60% [9, 10] and 10–15% [11], respectively. Oncogenic *KRAS* mutations are associated with resistance to EGFR inhibitors such as cetuximab [12].

PI3Ks are a family of lipid kinases that phosphorylate the 30-OH group on phosphatidylinositol in the plasma membrane. Subsequently, the serine/threonine kinase AKT is recruited to the cell membrane where it becomes phosphorylated and activated. In various types of cancer, the PI3K/AKT signaling cascade is critically involved in mediating survival and tumor cell growth [13, 14]. Furthermore, the PI3K/AKT signaling pathway is frequently activated in malignant tumors, including CRC, by growth factor receptor tyrosine kinases, by activating gene mutations of *KRAS* or *phosphatidylinositol-4,5-bisphosphate 3-kinase*, *catalytic subunit alpha* (*PIK3CA*), or by loss of function of the phosphatase PTEN [15, 16].

Here we have analyzed and compared the biological and molecular effects of four molecular cancer therapeutics, the multikinase inhibitor regorafenib [3], the inhibitor of the V600E/V600K mutant form of BRAF vemurafenib [17], the selective MEK1/MEK2 inhibitor trametinib [18], and the AKT inhibitor perifosine [19], in CRC cells in order to elucidate determinants of their efficiency or inefficiency.

Other than regorafenib, vemurafenib, trametinib, and perifosine are not established in the treatment of CRC. While BRAF-inhibitors such as vemurafenib have produced impressive response rates of approximately 60–80% in patients with *BRAF*-mutant metastatic malignant melanoma [20], vemurafenib is apparently much less efficient in *BRAF*-mutant CRC [21, meeting abstract]. As a possible mechanism of vemurafenib resistance, EGFR-mediated reactivation of ERK signaling has been proposed [22], but it has also been suggested that resistance to BRAF inhibition can be overcome with PI3K inhibition or demethylating agents [23]. In case of trametinib, encouraging preclinical data have been published that suggest direct antitumor activities on CRC cell lines both *in vitro* and *in vivo* [24] as well as an enhancement of the efficacy of 5-fluorouracil [25]. The results of clinical trials, however, are still awaited. Finally, perifosine was found to double the time to progression in one phase II trial for metastatic colon cancer [26], but later on failed its phase III clinical trial [27, meeting abstract]. On the other hand, perifosine has also been shown to act as a sensitizer to the anticolorectal cancer effects of curcumin; an effect that warrants further investigation [28]. Together, these findings indicate that all three drugs display inhibitory effects on CRC cells in preclinical settings but also illustrate that their clinical efficiency is either still unknown or questionable. Therefore, the use of these substances in our studies was most of all motivated by their molecular specificity and not their (uncertain) clinical efficiency.

In our studies, we took advantage of a panel of recently established low-passage cell lines that were derived from primary tumors of surgical CRC patients [29, 30]. In contrast to cell lines of high passage [31, 32], low-passage cancer cell lines well reflect the biology of the original tumor, such as growth behavior, morphology, and mutational profile and are, therefore, in our experience, a versatile tool to evaluate drug efficiencies in a preclinical context. To reflect the three molecular classes of CRC, cell lines with chromosomal instability (CIN), microsatellite instability (MSI), and a CpG island methylator phenotype were included into the investigations. With respect to CRC-typical molecular alterations, the cell lines were characterized by an individual, only partially overlapping molecular profile that included oncogenic mutations of *KRAS*, *BRAF* (V600E), and *PIK3CA* as well as loss or inactivation of the tumor suppressor genes *APC* and *TP53*. The study, therefore, also aimed at a systematic evaluation of relationships between the biological efficiency of the investigated SMI, the mutational profiles of the CRC cells, and the activity of downstream signaling pathways and target genes.

The results show that the efficacy of vemurafenib and trametinib in CRC cells depends on the presence of mutant *BRAF* (V600E) and an efficient inhibition of MEK/ERK signaling, whereas regorafenib action was largely independent of the molecular status of the cells and perifosine showed a cell line-specific action profile.

2. Materials and Methods

2.1. Reagents. Unless stated otherwise, all reagents were obtained from Sigma-Aldrich (Deisenhofen, Germany).

2.2. Cell Line Establishment Protocol and Cell Culture. Primary CRC resection specimens were obtained from surgery, with informed written patient consent. All procedures were approved by the Ethics Committee of the University of Rostock (reference number II HV 43/2004) in accordance with generally accepted guidelines for the use of human material. Establishment of the cell line HROC24 has been described before [30]. The other cell lines were either directly established from fresh tumor material (HROC18 and HROC43) or following xenografting (HROC46) in immunodeficient NMRI-*Foxn1*^{nu} mice. Cell line establishment protocol was adapted according to [30]. Briefly, single cell suspensions were seeded on collagen-coated plates in Dulbecco's MEM/Ham's F-12 (Biochrom, Berlin, Germany) supplemented with 10% fetal calf serum (FCS), 100 U/mL penicillin, and 100 μg/mL streptomycin (complete culture medium; all reagents from PAA Laboratories, Pasching, Austria) at 37°C in a 5% CO_2 humidified atmosphere. Continually growing cell cultures were regularly passaged. Cell lines used in this study did not exceed passage 50. Clinical, pathological, and molecular characteristics of the patients are summarized in Table 1. Noteworthy, all four cell lines were mutant for

Table 1: Clinical and pathological characteristics of patients and HROC cell lines.

Tumor ID	Age/Gender	Tumor location	TNM-Stage	UICC stage	Tumor type	Molecular type	Molecular alterations					
							APC	*TP53*	*KRAS*	*BRAF*	*PIK3CA*	*PTEN*
HROC18	65/f	caecum	G2T2N0M0 R0L0V0	I	Primary adenocarcinoma	spStd	mut	mut	wt	wt	mut	wt
HROC24	98/m	colon ascendens	G2T2N0M0 R0L0V1	I	Primary adenocarcinoma	spMSI-H	mut	wt	wt	mut	wt	wt
HROC43	72/m	colon ascendens	G3T3N2M0 R0L1V0	IIIb	Primary adenocarcinoma	CIMP-L	mut	mut	mut	wt	wt	wt
HROC46*	66/m	colon ascendens	G3T3N0M1 R2L0V1	IV	Primary adenocarcinoma	spStd	mut	wt	mut	wt	wt	wt

f: female, m: male, spStd: sporadic standard, spMSI: sporadic microsatellite instable, CIMP-L: CpG island methylator phenotype, and L: low, H: high. *Xenograft-derived cell line.

APC and wild-type for *PTEN*. One cell line (HROC24) expressed mutant *BRAF* (V600E), two cell lines (HROC43 and HROC46) oncogenic *KRAS*, and also two cell lines (HROC24 and HROC46) were mutant for *TP53*. HROC18 is the only cell line which harbors an E545K mutation of *PIK3CA* that increases the catalytic activity of the protein [33].

2.3. Quantification of DNA Synthesis. To analyze the effects of the SMI vemurafenib, perifosine, regorafenib, and trametinib (all from Selleckchem, Houston, TX, USA) on cell proliferation, DNA synthesis was measured using a 5-bromo-2′-deoxy-uridine (BrdU) incorporation assay kit (Roche Applied Science, Mannheim, Germany). Therefore, cells of the indicated CRC lines were plated in 96-well half-area microplates at equal seeding densities and allowed to adhere overnight in complete culture medium. The next day, the cells were serum-starved for 16 h before the FCS-free medium was substituted by complete culture medium supplemented with kinase inhibitors as indicated. After an incubation period of 24 h, BrdU labeling was initiated by adding labeling solution at a final concentration of 10 μM. Another 8 h later, labeling was stopped and BrdU uptake was measured according to the manufacturer's instructions. IC_{50} values were determined by interpolation from the dose response curves.

2.4. Detection of Dead Cells and Analysis of Cellular DNA Content by Flow Cytometry. HROC24 cells growing in 12-well plates in complete culture medium were exposed to SMI and combinations thereof for 48 h as indicated. Afterwards, the cells were harvested by trypsinization, resuspended in buffer for flow cytometry (PBS pH 7.4; 0.5% bovine serum albumin; 0.1% sodium azide) and kept on ice until measurement. Subsequently, the samples were labeled with propidium iodide (PI; 10 μg/mL). PI-positive (dead) cells were quantified using a FACSCalibur cytometer (BD Biosciences, Heidelberg, Germany).

In addition, cell death was verified by trypan blue staining of trypsinized cells as an independent method.

For the detection of the cellular DNA content, trypsinized HROC24 cells were pelleted by centrifugation, washed twice with PBS (pH 7.4), and resuspended in ice-cold 70% ethanol for at least 12 h at 4°C. After additional washing steps, the cells were incubated for 20 min in 400 μL PBS supplemented with 0.1 mg/mL RNase A (Roche Applied Science) at 37°C. Subsequently, 50 μg/mL PI was added and the samples were subjected to cytofluorometric analysis. 10.000 events were measured for each sample and the data stored in list mode for further analysis. The cell cycle distribution was calculated using the software tool *Cyflogic* (CyFlo Ltd, Finland). Cells of the Sub-G1 peak were considered apoptotic.

2.5. Immunoblotting. Cells of the indicated CRC lines were grown in 24-well plates in complete culture medium until reaching subconfluency before they were treated with SMI for 6 h. Afterwards, protein extracts were prepared and subjected to immunoblot analysis as published before [34], using polyvinylidene fluoride membrane for protein transfer. The following primary antibodies (all from New England BioLabs, Frankfurt, Germany, unless specified otherwise) were employed: anti-GAPDH (#2118), anti-phospho-AKT (P-AKT; #4060), anti-phospho-MEK (P-MEK1/2; #9154), anti-phospho-ERK1/2 (P-ERK1/2) (#4370), anti-AKT protein (#4691), anti-MEK1/2 (#8727), and anti-ERK1/2 (#06-182, Millipore, Billerica, MA, United States). The blots were developed using LI-COR reagents for an Odyssey Infrared Imaging System as previously described [35]. The signal intensities of the investigated proteins were quantified by means of the Odyssey software and raw data processed as described in the corresponding figure legend.

2.6. Quantitative Reverse Transcriptase-PCR Using Real-Time TaqMan Technology. HROC24 cells growing in 12-well plates were treated with SMI for 6 h as indicated. Afterwards, total RNA was isolated with TriFast reagent (PEQLAB Biotechnologie, Erlangen, Germany) according to the manufacturer's instructions. All further steps were performed with reagents from Life Technologies (Darmstadt, Germany). First, any traces of genomic DNA were removed employing the DNA-free kit. Next, 1 μg of RNA was reverse transcribed into cDNA by means of TaqMan Reverse Transcription Reagents and random hexamer priming. Relative quantification of target cDNA levels by real-time PCR was performed in an ABI Prism 7000 sequence detection system (Life Technologies). Therefore, TaqMan Universal PCR Master Mix and human gene-specific Assay-on-Demand kits with fluorescently labeled MGB probes were used. The following assays were employed: Hs99999140_m1 (*FOS*), Hs00355782_m1 (*CDKN1A*; *p21*), Hs00244839_m1 (*DUSP5*), Hs00180269_m1 (*BAX*), Hs00181225_m1 (*FAS ligand*; *FASLG*; *CD95L*), Hs01034249_m1 (*TP53*), Hs00765553_m1 (*cyclin D1*; *CCND1*), Hs00608023_m1 (*BCL2*), and Hs99999905_m1 (*GAPDH*; house-keeping gene control). PCR conditions were 95°C for 10 min, followed by 40 cycles of 15 s at 95°C/1 min at 60°C. The relative expression of each mRNA (n = 4–8 independent samples per experimental condition) compared with *GAPDH* was calculated according to the equation $\Delta Ct = Ct_{target} - Ct_{GAPDH}$. The relative amount of target mRNA in control cells and cells treated with kinase inhibitors as indicated was expressed as $2^{-(\Delta Ct)}$.

2.7. Statistical Analysis. Values are expressed as mean ± standard error of the mean (SEM) for the indicated number of separate cultures per experimental protocol. Statistical significance was checked using the Mann-Whitney U test. $P < 0.05$ (Bonferroni-adjusted as indicated in the figure legends) was considered to be statistically significant.

3. Results

3.1. Antiproliferative Effects of SMI on CRC Low-Passage Cell Lines. In initial studies, the four low-passage CRC cell lines were exposed to different doses of vemurafenib, trametinib, perifosine, and regorafenib, respectively, and cell proliferation was assessed by measuring the incorporation of BrdU into newly synthesized DNA (Figure 1).

As expected, the inhibitor of mutant BRAF, vemurafenib, efficiently inhibited DNA synthesis of HROC24 cells, the

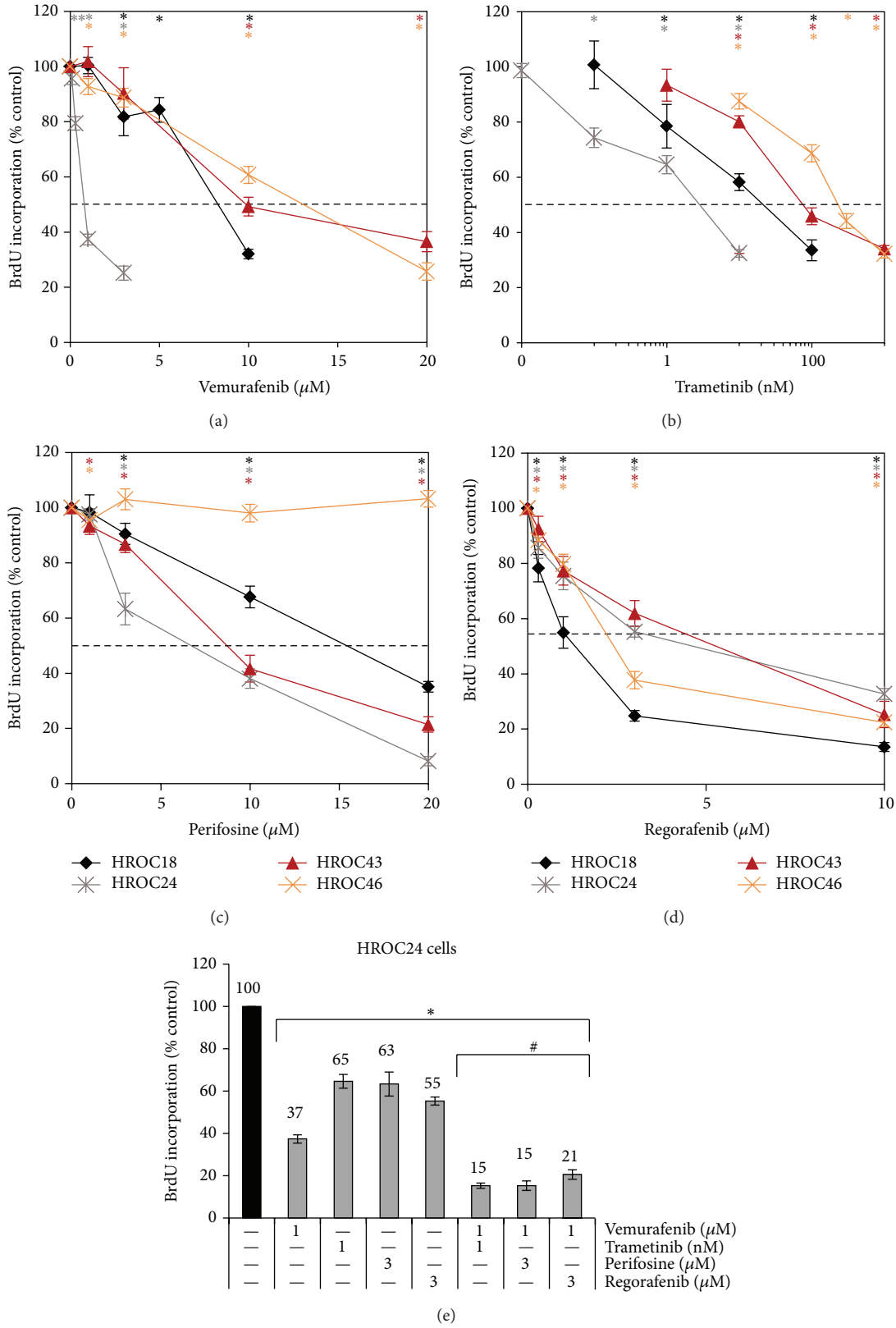

Figure 1: Effects of SMI on the BrdU incorporation of CRC cell lines. HROC18, HROC24, HROC43, and HROC46 cells growing in 96-well half-area microplates were treated with (a) vemurafenib, (b) trametinib (please note the logarithmic scale x-axis), (c) perifosine, and (d) regorafenib as indicated for 24 h, before DNA synthesis was assessed with the BrdU incorporation assay. In (e), HROC24 cells were incubated with combinations of SMI as indicated. One hundred percent BrdU incorporation corresponds to cells cultured without SMI. Data are presented as mean ± SEM ($n \geq 12$ separate cultures); $^{*}P < 0.004$ versus control cultures with Bonferroni-adjusted $\alpha = 0.0125$; $^{\#}P < 0.001$ versus cultures treated with either of the two combined substances alone with Bonferroni-adjusted $\alpha = 0.0038$.

Table 2: IC_{50} values of vemurafenib, perifosine, regorafenib, and trametinib (BrdU incorporation assay).

	Vemurafenib (μM)	Perifosine (μM)	Regorafenib (μM)	Trametinib (nM)
HROC18	8.3	15.4	1.3	39.9
HROC24	0.8	6.7	4.6	5.1
HROC43	9.9	8.7	5.3	89.2
HROC46	12.7	#	2.4	252

#: no inhibitory effects on BrdU incorporation under experimental conditions.

only cell line in this study that harbors the V600E *BRAF* oncogene (IC_{50} = 0.8 μM; Figure 1(a), Table 2). In contrast, for the other three cell lines IC_{50} values from 8.3–12.7 μM were determined. HROC24 was also the only cell line that was sensitive to low nanomolar (and even subnanomolar) concentrations of the MEK1/2 inhibitor trametinib (IC_{50} = 5.1 nM; Figure 1(b)). Of the other three CRC lines, HROC18 showed the highest sensitivity to trametinib (IC_{50} = 39.9 nM), HROC43 showed an intermediate responsiveness (IC_{50} = 89.2 nM), and HROC46 showed the poorest response (IC_{50} = 252 nM).

The AKT inhibitor perifosine inhibited proliferation of the CRC lines HROC24 and HROC43 with similar efficiency (IC_{50} = 6.7 μM and 8.7 μM, resp.), while HROC18 cells were less sensitive (IC_{50} = 15.4 μM) and HROC46 cells were resistant to the drug (Figure 1(c); small nonsystematic decrease at 1 μM only).

The response pattern to the multikinase inhibitor regorafenib differed from the one to all other drugs in that (i) similar IC_{50} values were determined for all four cell lines (ranging from 1.3 to 5.3 μM; Figure 1(d)) and (ii) HROC18 but not HROC24 was the most sensitive cell line.

In subsequent experiments, effects of SMI combinations were investigated employing HROC24 cells. The results show an additive action of vemurafenib when combined with any of the other three drugs (Figure 1(e)). In contrast, the simultaneous application of perifosine and trametinib did not result in additive effects of the drugs in any of the four CRC cell lines (data not shown).

3.2. Induction of Cell Death by SMI. For each SMI, the effects of two concentrations (selected based on the BrdU incorporation data) on cell death were determined by FACS analysis. As shown in Figure 2(a) for HROC24 cells, both concentrations of vemurafenib and perifosine as well as the higher concentrations of regorafenib and trametinib significantly increased the portion of PI-positive (dead) cells. For the higher SMI concentrations, these findings were largely confirmed by the results of trypan blue staining, except for that the effect of regorafenib was insignificant (Figure 2(b)). However, only perifosine (at 3 μM) but none of the other inhibitors caused the death of more than 12% of the cells (PI-staining data; Figure 2(a)). Furthermore, when vemurafenib was applied together with low doses of the other drugs, only its combination with perifosine significantly increased its cytostatic effects (Figure 2(a)).

To further analyze the mechanisms of cell death, apoptotic cells were quantified employing the Sub-G1 peak method. As shown in Figure 2(c), for each inhibitor, a portion of apoptotic cells was determined that largely overlapped with the portion of PI-positive cells (Figure 2(a)). Together, these data suggest apoptosis as the main cause of CRC cell death under the given experimental conditions.

3.3. Effects of SMI on RAS/RAF/MEK/ERK and PI3K/AKT Signaling in CRC Cells. We next studied how the four investigated SMI affected expression and phosphorylation of AKT, MEK1/2, and ERK1/2 in HROC18, HROC24, HROC43, and HROC46 cells. For each cell line, typical immunoblots are shown in Figures 3(a)–3(d), while the quantitative effects of the four SMI are presented in Figures 4(a)–4(d).

In agreement with its profile of biological activities, vemurafenib displayed consistent inhibitory effects exclusively on the *BRAF*-mutant HROC24 cells, where it efficiently blocked phosphorylation of MEK1/2 and ERK1/2 (Figure 4(a)) at concentrations that also significantly diminished cell growth. For the other three cell lines, even increases of P-MEK1/2 and P-ERK1/2 levels were observed. Similar to vemurafenib, trametinib inhibited MEK1/2 phosphorylation in HROC24 cells only (Figure 4(b)). However, since trametinib specifically inhibits MEK activity, not phosphorylation, the more meaningful findings refer to the phosphorylation of ERK1/2. Here, a dose-dependent inhibitory effect of the drug was observed in all four types of CRC cells, with HROC24, like in the biological assays, as the most sensitive cell line. Significant changes of P-AKT levels in response to vemurafenib and trametinib treatment were restricted to HROC46 cells, where vemurafenib at 10 μM caused a decrease and trametinib at 1 nM caused an increase of the P-AKT/AKT ratio.

As expected, the AKT inhibitor perifosine did not reduce MEK1/2 and ERK1/2 phosphorylation in any of the four cell lines (Figure 4(c)); in HROC43 and HROC46 cells *increased* P-ERK levels at a perifosine concentration of 1 μM were detected. In agreement with the biological data (Figure 1), perifosine inhibited phosphorylation of AKT in the susceptible cell line HROC24 but was inefficient in the resistant cell line HROC46. Like in the BrdU incorporation assay, HROC18 and HROC43 displayed an intermediate sensitivity.

Although regorafenib reduced DNA synthesis in all four CRC lines (Figure 1), it consistently diminished phosphorylation of MEK1/2 and ERK1/2 in HROC24 cells only (Figure 4(d)). For the other three cell lines, the occasional significant effects did not follow a systematic pattern. Phosphorylation of AKT was not inhibited in any of the cell lines tested.

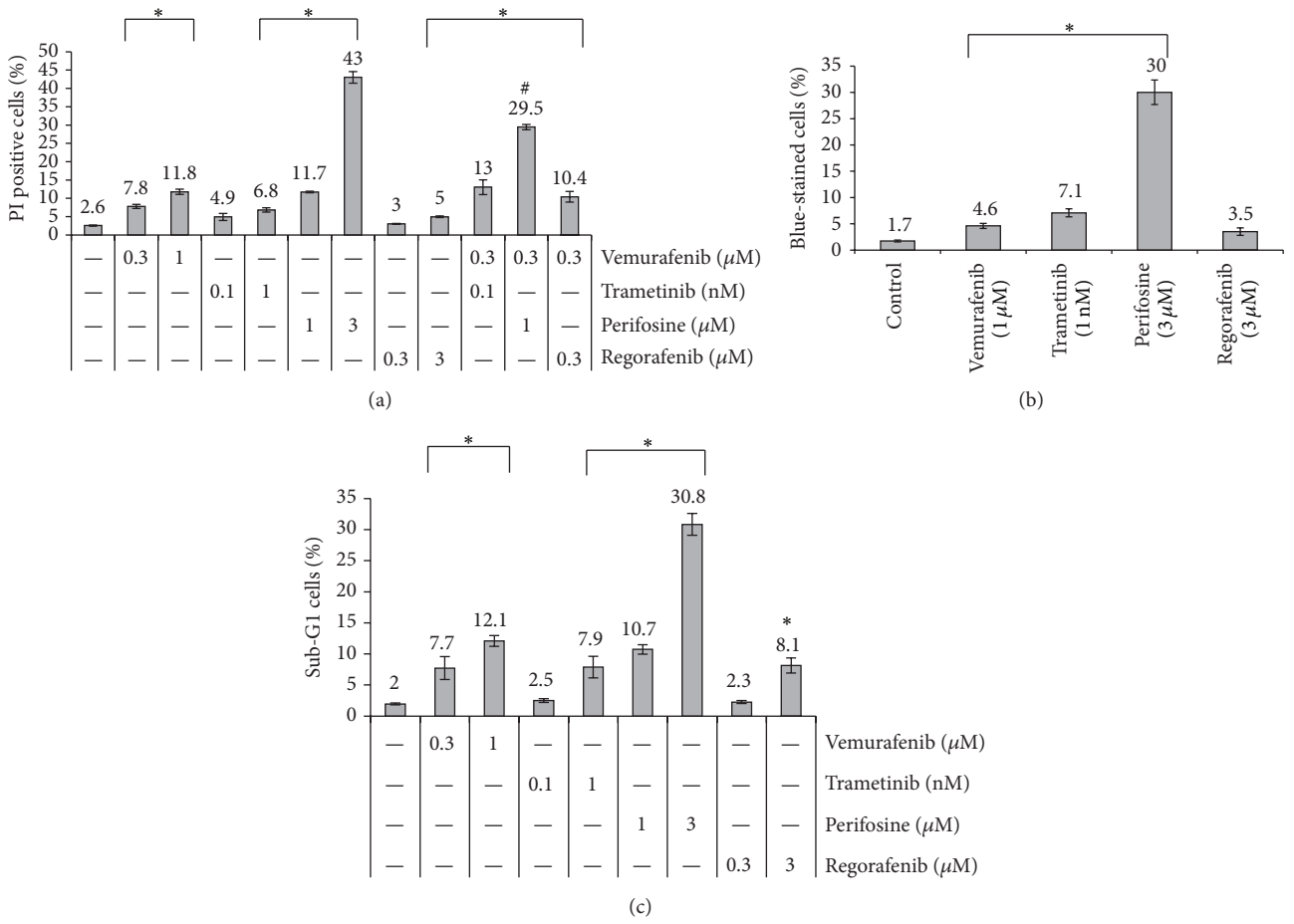

Figure 2: SMI-dependent death of HROC24 cells. HROC24 cells growing in 12-well plates were treated with SMI and combinations thereof for 48 h as indicated. Afterwards, they were subjected to (a) cytofluorometric quantification of dead (PI-positive) cells, (b) determination of cell death by trypan blue staining, and (c) detection of apoptotic (Sub-G1 peak) cells. The portion of dead/apoptotic cells is expressed as percent of the total cell count. Data from $n \geq 6$ separate cultures were used to calculate mean values ± SEM. (a): $^{*}P < 0.001$ versus control cells cultured without SMI and $^{\#}P < 0.002$ versus cells cultured with single SMI with Bonferroni-adjusted $\alpha = 0.00294$; (b): $^{*}P < 0.008$ versus control cultures with Bonferroni-adjusted $\alpha = 0.0125$; (c): $^{*}P < 0.001$ versus control cultures with Bonferroni-adjusted $\alpha = 0.00625$.

3.4. SMI Target Genes in HROC24 Cells. Using the CRC line HROC24, we also studied molecular effects of the investigated SMI at the level of gene expression. Therefore, a panel was chosen that covered target genes of RAS/RAF/MEK/ERK signaling (*FOS*, *DUSP5*), stimulators (*cyclin D1*/*CCND1*), and inhibitors (*CDKN1A*, *TP53*) of cell cycle progression as well as proapoptotic (*BAX*, *FASLG*) and antiapoptotic (*BCL2*) effectors. The results (Figure 5) indicate that the four SMI can be divided into two groups with different action profiles.

Vemurafenib and trametinib strongly inhibited the expression of *FOS* (Figure 5(a)) but caused no statistically significant changes of the mRNA levels of *CDKN1A* (d), *TP53* (e), *BAX* (f), *FASLG* (g), and *BCL2* (h). Partially discordant results were observed for *DUSP5* (b) and *cyclin D1* (c), where either only trametinib (at 1 nM; *DUSP5*) or vemurafenib (*cyclin D1*) displayed significant inhibitory effects (although the other drug showed by trend a similar effect in both cases). The other two SMI, perifosine and regorafenib, changed the mRNA levels of a larger panel of genes. In case of regorafenib, statistically significant inhibitory effects on the expression of *FOS* (a), *DUSP5* (b), *cyclin D1* (c), and *FASLG* (g) as well as a trend to a reduced expression of several other genes were observed. Perifosine diminished the mRNA levels of *cyclin D1* (c), *TP53* (e), *FASLG* (g), and *BAX* (h).

4. Discussion

Low-passage human cancer cell lines are increasingly acknowledged as advantageous preclinical models for testing drug efficiencies and analyzing the molecular basis of drug sensitivity and resistance [36, 37]. Compared to long-term established high-passage cell lines, they more closely resemble their parental primary cancers regarding genotype and phenotypic features and, therefore, offer improved chances to address clinically relevant questions in the field of cancer medicine [30–32, 36, 37]. Here, we took advantage of four low-passage CRC cell lines with well-defined molecular phenotypes [29, 30, and this study] to evaluate the biological and

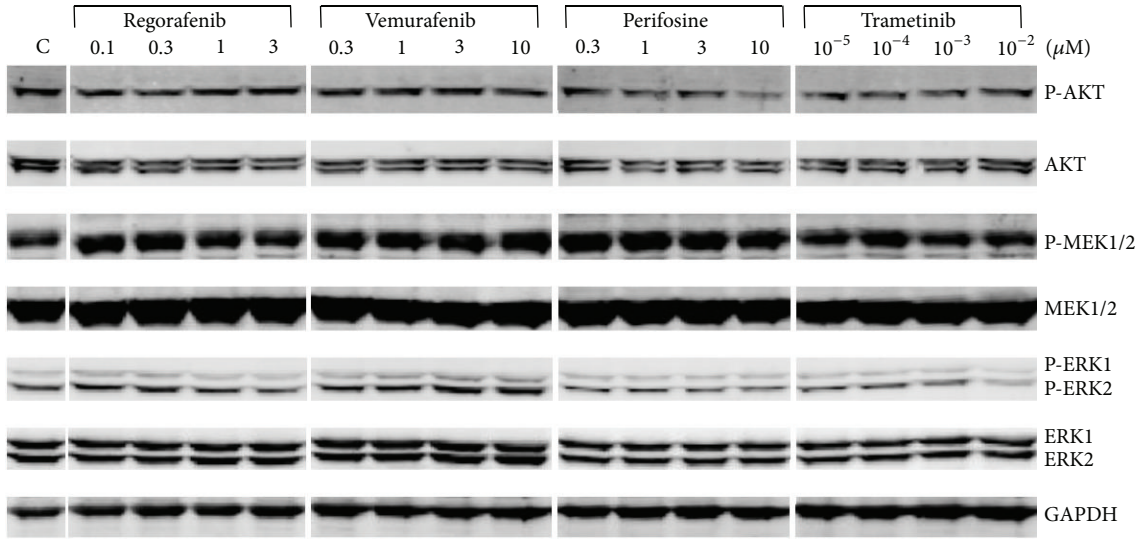

(a)

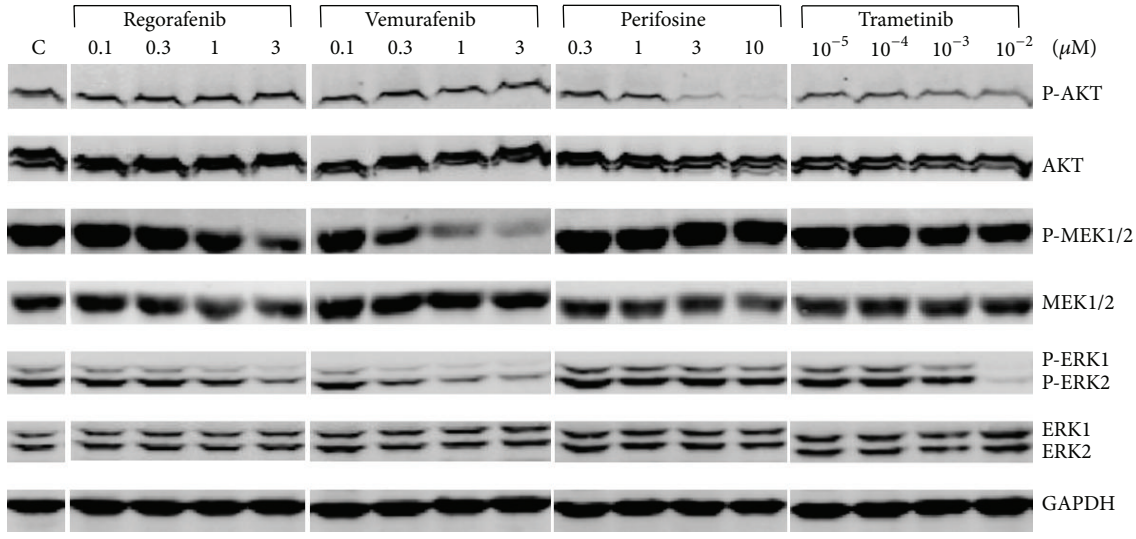

(b)

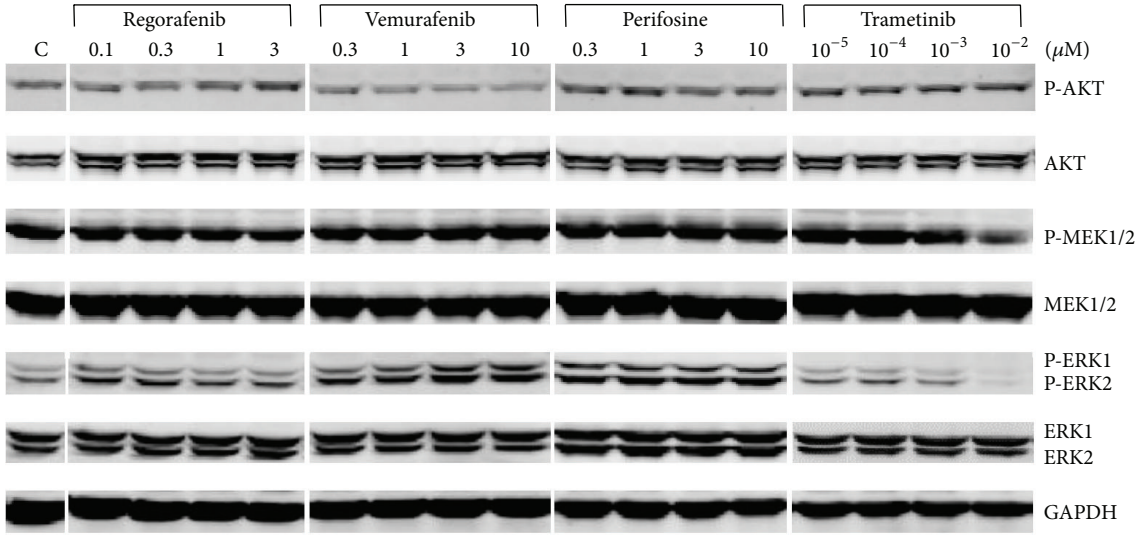

(c)

Figure 3: Continued.

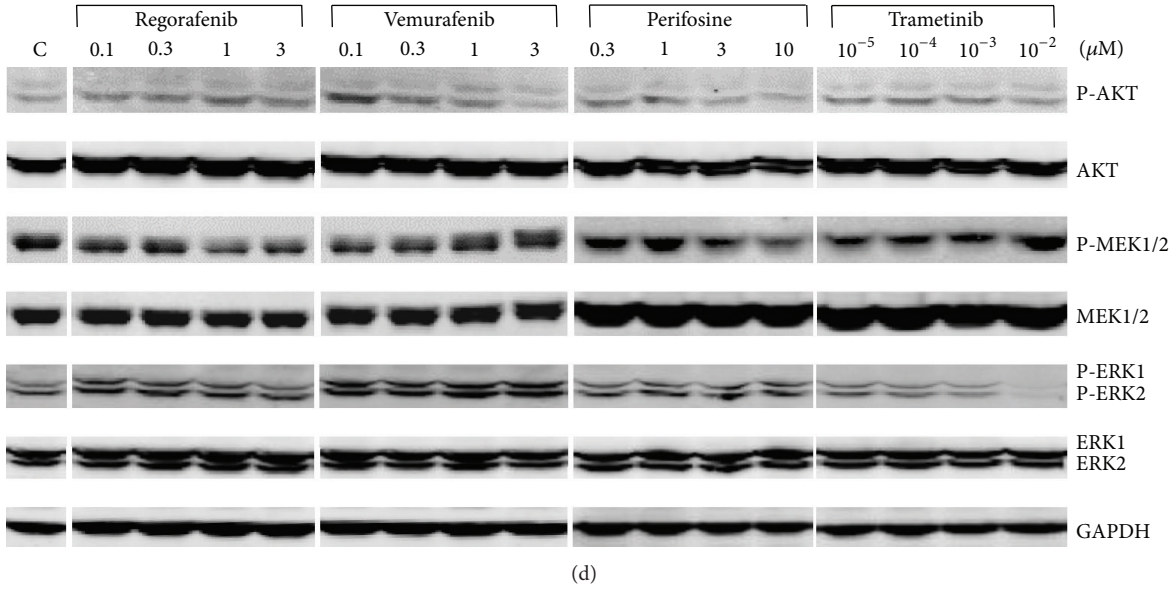

(d)

Figure 3: Effects of vemurafenib, trametinib, perifosine, and regorafenib on the phosphorylation of AKT, MEK1/2, and ERK1/2 in CRC cell lines. (a) HROC18, (b) HROC24, (c) HROC43, and (d) HROC46 cells were grown in 24-well plates to subconfluency before culture medium was supplemented with vemurafenib, trametinib, perifosine, and regorafenib at the indicated concentrations. Control cultures (C) were treated with solvent only. After an incubation period of 6 h, protein extracts from equal amounts of cells were subjected to immunoblot analysis. P-AKT, P-MEK1/2, P-ERK1/2, the respective total proteins, and GAPDH (for loading control) were detected using fluorescein- (IRDye-) labeled secondary antibodies. For each cell line, one representative blot is shown. For mean values of independent experiments, please refer to Figure 4.

molecular effects of selected SMI that interfere with signaling through two key mitogenic/antiapoptotic pathways in CRC cells, RAS/RAF/MEK/ERK, and PTEN/PI3K/AKT/mTOR. The studies were motivated by the fact that many drugs deemed active against a particular type of cancer are effective in a subset of patients only. To this end, however, predictive molecular biomarkers to stratify cancer patients for treatment are available in exceptional cases only (e.g., absence of oncogenic *KRAS* mutations as a prerequisite for treatment of CRC patients with anti-EGFR antibodies [12]).

Vemurafenib acts as specific inhibitor of the V600E/V600K mutant form of BRAF [17] and was therefore predicted to selectively target HROC24 cells, the only mutant *BRAF* cell line used in this study. Indeed, both biological and molecular data (Figures 1 and 4, resp.) pointed to a unique sensitivity of HROC24 cells to the drug. We considered these expected results as further support for our concept to identify links between the biological sensitivity of low-passage CRC lines and specific molecular alterations. Previous studies in commonly used high-passage *BRAF*-mutant lines have suggested that CRC cells are much less sensitive to vemurafenib than malignant melanoma cells due to an EGFR-mediated reactivation of ERK signaling [22]. Although our data are not contradictory to these findings, it is still interesting to note that vemurafenib almost completely blocked phosphorylation of MEK1/2 and ERK1/2 in HROC24 cells over at least 6 h at low micromolar concentrations.

In case of the specific MEK1/2 inhibitor trametinib [18], a graduated response of the four CRC cell lines was observed. Again, HROC24 cells were much more sensitive to the drug than the other three cell lines both at the levels of DNA synthesis (Figure 1) and signal transduction (Figure 4); a finding that is compatible with a strict dependency of HROC24 cells on a constitutive activation of the MEK/ERK signaling pathway by mutant BRAF. Unexpectedly, the only remaining wild-type *KRAS* cell line, HROC18, displayed the second-lowest IC_{50} value for trametinib in the BrdU incorporation assay, while the two CRC lines with oncogenic *KRAS* mutations, HROC43 and HROC46, were less sensitive. In HROC18, HROC43, and HROC46 cells, suppression of DNA synthesis did not correlate with the inhibition of ERK phosphorylation, which showed a similar dose dependency in all three cell lines. Finally, the *TP53* status was no predictor of the trametinib responsiveness. Together, our data suggest the presence of oncogenic *BRAF* as determinant of the efficiency of trametinib in CRC cells, an observation that is in line with similar findings in malignant melanoma [20]. At the level of gene expression, the effects of both vemurafenib and trametinib were largely consistent with the action profile of drugs that act by targeting the RAS/RAF/MEK/ERK signaling pathways. Thus, both drugs strongly inhibited the expression of the *FOS* gene, a key regulator of cell proliferation, differentiation, and survival that is transcriptionally regulated by the aforementioned signaling cascade [38].

For the AKT inhibitor perifosine [19], a comparison of the most sensitive cell line, HROC24, with largely resistant HROC46 cells revealed a correlation between the inhibition of DNA synthesis and reduction of AKT phosphorylation. On the other hand, the molecular basis of the complete biological resistance of HROC46 cells warrants further investigations,

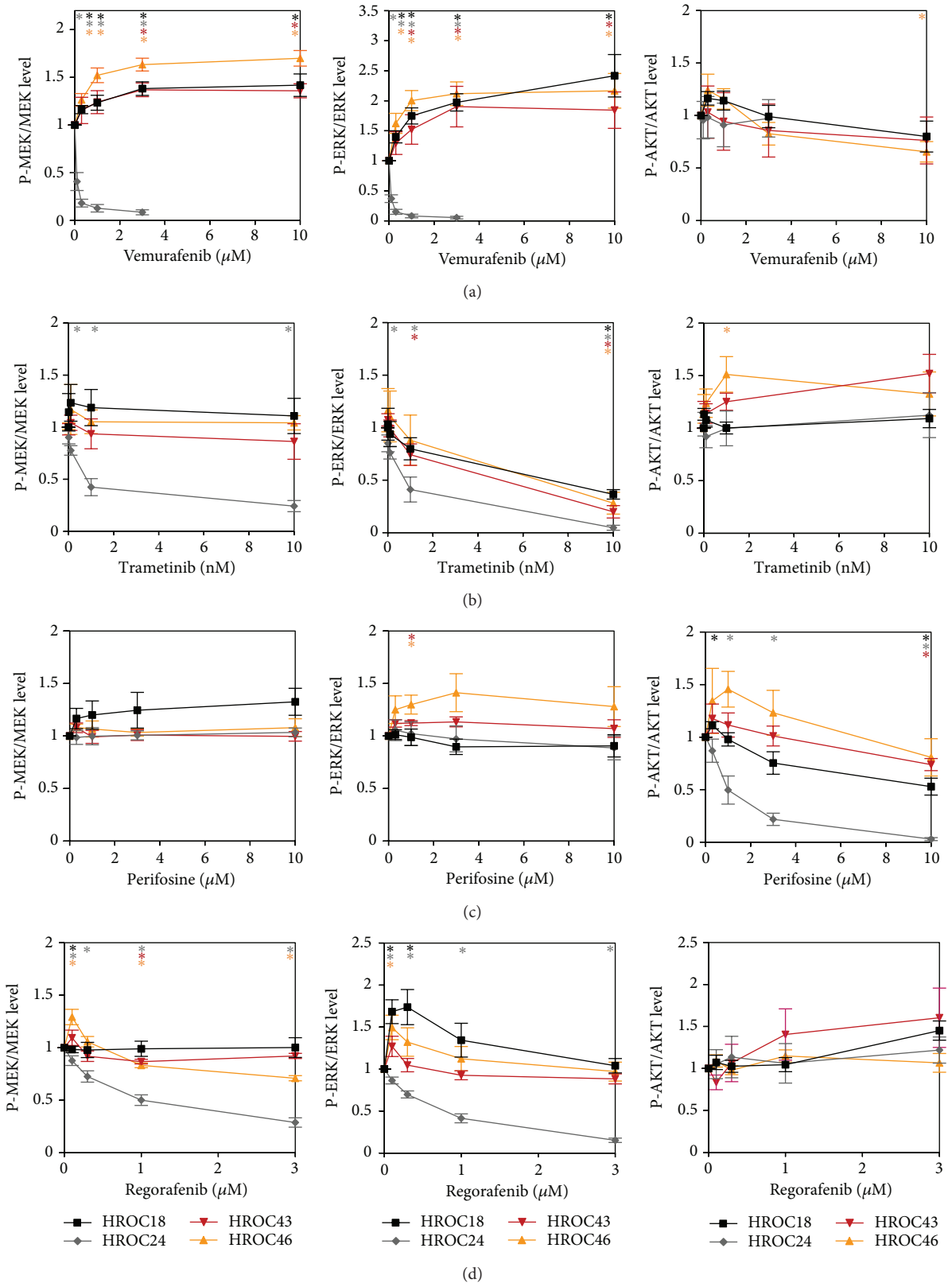

Figure 4: Quantitative analysis of the effects of vemurafenib, trametinib, perifosine, and regorafenib on signal transduction in CRC cell lines. The effects of (a) vemurafenib, (b) trametinib, (c) perifosine, and (d) regorafenib on fluorescence signal intensities of phosphoproteins (P-AKT, P-MEK1/2, and P-ERK1/2, resp.) and corresponding total proteins in HROC18 (black), HROC24 (grey), HROC43 (red), and HROC46 (orange) cells were quantified. Subsequently, the ratios P-MEK/MEK protein (left panels), P-ERK/ERK protein (middle panels), and P-AKT/AKT protein (right panels) were determined. A ratio of 1 corresponds to control cells cultured without SMI. Data of 5 independent experiments were used to calculate mean values ± SEM; $^{*}P < 0.01$ versus control cultures with Bonferroni-adjusted $\alpha = 0.0125$.

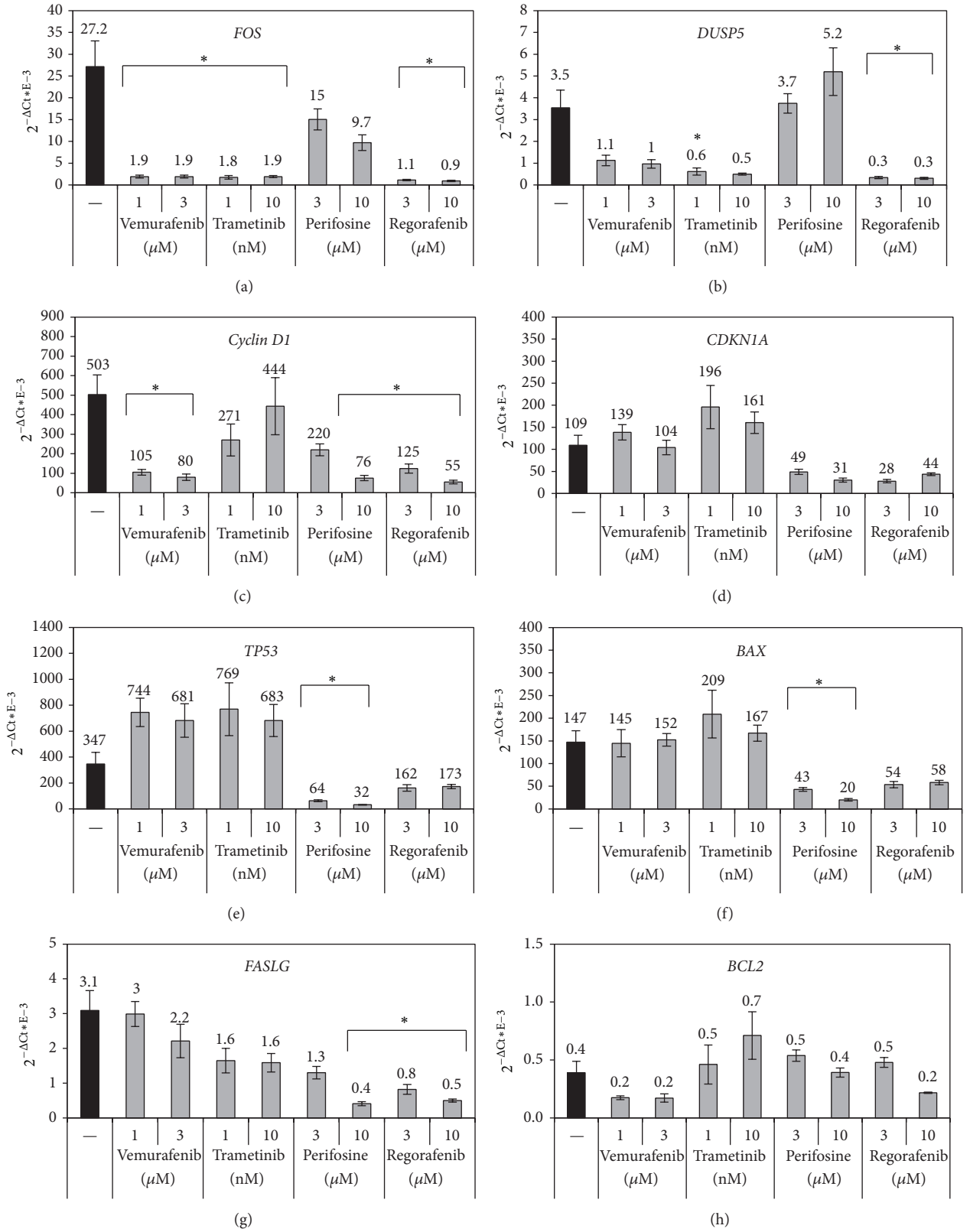

Figure 5: Gene expression profiles of SMI-treated HROC24 cells. Cultured HROC24 cells were exposed to SMI at the indicated concentrations for 6 hours. The mRNA expression of (a) *FOS*, (b) *DUSP5*, (c) *cyclin D1*, (d) *CDKN1A*, (e) *TP53*, (f) *BAX*, (g) *FASLG*, and (h) *BCL2* and the housekeeping gene *HPRT* was analyzed by real-time PCR and relative amounts of target mRNA were calculated as described in the "materials and methods" section. Data of $n = 4$–8 independent cultures were used to calculate mean values ± SEM. $^{*}P < 0.006$ versus control cultures with Bonferroni-adjusted $\alpha = 0.00625$.

since *PTEN* mutations were not detected and at least by trend a decrease of P-AKT levels at a perifosine concentration of 10 μM was observed. Noteworthy, HROC18, the only cell line in our investigation that carries the E545K mutation of *PIK3CA*, displayed an intermediate sensitivity to perifosine only.

In this study, perifosine was the only SMI that strongly affected cell survival by inducing apoptosis (shown for HROC24 cells; Figure 2). At the level of gene expression, however, the effects of perifosine were only in part in line with its proapoptotic efficiency (diminished levels of *cyclin D1*). Other effects of perifosine (inhibition of *TP53*, *BAX*, and *FASLG* expression) were unexpected and require follow-up studies for interpretation.

The multikinase inhibitor regorafenib [3] diminished the proliferation of all four CRC lines with similar efficiency (IC_{50} values in the low micromolar range). Given that cell lines of all three molecular classes of CRC and with a different mutation status of *KRAS*, *BRAF*, *PIK3CA*, and *TP53* were studied, these data suggest regorafenib efficiency as quite robust against specific molecular alterations. At the level of gene expression, a broad-range inhibitory effect of regorafenib was observed that fits its action profile as a multikinase inhibitor. Surprisingly, however, regorafenib inhibited phosphorylation of MEK1/2 and ERK1/2 exclusively in HROC24 cells and AKT phosphorylation even not at all. We therefore hypothesize that both signaling pathways are not essential for the inhibition of DNA synthesis and gene expression in low-passage HROC cells by regorafenib.

Interestingly, the combination of vemurafenib with any of the other three drugs resulted in additive inhibitory effects on the proliferation of HROC24 cells. Combination therapy with BRAF and MEK inhibition is currently in clinical development for the treatment of *BRAF* mutated malignant melanoma [39]. Based on our data, we suggest that further preclinical studies should address the question if CRC might be another suitable target for such a combination of drugs. We expand this conclusion to the simultaneous application of vemurafenib and regorafenib or a specific AKT inhibitor, since all these drug combinations showed similar potencies in our assays. As a next step, we are planning *in vivo* studies in mice with xenografted tumors to validate and expand the results of our *in vitro* investigations.

5. Conclusions

Together, the results of this study have provided novel insights into the molecular determinants of SMI efficiencies in CRC cells. Specifically, a MSI-positive cell line with mutant *BRAF*, HROC24, was most sensitive not only to vemurafenib but also to trametinib and perifosine treatment. The multikinase inhibitor regorafenib displayed growth-inhibitory effects that were largely independent of the mutational profile and the molecular class of the tumor. Combinations of regorafenib with specific SMI such as vemurafenib (in *BRAF*-mutant tumors), trametinib and perifosine warrant further evaluation. Low-passage cell lines, like the ones used in this study, are relevant preclinical models and therefore advantageous for the testing of novel targeted therapeutics.

Conflict of Interests

The authors declare that there is no conflict of interests regarding the publication of this paper.

Authors' Contribution

Falko Lange and Benjamin Franz contributed equally.

Acknowledgment

The authors gratefully acknowledge the excellent technical assistance of Mrs. Katja Bergmann.

References

[1] R. Siegel, J. Ma, Z. Zou, and A. Jemal, "Cancer statistics, 2014," *CA: Cancer Journal for Clinicians*, vol. 64, no. 1, pp. 9–29, 2014.

[2] Y.-D. Cheng, H. Yang, G.-Q. Chen, and Z.-C. Zhang, "Molecularly targeted drugs for metastatic colorectal cancer," *Drug Design, Development and Therapy*, vol. 7, pp. 1315–1322, 2013.

[3] S. M. Wilhelm, J. Dumas, L. Adnane et al., "Regorafenib (BAY 73-4506): a new oral multikinase inhibitor of angiogenic, stromal and oncogenic receptor tyrosine kinases with potent preclinical antitumor activity," *International Journal of Cancer*, vol. 129, no. 1, pp. 245–255, 2011.

[4] A. Grothey, E. Van Cutsem, A. Sobrero et al., "Regorafenib monotherapy for previously treated metastatic colorectal cancer (CORRECT): an international, multicentre, randomised, placebo-controlled, phase 3 trial," *The Lancet*, vol. 381, no. 9863, pp. 303–312, 2013.

[5] T. Efferth, "Signal transduction pathways of the epidermal growth factor receptor in colorectal cancer and their inhibition by small molecules," *Current Medicinal Chemistry*, vol. 19, no. 33, pp. 5735–5744, 2012.

[6] E. Martinelli, T. Troiani, E. D'Aiuto et al., "Antitumor activity of pimasertib, a selective MEK 1/2 inhibitor, in combination with PI3K/mTOR inhibitors or with multi-targeted kinase inhibitors in pimasertib-resistant human lung and colorectal cancer cells," *International Journal of Cancer*, vol. 133, no. 9, pp. 2089–2101, 2013.

[7] S. Yoon and R. Seger, "The extracellular signal-regulated kinase: multiple substrates regulate diverse cellular functions," *Growth Factors*, vol. 24, no. 1, pp. 21–45, 2006.

[8] C. Montagut and J. Settleman, "Targeting the RAF-MEK-ERK pathway in cancer therapy," *Cancer Letters*, vol. 283, no. 2, pp. 125–134, 2009.

[9] S. Ogino, J. A. Meyerhardt, N. Irahara et al., "KRAS mutation in stage III colon cancer and clinical outcome following intergroup trial CALGB 89803," *Clinical Cancer Research*, vol. 15, no. 23, pp. 7322–7329, 2009.

[10] M. Brink, A. F. P. M. de Goeij, M. P. Weijenberg et al., "K-ras oncogene mutations in sporadic colorectal cancer in The Netherlands Cohort Study," *Carcinogenesis*, vol. 24, no. 4, pp. 703–710, 2003.

[11] H. Davies, G. R. Bignell, C. Cox et al., "Mutations of the BRAF gene in human cancer," *Nature*, vol. 417, no. 6892, pp. 949–954, 2002.

[12] P. M. Wilson, M. J. LaBonte, and H.-J. Lenz, "Molecular markers in the treatment of metastatic colorectal cancer," *The Cancer Journal*, vol. 16, no. 3, pp. 262–272, 2010.

[13] K.-K. Wong, J. A. Engelman, and L. C. Cantley, "Targeting the PI3K signaling pathway in cancer," *Current Opinion in Genetics & Development*, vol. 20, no. 1, pp. 87–90, 2010.

[14] S. Ward, Y. Sotsios, J. Dowden, I. Bruce, and P. Finan, "Therapeutic potential of phosphoinositide 3-kinase inhibitors," *Chemistry & Biology*, vol. 10, no. 3, pp. 207–213, 2003.

[15] N. T. Ihle, G. Powis, and S. Kopetz, "PI-3-Kinase inhibitors in colorectal cancer," *Current Cancer Drug Targets*, vol. 11, no. 2, pp. 190–198, 2011.

[16] T. L. Yuan and L. C. Cantley, "PI3K pathway alterations in cancer: variations on a theme," *Oncogene*, vol. 27, no. 41, pp. 5497–5510, 2008.

[17] J. Tsai, J. T. Lee, W. Wang et al., "Discovery of a selective inhibitor of oncogenic B-Raf kinase with potent antimelanoma activity," *Proceedings of the National Academy of Sciences of the United States of America*, vol. 105, no. 8, pp. 3041–3046, 2008.

[18] A. G. Gilmartin, M. R. Bleam, A. Groy et al., "GSK1120212 (JTP-74057) is an inhibitor of MEK activity and activation with favorable pharmacokinetic properties for sustained in vivo pathway inhibition," *Clinical Cancer Research*, vol. 17, no. 5, pp. 989–1000, 2011.

[19] S. B. Kondapaka, S. S. Singh, G. P. Dasmahapatra, E. A. Sausville, and K. K. Roy, "Perifosine, a novel alkylphospholipid, inhibits protein kinase B activation," *Molecular Cancer Therapeutics*, vol. 2, no. 11, pp. 1093–1103, 2003.

[20] K. T. Flaherty, I. Puzanov, K. B. Kim et al., "Inhibition of mutated, activated BRAF in metastatic melanoma," *The New England Journal of Medicine*, vol. 363, no. 9, pp. 809–819, 2010.

[21] S. Kopetz, J. Desai, E. Chan et al., "PLX4032 in metastatic colorectal cancer patients with mutant BRAF tumors," *Journal of Clinical Oncology*, vol. 28, supplement, abstract 3534, no. 15, 2010.

[22] R. B. Corcoran, H. Ebi, A. B. Turke et al., "EGFR-mediated reactivation of MAPK signaling contributes to insensitivity of BRAF-mutant colorectal cancers to RAF inhibition with vemurafenib," *Cancer Discovery*, vol. 2, no. 3, pp. 227–235, 2012.

[23] M. Mao, F. Tian, J. M. Mariadason et al., "Resistance to BRAF inhibition in BRAF-mutant colon cancer can be overcome with PI3K inhibition or demethylating agents," *Clinical Cancer Research*, vol. 19, no. 3, pp. 657–667, 2013.

[24] T. Yamaguchi, R. Kakefuda, N. Tajima, Y. Sowa, and T. Sakai, "Antitumor activities of JTP-74057 (GSK1120212), a novel MEK1/2 inhibitor, on colorectal cancer cell lines in vitro and in vivo," *International Journal of Oncology*, vol. 39, no. 1, pp. 23–31, 2011.

[25] M. Watanabe, Y. Sowa, M. Yogosawa, and T. Sakai, "Novel MEK inhibitor trametinib and other retinoblastoma gene (RB)-reactivating agents enhance efficacy of 5-fluorouracil on human colon cancer cells," *Cancer Science*, vol. 104, no. 6, pp. 687–693, 2013.

[26] J. C. Bendell, J. Nemunaitis, S. J. Vukelja et al., "Randomized placebo-controlled phase II trial of perifosine, plus capecitabine as second- or third-line therapy in patients with metastatic colorectal cancer," *Journal of Clinical Oncology*, vol. 29, no. 33, pp. 4394–4400, 2011.

[27] J. C. Bendell, T. Ervin, N. Senzer et al., "Results of the X-PECT study: a phase III randomized double-blind, placebo-controlled study of perifosine plus capecitabine (P-CAP) versus placebo plus capecitabine (CAP) in patients (pts) with refractory metastatic colorectal cancer (mCRC)," *Journal of Clinical Oncology*, vol. 30, 2012.

[28] M. B. Chen, X. Y. Wu, G. Q. Tao et al., "Perifosine sensitizes curcumin-induced anti-colorectal cancer effects by targeting multiple signaling pathways both in vivo and in vitro," *International Journal of Cancer*, vol. 131, no. 11, pp. 2487–2498, 2012.

[29] M. Linnebacher, C. Maletzki, C. Ostwald et al., "Cryopreservation of human colorectal carcinomas prior to xenografting," *BMC Cancer*, vol. 10, article 362, 2010.

[30] C. Maletzki, S. Stier, U. Gruenert et al., "Establishment, characterization and chemosensitivity of three mismatch repair deficient cell lines from sporadic and inherited colorectal carcinomas," *PLoS ONE*, vol. 7, no. 12, Article ID e52485, 2012.

[31] B. S. Danes, P. Deangelis, F. Traganos, M. R. Melamed, and T. Alm, "Demonstration of altered cellular DNA content distribution in long-term colon epithelial cell lines with colon cancer genotypes," *Scandinavian Journal of Gastroenterology*, vol. 23, no. 7, pp. 840–846, 1988.

[32] J. Bocsi and A. Zalatnai, "Establishment and long-term xenografting of human pancreatic carcinomas in immunosuppressed mice: changes and stability in morphology, DNA ploidy and proliferation activity," *Journal of Cancer Research and Clinical Oncology*, vol. 125, no. 1, pp. 9–19, 1999.

[33] S. Kang, A. G. Bader, and P. K. Vogt, "Phosphatidylinositol 3-kinase mutations identified in human cancer are oncogenic," *Proceedings of the National Academy of Sciences of the United States of America*, vol. 102, no. 3, pp. 802–807, 2005.

[34] F. Lange, K. Rateitschak, C. Kossow, O. Wolkenhauer, and R. Jaster, "Insights into erlotinib action in pancreatic cancer cells using a combined experimental and mathematical approach," *World Journal of Gastroenterology*, vol. 18, no. 43, pp. 6226–6234, 2012.

[35] F. Lange, K. Rateitschak, B. Fitzner, R. Pöhland, O. Wolkenhauer, and R. Jaster, "Studies on mechanisms of interferon-gamma action in pancreatic cancer using a data-driven and model-based approach," *Molecular Cancer*, vol. 10, article 13, 2011.

[36] H. Kamiyama, S. Rauenzahn, J. S. Shim et al., "Personalized chemotherapy profiling using cancer cell lines from selectable mice," *Clinical Cancer Research*, vol. 19, no. 5, pp. 1139–1146, 2013.

[37] B. Vécsey-Semjén, K.-F. Becker, A. Sinski et al., "Novel colon cancer cell lines leading to better understanding of the diversity of respective primary cancers," *Oncogene*, vol. 21, no. 30, pp. 4646–4662, 2002.

[38] E. Tulchinsky, "Fos family members: regulation, structure and role in oncogenic transformation," *Histology and Histopathology*, vol. 15, no. 3, pp. 921–928, 2000.

[39] K. T. Flaherty, J. R. Infante, A. Daud et al., "Combined BRAF and MEK inhibition in melanoma with BRAF V600 mutations," *The New England Journal of Medicine*, vol. 367, no. 18, pp. 1694–1703, 2012.